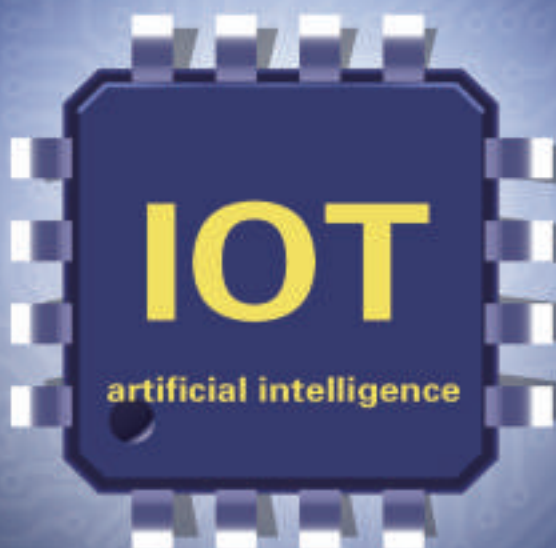


# ZTE COMMUNICATIONS

An International ICT R&D Journal Sponsored by ZTE Corporation

June 2015, Vol. 13 No. 2

## **SPECIAL TOPIC:** **Using Artificial Intelligence in the** **Internet of Things**



# ZTE Communications Editorial Board

## Chairman

**Houlin Zhao:** International Telecommunication Union (Switzerland)

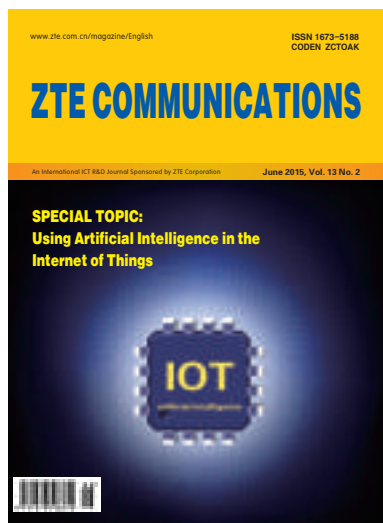
## Vice Chairmen

**Lirong Shi:** ZTE Corporation (China)    **Chengzhong Xu:** Wayne State University (USA)

## Members (in Alphabetical Order):

Chang Wen Chen	The State University of New York at Buffalo (USA)
Chengzhong Xu	Wayne State University (USA)
Connie Chang-Hasnain	University of California, Berkeley (USA)
Fa-Long Luo	Element CXI (USA)
Fuji Ren	The University of Tokushima (Japan)
Guifang Li	University of Central Florida (USA)
Honggang Zhang	Université Européenne de Bretagne (France)
Houlin Zhao	International Telecommunication Union (Switzerland)
Huifang Sun	Mitsubishi Electric Research Laboratories (USA)
Jianhua Ma	Hosei University (Japan)
Jiannong Cao	Hong Kong Polytechnic University (Hong Kong, China)
Jinhong Yuan	University of New South Wales (Australia)
Keli Wu	The Chinese University of Hong Kong (Hong Kong, China)
Kun Yang	University of Essex (UK)
Lirong Shi	ZTE Corporation (China)
Shigang Chen	University of Florida (USA)
Shuguang Cui	Texas A&M University (USA)
Victor C. M. Leung	The University of British Columbia (Canada)
Wanlei Zhou	Deakin University (Australia)
Weihua Zhuang	University of Waterloo (Canada)
Wen Gao	Peking University (China)
Wenjun (Kevin) Zeng	University of Missouri (USA)
Xiaodong Wang	Columbia University (USA)
Yi Pan	Georgia State University (USA)
Yingfei Dong	University of Hawaii (USA)
Yueping Zhang	Nanyang Technological University (Singapore)
Zhenge (George) Sun	ZTE Corporation (China)
Zhili Sun	University of Surrey (UK)

# ► CONTENTS



Submission of a manuscript implies that the submitted work has not been published before (except as part of a thesis or lecture note or report or in the form of an abstract); that it is not under consideration for publication elsewhere; that its publication has been approved by all co-authors as well as by the authorities at the institute where the work has been carried out; that, if and when the manuscript is accepted for publication, the authors hand over the transferable copyrights of the accepted manuscript to *ZTE Communications*; and that the manuscript or parts thereof will not be published elsewhere in any language without the consent of the copyright holder. Copyrights include, without spatial or timely limitation, the mechanical, electronic and visual reproduction and distribution; electronic storage and retrieval; and all other forms of electronic publication or any other types of publication including all subsidiary rights.

Responsibility for content rests on authors of signed articles and not on the editorial board of *ZTE Communications* or its sponsors.

All rights reserved.

## Special Topic: Using Artificial Intelligence in the Internet of Things

Guest Editorial 01  
Fuji Ren and Yu Gu

IOT: Advanced Direction of the Internet of Things 03  
Yixin Zhong

An Instance-Learning-Based Intrusion-Detection System for Wireless Sensor Networks 07  
Shuai Fu, Xiaoyan Wang, and Jie Li

Forest Fire Detection Using Artificial Neural Network Algorithm Implemented in Wireless Sensor Networks 12  
Yongsheng Liu, Yansong Yang, Chang Liu, and Yu Gu

WeWatch: An Application for Watching Video Across Two Mobile Devices 17  
Fuji Ren, Mengni Chen, and Yu Gu

A Parameter-Detection Algorithm for Moving Ships 23  
Yaduan Ruan, Juan Liao, Jiang Wang, Bo Li, and Qimei Chen

## Review

Inter-WBAN Coexistence and Interference Mitigation 28  
Bin Liu, Xiaosong Zhao, Lei Zou, and Chang Wen Chen

# ▶ CONTENTS

## ZTE COMMUNICATIONS

Vol. 13 No. 2 (Issue 46)

Quarterly

First English Issue Published in 2003

### Supervised by:

Anhui Science and Technology Department

### Sponsored by:

Anhui Science and Technology Information  
Research Institute and ZTE Corporation

### Staff Members:

Editor-in-Chief: Sun Zhenge

Executive Associate

Editor-in-Chief: Huang Xinming

Editor-in-Charge: Zhu Li

Editors: Paul Sleswick, Xu Ye, Yang Qinyi,  
Lu Dan

Producer: Yu Gang

Circulation Executive: Wang Pingping

Assistant: Wang Kun

### Editorial Correspondence:

Add: 12F Kaixuan Building,

329 Jinzhai Road,

Hefei 230061, P. R. China

Tel: +86-551-65533356

Fax: +86-551-65850139

Email: magazine@zte.com.cn

### Published and Circulated

(Home and Abroad) by:

Editorial Office of

*ZTE Communications*

### Printed by:

Hefei Tiancai Color Printing Company

### Publication Date:

June 25, 2015

### Publication Licenses:

ISSN 1673-5188

CN 34-1294/TN

### Advertising License:

皖合工商广字0058号

### Annual Subscription:

RMB 80

## Research Papers

### A Visual Lossless Image-Recompression Framework

36

Ping Lu, Xia Jia, Hengliang Zhu, Ming Liu, Shouhong Ding, and Lizhuang Ma

### Channel Modeling for Air-to-Ground Wireless Communication

41

Yingcheng Shi, Di He, Bin Li, and Jianwu Dou

### Terminal-to-Terminal Calling for GEO Broadband Mobile Satellite Communication

46

Qing Wang, Minjiong Zhu, Jie Zhou, Zhen Gao, and Jinsheng Yang

### Community Discovery with Location-Interaction Disparity in Mobile Social Networks

53

Danmeng Liu, Wei Wei, Guojie Song, and Ping Lu

## Roundup

### Introduction to *ZTE Communications*

02

### *ZTE Communications* Call for Papers

11

—Special Issue on Smart City: Key Technologies and Practices

### *ZTE Communications* Call for Papers

35

—Special Issue on Optical Wireless Communications

### New Members of *ZTE Communications* Editorial Board

62

# Using Artificial Intelligence in the Internet of Things

## ► Fuji Ren



Dr. Fuji Ren is a professor in the Faculty of Engineering, University of Tokushima, Japan. His research interests include information science, artificial intelligence, language understanding and communication, and affective computing. He is a member of IEICE, CAAI, IEEJ, IPSJ, JSAP, AAMT, and a senior member of IEEE. He is a fellow of the Japan Federation of Engineering Societies and president of the International Advanced Information Institute.

member of IEEE. He is a fellow of the Japan Federation of Engineering Societies and president of the International Advanced Information Institute.

## ► Yu Gu



Dr. Yu Gu is a professor in the School of Computer and Information, Hefei University of Technology, China. He has published more than 40 papers in international journals and conference proceedings, including IEEE Commun. Surveys and Tutorials, IEEE Trans. Parallel and Distributed Systems (TPDS), Ad Hoc

Networks (Elsevier), and Wireless Commun. and Mobile Comput (Wiley). He received the Excellent Paper Award at IEEE Scalcom 2009. His research interests include information science, pervasive computing, and wireless networks, in particular, wireless sensor networks.

**T**he Internet of Things (IoT) has received much attention over the past decade. With the rapid increase in the use of smart devices, we are now able to collect big data on a daily basis. The data we are gathering (and related problems) are becoming more complex and uncertain. Researchers have therefore turned to artificial intelligence (AI) to efficiently deal with the problems created by big data.

This special issue deals with the technology and applications of AI in the IoT and is a forum for scientists, engineers, broadcasters, manufacturers, software developers, and other related professionals to discuss related issues. The topics addressed in this special issue include current research progress, real-world applications, and security issues related to AI in IoT. The call-for-papers attracted a number of excellent submissions. After two-round reviews, five papers were selected for publication. These papers are organized in three groups. The first group comprises one overview paper that outlines the technical progress of IoT. The second group comprises two papers addressing security issues in IoT. The last group comprises two papers that present some interesting real-world applications that will benefit daily life.

The first paper, "I<sup>2</sup>oT: Advanced Direction of the Internet of Things," gives an excellent vision of how AI technologies can be combined with IoT. The author introduces the principle and conceptual model of intelligent IoT (I<sup>2</sup>oT in short), which results from the integration of AI and IoT and is the most promising version of IoT. In the final section of the paper, the author makes recommendations for further study and standardization.

The wireless sensor network (WSN) is a key enabler of IoT because of its great sensing ability and ability to generate and process big data. Using AI to handle big data in a WSN is a critical research topic and deserves much effort. The next two papers, "An Instance-Learning-Based Intrusion-Detection System for Wireless Sensor Networks" and "Forest Fire Detection Using Artificial Neural Network Algorithm Implemented in Wireless Sensor Networks" fall within this scope. The former addresses the intrusion-detection issue in WSNs and presents an instance-learning-based intrusion-detection system (IL-IDS) to protect the network from routing attacks. By mining historical data (instances), critical rules about attacks can be created to help build a routing mechanism that is more robust to malicious behaviour. The latter paper deals with a more specific application, i.e., forest fire detection using an artificial neural network algorithm in a WSN. Forest fires threaten forest resources, human lives, and surrounding environments. The authors build a forest fire detection system that takes advantage of the unique features of a WSN, such as easy deployment, efficient data collection and environmental monitoring. An artificial neural network algorithm is designed to improve multi-criteria detection, which helps decrease the possibility of false alarms the system cost.

The last group comprises two papers about real-world applications of IoT: "We

**Guest Editorial**

Fuji Ren and Yu Gu

Watch: An Application for Watching Video Access Two Mobile Devices” and “A Parameter-Detection Algorithm for Moving Ships.” With the rapid development of wireless communications and embedded computing, IoT is no longer a concept but is gradually becoming a reality. One of the consequences of this trend is that people are surrounded by smart devices, which are changing almost every aspect of daily life. The former paper explores the blossoming of smart devices for a better viewing experience. It presents a unified platform based on Android where different devices can share screens. For instance, it allows a video to be played simultaneously on two devices that are close to each other. It provides a better way of watching videos by putting the screens of the two devices close together. However, the distance between the two screens needs to be accurately measured. This paper discusses a distance-measuring mechanism based on Wi-Fi signal decay. By mining training data, the system can adaptively improve the measurement accuracy.

The vision-based technique is a general AI technique that involves abstracting information from dynamic or static pic-

tures. It is essential for the fast approach of IoT. In the latter paper, the authors propose an algorithm for detecting the parameters of a moving ship in an inland river. Numerous different vision-based parameter-detection approaches have been used in traffic monitoring systems; however, few have been applied to waterway transport because of complexities such as rippling water and lack of calibration objects. The authors discuss interactive calibration without a reference as well as detection of a moving ship using an optimized visual foreground-detection algorithm. This reduces the likelihood of false detection in dynamic water-based scenarios and improves the detection of ship size, speed and flow. The traffic parameter detection algorithm has been trialled in the Beijing - Hangzhou Grand Canal and has an accuracy of more than 90% for all parameters.

We thank all authors for their valuable contributions and we express our sincere gratitude to all the reviewers for their timely and insightful expert reviews. It is hoped that the contents in this special issue are informative and useful from the aspects of technology, standardization, and implementation.

**Roundup**

## Introduction to *ZTE Communications*



*ZTE Communications* is a quarterly, peer-reviewed international technical journal (ISSN 1673-5188 and CODEN ZCTOAK) sponsored by ZTE Corporation, a major international provider of telecommunications, enterprise and consumer technology solutions for the Mobile Internet. The journal publishes original academic papers and research findings on the whole range of communications topics, including communications and information system design, optical fiber and electro-optical engineering, microwave technology, radio wave propagation, antenna engineering, electromagnetics, signal and image processing, and power engineering. The journal is designed to be an integrated forum for university academics and industry researchers from around the world. *ZTE Communications* was founded in 2003 and has a readership of 5500. The English version is distributed to universities, colleges, and research institutes in more than 140 countries. It is listed in Inspec, Cambridge Scientific Abstracts (CSA), Index of Copernicus (IC), Ulrich's Periodicals Directory, Norwegian Social Science Data Services (NSD), Chinese Journal Fulltext Databases, Wanfang Data — Digital Periodicals, and China Science and Technology Journal Database. Each issue of *ZTE Communications* is based around a Special Topic, and past issues have attracted contributions from leading international experts in their fields.



# I<sup>2</sup>oT: Advanced Direction of the Internet of Things

Yixin Zhong

(University of Posts and Telecommunications, Beijing 1000876, China)

## Abstract

The Internet of Things (IoT) is still in its infancy because of the limited capability of its embedded processor. In the meantime, research on artificial intelligence (AI) has made plenty of progress. The application of AI to IoT will significantly increase the capabilities of IoT, and this will benefit both economic and social development. In this paper, the elementary concepts and key technologies of AI are explained, and the model and principle of intelligent IoT, denoted I<sup>2</sup>oT, resulting from the integration of AI and IoT are discussed. I<sup>2</sup>oT will be the most promising version of IoT. Finally, recommendations for further study and standardization of I<sup>2</sup>oT are made.

## Keywords

Internet of Things; artificial intelligence; knowledge producing; strategy formulation; intelligent internet of things

## 1 Introduction

There are two main motivations for expanding the Internet to the Internet of Things (IoT). The first motivation is to expand the amount of information shared by databases and objects in the real world. The second motivation is to enable users not only to share information but also control objects in the real world. These make IoT much more attractive in society. In other words, IoT is a good advancement of the conventional Internet.

In terms of technological development, however, IoT is still in its infancy and can be greatly improved by endowing IoT functions with much more intelligence [1]. Significant progress has been made in artificial intelligence (AI) over the past decade. All AI technologies needed to make IoT more intelligent and evolve into I<sup>2</sup>oT are now feasible. The main concern at the moment is how to understand and effectively apply AI technologies to current IoT systems.

## 2 A Brief Description of IoT

The purpose of IoT is to expand the functions of existing Internet and make it more useful. With IoT, users can share not only information provided by humans and contained in databases but also information provided by things in physical world. The simplified functional model of IoT is shown in Fig. 1.

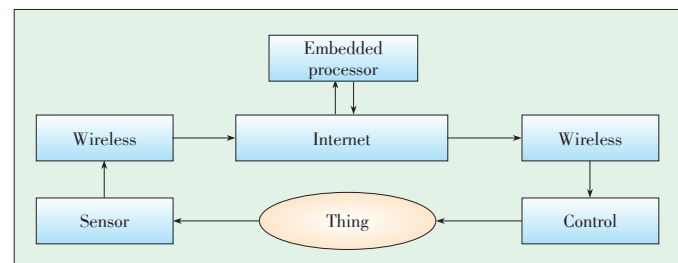
As in Fig. 1, IoT has sensors, for acquiring information about the state of things; an embedded processor, for producing orders that regulate the state of things; wireless technology,

for transferring information from sensors to Internet and Internet to controller; and control unit, for executing human orders regulating the state of things.

Take IoT for maintaining room temperature for example. A standard room temperature is designated in advance, and the actual room temperature is acquired by the sensor(s) and transferred via wireless to Internet. After receiving the actual room temperature, the embedded processor compares it with the designated value and generates an order to regulate the room temperature and keep it within a certain range. This order is immediately sent to the control unit via the Internet and wireless unit and is executed by the actuator of the control unit.

If information about the state of the thing concerned can be acquired by sensors and controlled by actuators, and if the function performed by the embedded processor is not too complicated, the IoT technology is feasible.

If physical things and their environment in IoT become complex, the functions of the required embedded processors also become complex, and conventional technologies of the current



▲ Figure 1. Simplified functional model of IoT.

IoT will no longer be satisfactory.

Unfortunately, problems with complex factors are very often important to economic and social development. A typical example is air pollution over a large area. Another typical example is global warming. People want to know information about the air quality and weather conditions and control them in certain ways. Therefore, efficiently dealing with complex problems is an unavoidable responsibility of scientists.

The most promising approach to handling such complex problems is artificial intelligent. The reason for this proposal is the fact that central need for solving complex problems is the learning ability.

### 3 Fundamental Concepts and Principles of Artificial Intelligence

In a narrow sense, AI has traditionally implied the simulation of logical human thinking using computer technology. Within this framework, the fields of artificial neural networks (ANNs) [2]–[4] and sensor-motor systems (SMSs) [5]–[7] were considered extraneous, even though both fields have been concerned with simulating the functions of the human brain. ANN and SMS had to form a new discipline called computational intelligence (CI). Computational intelligence has become the other approach to AI. It is more reasonable for the term AI to encompass both AI in narrow sense and CI. In the contemporary sense, AI is now re-termed unified AI [8]–[9].

In this paper, AI means unified AI, a general term representing the theory and technology related to simulating intellectual abilities of human being, including the ability to understand and solve problems. What follows is a brief explanation of how AI can handle complex problems [10]–[12].

What AI simulates and offers is not anything else but the learning ability of human beings, i.e., learning to understand and solve the problem. Therefore, learning is the central feature in AI and learning-technology is the key to handling problems.

The simplest model for AI is roughly abstracted in Fig. 2.

Ontological information (OI) in Fig. 2 is information about the state and pattern of the state variance that are presented by the object in the environment of the outside world and that are the resources and clues for learning to understand the problem. On the other hand, the subject's action or reaction applied to the object can be learnt based on an understanding of the problem.

A more specific functional model of the technologies in AI is shown in Fig. 3. In Fig. 3, AI technologies are interconnected and interact with each other.

#### 3.1 Categories of AI Technology

##### 3.1.1 Perception

This technology is used to acquire the OI about the object or

problem in its environment. It is also the technology for converting OI to epistemological information (EI).

Epistemological information is information perceived by the subject about the trinity of the form (syntactic information), content/meaning (semantic information), and utility/value (pragmatic information) concerning OI.

Unlike the traditional concept of information proposed by Claude Shannon, EI comprises the trinity of the form, content/meaning, and utility/value and is the basis of learning. This is why EI is also often called comprehensive information.

The essential function of perception is to convert OI to EI. This is the first class of information conversion in AI.

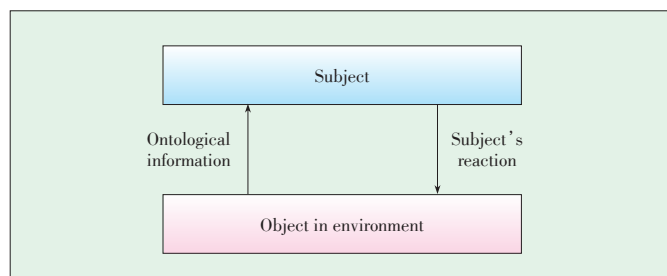
##### 3.1.2 Cognition

The main function of cognition technology is to convert EI, which is perceived by the subject from OI, into the corresponding knowledge about the object. This is the second class of information conversion needed in AI. The only possible approach to converting EI to knowledge must be learning—there is no other way.

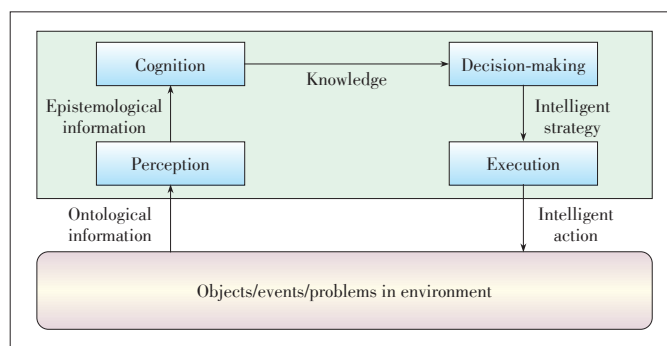
##### 3.1.3 Decision-Making

The technology used in decision-making converts EI to intelligent strategy (IS) based on knowledge support and is directed by the goal of problem solving. The strategy is just the procedural guidance for problem-solving. This is the third class of information conversion in AI.

The radical function of decision-making technology is learning to find the optimal solution for a given problem. There are usually a number of ways of achieving the designated goal from



▲ Figure 2. A simplified functional model for AI.



▲ Figure 3. A more specific functional model of AI.



a starting point expressed by EI. A decision should be made through intelligent use, via learning, of the relevant knowledge provided.

### 3.1.4 Strategy-Execution

This technology is used to convert the IS into intelligent action (IA) that will solve the problem.

### 3.1.5 Strategy-Optimization

Because of various non-ideal factors in all sub-processes in Fig. 3, there are often errors when intelligent action is applied. These errors are regarded as new information and are fed back to the input of the perception of the model. With this new information, the knowledge can be improved via learning, and the strategy can be optimized. Such an optimization process might continue many times until the error is sufficiently small.

In sum, all the AI technologies hereto mentioned are learning-based, and this is why AI is powerful.

## 3.2 Implementation Issues for the Three Classes of Information Conversion

Perception technology can be implemented using the model in Fig. 4, which converts OI to EI, the trinity of  $X$ ,  $Y$  and  $Z$ , and is the first class of information conversion.

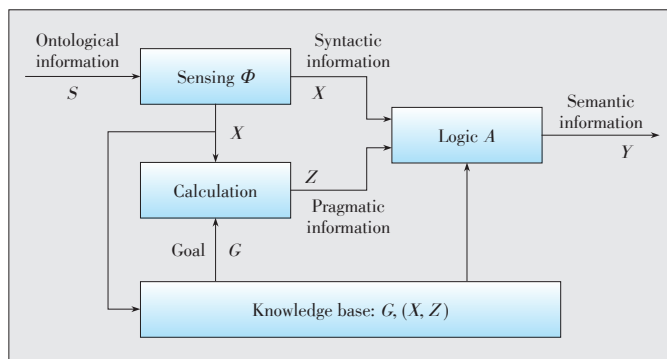
Fig. 4 shows that the ontological information (denoted  $S$ ) is applied to the input of the perception model and mapped to the corresponding syntactic information (denoted  $X$ ). Next, the pragmatic information (denoted  $Z$ ) can be retrieved from the knowledge base, in which many  $X$ - $Z$  pairs,  $\{X(i), Z(i)\}$ , are stored. When  $X$  is matched with  $X(i_0)$ , then  $Z(i_0)$  is regarded as the pragmatic information corresponding to  $X$ . In case no math can be found, the equation can be used to find  $Z$ ;

$$Z = \text{Cor}(X, G) \quad (1)$$

where  $X$  and  $G$  are expressed as vectors; and Cor is the correlation operation. Because  $X$  and  $Z$  are now available, the semantic information  $Y$  can be inferred from:

$$Y = \lambda(X, Z) \varepsilon S \quad (2)$$

where  $S$  is the space of semantic information, and  $\lambda$  is the logic



▲ Figure 4. Model of the first class of information conversion.

operation mapping the pair of  $(X, Z)$  to  $Y$  in  $S$ . This means that  $Y$  is a subset of  $S$  when both  $X$  and  $Z$  are simultaneously valid. In other words,  $Y$  is determined by the joint conditions of  $X$  and  $Z$  (Fig. 5).

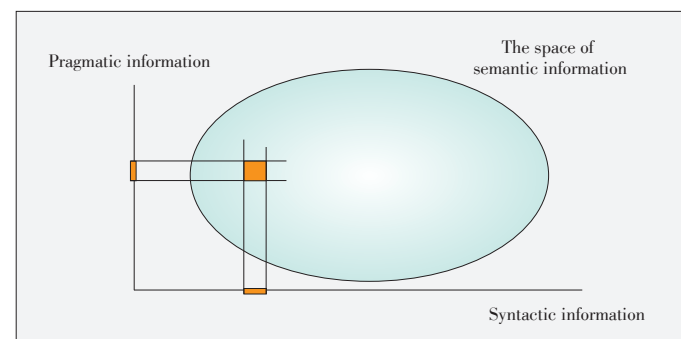
As a result, OI is converted into EI, which is the trinity of  $X$ ,  $Y$  and  $Z$ , via the model in Fig. 4. This technology is completely feasible in practice.

Cognition technology can be implemented using the model in Fig. 6, with which EI is converted to knowledge. This is the second class of information conversion.

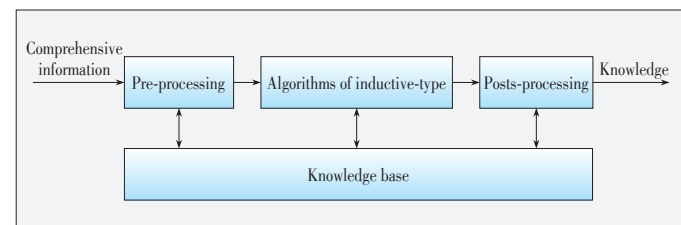
According to the definitions of information and knowledge, information is the phenomenon in nature and knowledge is the essence in nature. Thus, knowledge can be established using inductive-type algorithms (Fig. 6). In Fig. 6, comprehensive information is another name for EI.

The technology for decision-making can be implemented using the model in Fig. 7, which converts EI to IS based on the support of the related knowledge and guided by the goal of problem solving given beforehand.

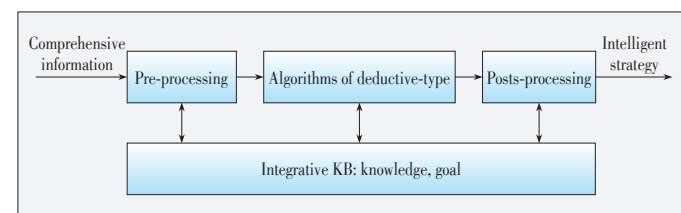
The model in Fig. 7 is quite similar to that in Fig. 6; however, the big difference between them is the principal algorithms. In Fig. 6, the algorithms are inductive type whereas in Fig. 7 they are deductive type.



▲ Figure 5.  $Y = \lambda(X, Z)$ .



▲ Figure 6. Model of second-class of information conversion.



▲ Figure 7. Model of third class of information conversion.

## FoT: Advanced Direction of the Internet of Things

Yixin Zhong

In AI theory and technology, the three classes of information conversion (IC) are the nucleus and novelty. Nevertheless, the sub-process of strategy execution is a kind of normal technology, converting the intelligent strategy into intelligent action, and therefore is not necessary to explain here anymore.

In sum, the key issue in AI theory and technology is to successively derive the EI (first class of IC) and knowledge (second-class IC) in order to deeply understand the object concerned and then produce an intelligent strategy (third-class IC) based on OI, EI, knowledge, and the goal of the system in order to regulate the object.

## 4 A Conceptualized Model of FoT

The functioning ability of IoT is mainly limited by the performance of the embedded processor, which often fails to produce a strategy that is intelligent enough to deal with complex problems. Therefore, strengthening the embedded processor is the key to improving IoT.

Because the intelligent strategy can be derived from the three classes of IC in AI, it is feasible to use these three classes of IC to replace the embedded processor in IoT and transform IoT into FoT, which is a much more intelligent version of IoT (Fig. 8).

Comparing the conceptual model in Fig. 8 with that in Fig. 1, there is almost no difference between these two models except the replacement of embedded processor by the nucleus of AI technology, i.e., first, second and third class of IC. This is the most effective way of transforming IoT into FoT.

Because of the strong learning abilities offered by the three classes of IC in AI, the FoT will be much more powerful than the conventional IoT and will be able to handle the complex problems mentioned in section 2. The intelligent strategy needed to tackle complex problems can, in principle, be derived from the three classes of IC based on OI, EI, relevant knowledge, and the designated goal for solving problems in a manner similar to humans.

## 5 Conclusion

In conclusion, the following two points are emphasized:

- 1) IoT will have to be capable of intelligently handling complex problems. This will be an increasingly serious chal-

lenge. It is strongly recommended that the embedded processor be replaced by the three classes of IC technology in AI. In this way, IoT will become FoT and meet the demands of applications for economic and social development.

- 2) Broadly speaking, the real significance of AI is that it implements the great law of information conversion and intelligence creation, according to which information is the means and intelligence creation is the purpose. This is the radical law that governs all information activities in the information era. Arguably, this law will be more significant than the law of energy conversion and conservation in physical science in industrial era.

## References

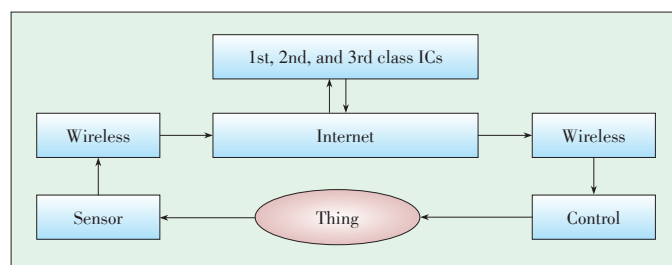
- [1] D. Kyriazis and T. Varvarigou, "Smart, autonomous and reliable internet of things," in *International Conference on Emerging Ubiquitous Systems and Pervasive Networks*, Niagara Falls, Canada, 2013. doi:10.1016/j.procs.2013.09.059.
- [2] W. C. McCulloch and W. Pitts, "A logic calculus of the ideas immanent in nervous activity," *Bulletin of Mathematical Biophysics*, no. 5, pp. 115–133, 1943.
- [3] D. E. Rumelhart, *Parallel Distributed Processing*. MA, USA: MIT Press, 1986.
- [4] J. Hopfield, "Neural networks and physical systems with emergent collective computational abilities," *Proceedings of the National Academy of Sciences*, vol. 79, pp. 2554–2558, 1982.
- [5] R. A. Brooks, "Intelligence without representation," *Artificial Intelligence*, no. 47, pp. 139–159, 1991.
- [6] R. A. Brooks, "Elephant cannot play chess," *Autonomous Robots*, no. 6, pp. 3–15, 1990.
- [7] M. Wooldridge and N. Jennings, *Intelligent Agents*. Germany: springer-verlag, 1995.
- [8] N. Nilsson, *Artificial Intelligence: A New Synthesis*. San Mateo, USA: Morgan Kaufmann Publishers, 1998.
- [9] S. Russell and P. Norvig, *Artificial Intelligence: A Modern Approach*. Beijing, China: Pearson Education, Inc., as Prentice Hall, Inc., and Tsinghua University Press, 2006.
- [10] Y. Zhong, *Principles of Cognetics in Machine (in Chinese)*. Beijing, China: Science Press, 2007.
- [11] Y. Zhong, *Principles of Advanced Intelligence (in Chinese)*. Beijing, China: Beijing Science Press, 2014.
- [12] Y. Zhong, "Principles of Information Conversion (in Chinese)," *Science Bulletin*, vol. 58, no. 14, pp. 1300–13–6, 2013.

Manuscript received: 2015-04-11

## Biography

**Yixin Zhong** (zyx@bupt.edu.cn) received the BS and MS degrees from Beijing University of Posts and Telecommunications (BUPT) in 1962 and 1965. From 1979 to 1981, he was an academic visitor to the Department of Electrical Engineering, Imperial College of Science and Technology, London. He is now a professor in the Department of Intelligence Science, School of Computing, BUPT. From 1993 to 2005, he was an associated editor of *IEEE Transactions on Neural Networks*. From 2001 to 2002, he was chair of APNNA. From 2001 to 2010, he was president of the Chinese Association for Artificial Intelligence. From 2007 to 2009, he was vice-president of WFEO and the chair of WFEO-CIC. He has also been the general chair or program chair for a number of international conferences on communications, information science, and artificial intelligence. He is now the honorary president of International Society for Information Studies. His research and teaching interests include information theory, neural networks, cognitive science, and artificial intelligence. He received a number of national awards from the Chinese government and academic organizations. He received the Outstanding Leadership Award from International Neural Network Society (INNS) in 1994, President's Award from Asia-Pacific Neural Network Assembly (APNNA) in 2002, Outstanding Contributor Award from World Federation of Engineering Organizations (WFEO) in 2010, National Outstanding Researcher and Professor in 2011, and Life Achievement Award from China Association for Artificial Intelligence in 2012.

He has published more than 450 papers and 18 books in related fields.



▲ Figure 8. Simplified functional model of FoT.

# An Instance-Learning-Based Intrusion-Detection System for Wireless Sensor Networks

Shuai Fu<sup>1</sup>, Xiaoyan Wang<sup>2</sup>, and Jie Li<sup>1</sup>

(1. Department of Computer Science, University of Tsukuba, Tsukuba, Japan;

2. Information Systems Architecture Science Research Division, National Institute of Informatics, Tokyo, Japan)

## Abstract

This paper proposes an instance-learning-based intrusion-detection system (IL-IDS) for wireless sensor networks (WSNs). The goal of the proposed system is to detect routing attacks on a WSN. Taking an existing instance-learning algorithm for wired networks as our basis, we propose IL-IDS for handling routing security problems in a WSN. Attacks on a routing protocol for a WSN include black hole attack and sinkhole attack. The basic idea of our system is to differentiate the changes between secure instances and attack instances. Considering the limited resources of sensor nodes, the existing algorithm cannot be used directly in a WSN. Our system mainly comprises four parts: feature vector selection, threshold selection, instance data processing, and instance determination. We create a feature vector form composed of the attributes that changes obviously when an attack occurs within the network. For the data processing in resource-constrained sensor nodes, we propose a data-reduction scheme based on the clustering algorithm. For instance determination, we provide a threshold-selection scheme and describe the concrete instance-determination mechanism of the system. Finally, we simulate and evaluate the proposed IL-IDS for different types of attacks.

## Keywords

WSN; security; intrusion-detection system; instance learning; black hole

## 1 Introduction

Wireless sensor networks (WSNs) contain a number of distributed sensors that are constrained in terms of energy, memory, computation, and bandwidth (PCs). The development of WSNs was motivated by military applications, such as battlefield surveillance. Now, WSNs are widely used for industrial and civilian applications, including industrial process monitoring and control, machine health monitoring, and environment and habitat monitoring.

As WSNs have developed, security problems in WSNs have attracted more and more attention. Currently, most research on these problems is focused on prevention mechanisms, such as secure routing protocols, cryptography, and authentication. Such mechanisms are usually the first line of defense; however, because of the particularities of WSNs, we cannot rely on intrusion-prevention techniques alone. In practical situations, intrusion-detection systems are needed to detect both known security exploits and novel attacks that have not yet been experienced.

Intrusion-detection is the process of identifying activities that violate the security policy of the system [1]. Such tech-

niques are traditionally categorized as anomaly detection and misuse detection. Anomaly detection is based on the normal behavior of the subject; any action that significantly deviates from this normal behavior is considered intrusive. Misuse detection catches intrusions in terms of the characteristics of known attacks or system vulnerabilities. Any action that conforms to the pattern of a known attack or vulnerability is considered intrusive [2].

There are many intrusion-detection algorithms, but few of them are designed for WSNs. We propose an instance learning-based intrusion-detection system (IL-IDS) based on an existing instance-based learning algorithm [3] for a wireless sensor networks.

## 2 Related Works

Our proposed intrusion-detection system is mainly designed for routing security in a WSN. In this section, we introduce several kinds of attack against a WSN and summarize related works on intrusion-detection systems for WSNs.

### 2.1 Routing Attacks on a Wireless Sensor Network

Before describing intrusion-detection algorithms, it is neces-

## An Instance-Learning-Based Intrusion-Detection System for Wireless Sensor Networks

Shuai Fu, Xiaoyan Wang, and Jie Li

sary to introduce several kinds of routing attack on a WSN. Such attacks include bogus routing information, selective-forwarding, sinkhole attack, Sybil attack, worm hole attack, and hello flood attack (**Table 1**).

▼ **Table 1. Types of routing attack on a WSN**

Routing attack	Description
Bogus routing information	By spoofing, altering, or replaying routing information, an attacker may be able to create routing loops or attract or repel network traffic.
Selective forwarding	Malicious nodes refuse to forward certain messages or even simply drop them, ensuring that they are not propagated any further.
Sinkhole attacks	Lure all traffic from nodes in a region to a compromised node.
Sybil attack	Single node presents multiple identities to other nodes in the network.
Worm holes	An attacker receives packets at one point in the network and tunnels them to another point in the network, and then replays them into the network from that point.
Hello flood attack	Broadcast high quality HELLO packets.

### 2.2 Intrusion Detection for a WSN

The intrusion-detection system designed by C. E. Loo *et al.* is based on a fixed-width clustering algorithm [4]. The audit data is divided into different clusters with fixed widths. The authors assume that less than  $y\%$  of the data consists of abnormal traffic samples and label the cluster normal or anomalous according to the point number of the cluster. Then, the authors decide whether newly observed data is normal or not by computing the distance to the cluster.

The other work is an intrusion-detection system designed by K. Ioannis *et al.* [5]. The authors use each node in the WSN to monitor whether its neighbors forward messages received from it. Looking at the transmission rate, the authors can determine which nodes are compromised. However, this kind of approach only focuses on selective-forwarding attacks and black hole attacks.

## 3 System Design

We propose an IL-IDS based on an existing instance-learning algorithm. Because of resource constraints in terms of energy, memory, computational speed, and bandwidth in a WSN, we modify the algorithm to make it suitable for the WSN. Here, we describe the four aspects of the algorithm:

- feature vector selection. This involves constructing feature vectors that show the network state. An obvious change in the feature vector means that an attack is occurring in the network.
- threshold selection. This involves determining the threshold  $r$  used to label instances as normal or not.
- Instance data processing. This involves collecting instance data and reducing instance samples for WSNs.
- Intrusion - detection process. This involves using the con-

crete processes from data collection to determine whether a newly observed instance is normal or not.

### 3.1 Feature Vector Selection

Constructing the sequence of feature vectors is an important issue. Feature vectors need to be designed so that they change obviously when an attack occurs. The feature vector we selected is shown in **Table 2**.

The features are classified as traffic-related or non-traffic-related. Traffic-related features describe conditions of the traffic flow through the node, and non - traffic - related features describe the routing conditions of the sensor node. From the definition of similarity, the two adjacent features interact with each other.

The ten features in Table 1 correspond to the feature vector  $\mathbf{X}=(x_0,x_1,...,x_9)$ . If behavior is abnormal, the attributes of feature vector change obviously.

In the instance -based learning algorithm, a change in the feature vector means the similarity becomes less than normal. In addition, by computing the similarity between normal data and abnormal data, we can infer whether a new instance represents abnormal behavior.

### 3.2 Threshold Selection

Selecting the threshold  $r$  requires a judgment to be made on whether the feature vector is normal or abnormal. Furthermore, determination of  $r$  depends on the tolerance of the routing protocol to errors and attacks. From simulation, we obtained many data samples and found that they followed a normal distribution. The threshold can be determined by a confidence level. In simulation, we made  $r$  to be 0.05. If the difference between the similarity and maximum similarity is greater than  $r$ , the observed instance is different from the sample instance. It is necessary to verify  $r$  through simulation.

### 3.3 Instance Data Processing

First, we count the attributes in Table 1 every fixed interval  $T$  and obtain the results as feature vectors. From experiments,

▼ **Table 2. Make-up of the feature vector**

	Feature description
1	Number of data packets received
2	Number of route requests received
3	Number of route requests sent
4	Number of route requests dropped
5	Number of data packets dropped
6	Number of route requests replies received
7	Number of route request replies forwarded
8	Number of route request replies sent
9	Number of route errors received
10	Number of route errors sent

we obtain the data sequences  $D$ . However, this creates a problem because we cannot store all the audit data in the sensor—its memory is too small. The instances of data processing is only the data reduction; therefore, we use a clustering algorithm to reduce the number of samples and only use several instances to represent all of them. The data reduction can be divided into two parts: adding instances into clusters and updating the centers of clusters.

In **Algorithm 1**, we have an instance collection  $D\{Y_1, Y_2, \dots, Y_n\}$ , where  $Y$  is a sample of a feature vector and  $Y_i = \langle y_1, y_2, \dots, y_l \rangle$ . We randomly choose several instances to be the centroids of the clusters in  $D$ . These centroids have the smallest mean distance to all the other instances in the cluster and form a centroid collection  $Cen\{C_1, C_2, \dots, C_m\}$ . Our aim is to represent all instances by the centroid collection.

After creating the centroid collection, we add each instance into the clusters by computing the distance to the centroid of the cluster and finding  $Distance_{cen}(Y_i)$ , where  $Distance_{cen}(Y_i) = \min_{C \in Cen} \{Distance(Y_i, C)\}$ . Each instance should belong to the cluster with the shortest distance between the instance and its centroid.

#### Algorithm 1: Instance Collection

**Input:** Instances collection  $D\{Y_1, Y_2, \dots, Y_n\}$ , where  $Y_i = \langle y_1, y_2, \dots, y_l \rangle$   
 Randomly choose  $m$  instances in  $D$  get the collection of centroids  $Cen\{C_1, C_2, \dots, C_m\}$ ;  
 Where  $C_i$  represents the centroid of  $cluster_i\{C_i\}$ ;  
 The number of instances in  $cluster_i$ :  $m_i$ ;  
 The radius of  $cluster_i$ :  $R_i$ ;  
**while**  $D_i \neq \Phi$  **do**  
   **for each instance**  $Y_i \in D$  **do**  
     Find  $Distance_{cen}(Y_i) = \min_{C \in Cen} \{Distance(Y_i, C)\}$ ;  
      $cluster_i = cluster_i \cup Y_i$ ;  
     Compute the mean distance from  $Y_i$  to each instance in  $cluster_i$  represented by  $\bar{R}_i(Y_i)$ ;  
     **if**  $m_i = 1$  **then**  
        $R_i = \bar{R}_i(Y_i)$ ;  
     **else if**  $m_i > 1$  **then**  
       **if**  $R_i > \bar{R}_i(Y_i)$  **then**  
          $C_i = Y_i$ ;  
          $R_i = \bar{R}_i(Y_i)$ ;  
          $Cen = Cen - C_i + Y_i$ ;  
       **else**  
         **continue**;

Then we update the centroid and radius of the cluster. If there is only one instance in the cluster, the new radius is the distance between the two instances. Otherwise, we compute the distance between every two instances in the cluster and make the instance that is the closest mean distance to all other instances in the cluster the new centroid. We do this until all

the instances are added to clusters.

### 3.4 Intrusion-Detection Process

Intrusion detection can be divided into two steps: 1) data collection and processing and 2) instance determination. Each sensor node can count the values of parameters in the feature vector. For each node in  $T$ , we obtain a sample of the feature vector. Over time, each node can collect and process a mass of instance data. This data is processed in three steps:

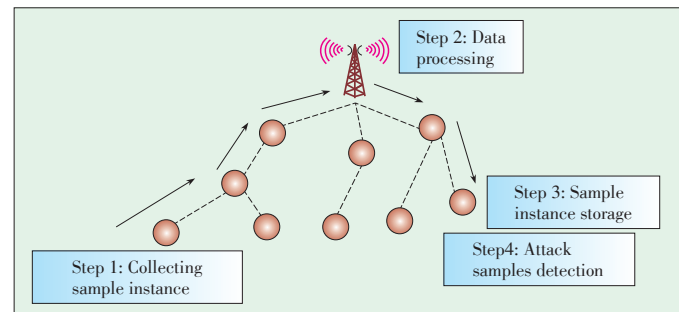
- 1) Data is transmitted to the base station.
- 2) The base station clusters the data according to Algorithm 1.
- 3) The centroid collection is stored in each sensor node.

After audit data is processed and stored, we monitor the related data in each  $T$  and obtain a new observed feature vector. Then, we compute  $Sim(X, D_{cent})$  and  $Dist(X, D_{cent})$ . If  $Dist(X, D_{cent})$  is greater than the radius of the centroid collection,  $X$  is abnormal; otherwise, we compare  $Sim(X, D_{cent})$  with  $r$ . If  $Sim(X, D_{cent}) > r$ , then  $X$  is normal. The system described above is shown in **Fig. 1**.

## 4 Performance Evaluation

### 4.1 Parameter Settings

As shown in **Table 3**, we set 300 nodes randomly distributed over  $500 \times 500 \text{ m}^2$ . These nodes included one base station and one compromised node. The compromised node generated a black hole and affected the nodes near it. The sensor nodes used the Constant Bit Rate (CBR) transport protocol and the



▲ **Figure 1.** The proposed IL-IDS.

▼ **Table 3.** Parameter settings

Simulation Tool	Ns2.32
Number of nodes	300
Transmission range	250 m
Simulation time	200 s
Range	$500 \times 500 \text{ m}^2$
Routing protocol	AODV
Transport protocol	50 CBRs
Maximum speed	40 m/s
AODV: ad hoc on-demand distance vector    CBR: constant bit rate	



An Instance-Learning-Based Intrusion-Detection System for Wireless Sensor Networks

Shuai Fu, Xiaoyan Wang, and Jie Li

Ad hoc On-Demand Distance Vector (AODV) routing protocol. The movement of all nodes except the base station was randomly generated.

4.2 Performance Metrics

In the simulation, we used three metrics to evaluate system performance and the usability of the algorithm in the WSN: 1) similarity of observed instances, 2) number of packets received every interval, and 3) rate of intrusion detection. We defined the similarity between two instances. The smaller the similarity, the more possible it was that an observed instance was as an attack. The number of packets received is the most important characteristic in feature vectors for a black hole attack. The more obviously the number of packets received changes, the greater the possibly a black hole attack is occurring in the WSN. Then we reviewed the rate of the intrusion-detection system during a black hole attack or sinkhole attack.

4.3 Simulation Results

We simulated two kinds of attack against a WSN: black hole and sinkhole.

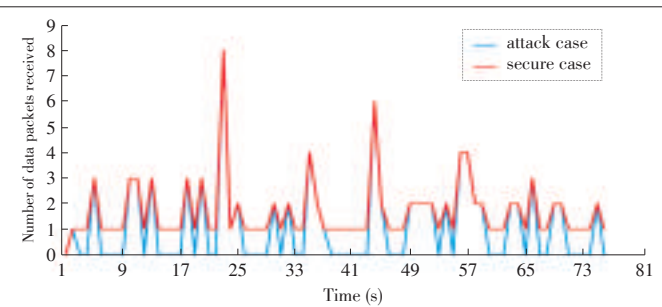
4.3.1 Black Hole Attack

In a selective-forwarding attack, malicious nodes may refuse to forward certain messages and simply drop them (black hole), which means that they are not propagated any further. For example, a malicious node behaves like a black hole and refuses to forward every packet it sees. We instigate a black hole attack in a WSN by making the malicious node drop packets. The impact on the sensor network was not obvious; only the number of packets received by the neighbor of the malicious node was reduced (Fig. 2). Table 4 shows one node's feature vectors for secure and attack scenarios. If there is a black hole node near the observed node, the number of data packets received decreases because the malicious node does not forward any packets and just drops them.

We observe the change of packets received for secure and attack scenarios. When an attack occurs, the number of packets received changes markedly.

4.3.2 Sinkhole Attack

The main purpose of a sinkhole attack is to lure all traffic



▲ Figure 2. Number of packets received for secure and attack scenarios.

from nodes in a region to a compromised node. This is achieved by forging or altering route packet information to make a compromised node look very attractive to the routing algorithm. Neighboring nodes assume that the compromised node is the best path to their destinations. A sinkhole attack can also be a platform for other attacks, e.g., a selective-forwarding attack [6]. Because all the traffic flows through the compromised node, a selective-forwarding attack is more effective and easier to launch.

We simulated a sinkhole attack in the malicious node, which broadcasted high-quality routing packets in order to attract its neighbor. The effect increased when combined with a sink hole based on a black hole.

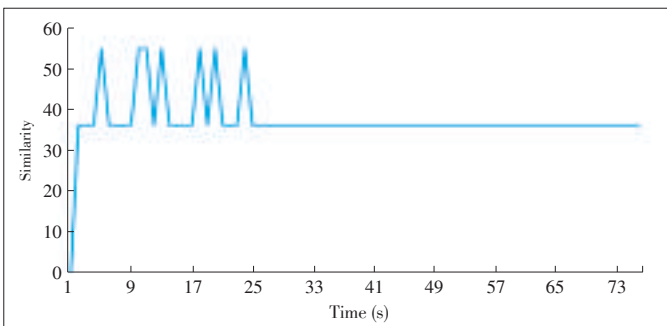
Fig. 3 shows the result of 75 attacking instances under sink hole attack. Fig. 4 shows that similarity for a sink hole is smaller than that for a black hole attack.

5 Conclusion

In this paper, we propose an IL-IDS for WSNs. Because of resource constraints on sensor nodes, the existing intrusion-detection algorithm cannot be directly used in a WSN. Our proposed IL-IDS comprises a feature vector and threshold-selection scheme, a data-reduction method, and a detailed work process of the system. Through simulation, we show that the per-

▼ Table 4. Feature vectors in one node for secure and attack scenarios

	Secure	Attack
Number of data packets received	4	1
Number of route requests received	4	1
Number of route requests sent	0	0
Number of route requests dropped	0	0
Number of data packets dropped	0	0
Number of route requests replies received	0	0
Number of route request replies forwarded	0	0
Number of route request replies sent	1	1
Number of route errors received	0	0
Number of route errors sent	0	0

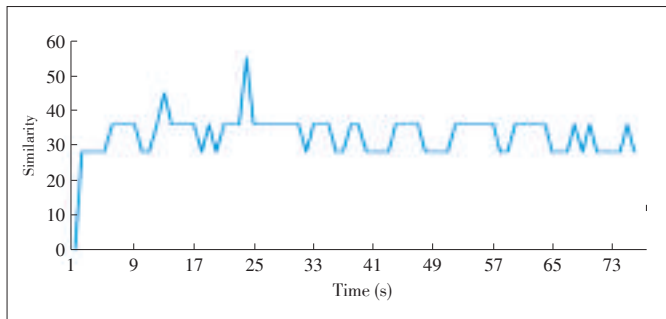


▲ Figure 3. Similarity change for 75 observed attacking instances under black hole.



## An Instance-Learning-Based Intrusion-Detection System for Wireless Sensor Networks

Shuai Fu, Xiaoyan Wang, and Jie Li



▲ Figure 4. Similarity change for 75 attacking instances under sink hole.

formance of our intrusion-detection system for black hole attacks and sinkhole attacks.

## References

- [1] P. Ning and S. Jajodia. Intrusion detection techniques [Online]. Available: <http://discovery.csc.ncsu.edu/Courses/csc774-S03/IDTechniques.pdf>
- [2] C. Karlof and D. Wagner, "Secure routing in wireless sensor networks: attacks and countermeasures," in *Proceedings of the First IEEE International Workshop on Sensor Network Protocols and Applications*, Anchorage, AK, USA, 2003, pp. 113–127. doi: 10.1109/SNPA.2003.1203362.
- [3] T. Lane and C. E. Brodley, "Temporal sequence learning and data reduction for anomaly detection," *ACM Transactions on Information and System Security*, vol. 2, no. 3, pp. 295–331. doi: 10.1145/322510.322526.
- [4] C. E. Loo, M. Y. Ng, C. Leckie, and M. palaniswami, "Intrusion detection for routing attacks in sensor networks," *International Journal of Distributed Sensor Networks*, vol. 2, no. 4, pp. 313–332, 2006.
- [5] K. Ioannis, T. Dimitrou, and F. C. Freiling, "Towards intrusion detection in wireless sensor networks," in *3th European Conference on Wireless Sensor Networks (EWSN'07)*, Delft, the Netherlands, 2007.
- [6] Ian F. Akyildiz, W. Su, Y. Sankarasubramanian, and E. Cayirci, "Wireless sen-

sor networks: A survey," *Computer Networks Elsevier Journal*, vol. 38, no. 4, pp. 393–422, 2002.

Manuscript received: 2015-04-10

## Biographies

**Shuai Fu** (fs0818@gmail.com) received his MS degree in computer science from University of Tsukuba, Japan. He is currently a PhD candidate in the Department of Computer Science, University of Tsukuba. His research interests include security and mobility management in wireless networks.

**Xiaoyan Wang** (wxyability@hotmail.com) received his BE degree from Beihang University, China, in 2004. He received his ME and PhD degrees from the University of Tsukuba, Japan, in 2010 and 2013. He is currently assistant professor in the Information Systems Architecture Science Research Division, National Institute of Informatics, Japan. His research interests include wireless communications and networks, with an emphasis on cognitive radio networks, game theory approaches, and cooperative communications.

**Jie Li** (lijie@cs.tsukuba.ac.jp) received his BE degree in computer science from Zhejiang University, China. He received his ME degree in electronic engineering and communication systems from China Academy of Posts and Telecommunications, Beijing. He received his Dr. Eng. degree from the University of Electro-Communications, Japan. He is currently a professor in the Department of Engineering, Information and Systems, University of Tsukuba, Japan. His research interests include mobile distributed computing and networking, network security, mobile cloud computing, OS, modeling and performance evaluation of information systems. He is a senior member of IEEE and ACM and a member of Information Processing Society of Japan. He has served as a secretary for Study Group on System Evaluation of IPSJ and has been on several editorial boards of IPSJ journals. He has been on the steering committees of the SIG of System EVALuation (EVA) of IPSJ, SIG of DataBase System (DBS) of IPSJ, and SIG of MoBiLe Computing and Ubiquitous Communications of IPSJ. He has co-chaired several international symposiums and workshops. He has also been in the program committees of several international conferences, including IEEE INFOCOM, IEEE ICDCS, IEEE ICC, IEEE GLOBECOM, and IEEE MASS.

## Roundup

## Call for Papers

### ZTE Communications Special Issue on Smart City: Key Technologies and Practices

Though the smart city has been one of the hottest fields due to its great potentials to make our world smarter and more efficient with using digital technologies, it is still necessary to clarify what are fundamental infrastructures and platforms as well as successful practices for truly smart cities. Therefore, the ZTE special issue is focused on key technologies and representative practices in building smart cities. We solicit papers in the topics including but not limited to the following:

- Survey/Review of Smart City Technologies and Applications
- Smart City Infrastructures for Sensing, Networking, IoT, Cloud, etc.
- Smart City Platforms for Programming, Big Data Processing, Services, etc.
- Smart City Practices, Cases Studies and Applications

## Paper Submissions

Prepare your paper with using the template and following the

guideline below.

Template: <http://cis.k.hosei.ac.jp/~jianhua/zte/template.docx>

Guideline: <http://cis.k.hosei.ac.jp/~jianhua/zte/guideline.pdf>

Send your paper via email attachment to the SI's editors

## Important Dates

Paper Submission Due: August 15, 2015

Paper Review Notification: September 10, 2015

Semi-Final Manuscript Submission: September 30, 2015

Final Manuscript Editing and Proofreading: November 15, 2015

Paper Publication and Special Issue Printing: December 15, 2015

## Guest Editors

**Jianhua Ma**, Hosei University, Japan (Email: [jianhua@hosei.ac.jp](mailto:jianhua@hosei.ac.jp))

**Weifeng Lv**, Beihang University, China (Email: [lwf@buaa.edu.cn](mailto:lwf@buaa.edu.cn))

# Forest Fire Detection Using Artificial Neural Network Algorithm Implemented in Wireless Sensor Networks

Yongsheng Liu<sup>1</sup>, Yansong Yang<sup>1</sup>, Chang Liu<sup>1</sup>, and Yu Gu<sup>2</sup>

(1.Network Technology Research Institute, China United Network Communications Corporation Limited, Beijing 100048, China;

2. Department of Computer Science, Hefei University of Technology, Hefei 230009, China)

## Abstract

A forest fire is a severe threat to forest resources and human life. In this paper, we propose a forest-fire detection system that has an artificial neural network algorithm implemented in a wireless sensor network (WSN). The proposed detection system mitigates the threat of forest fires by provide accurate fire alarm with low maintenance cost. The accuracy is increased by the novel multi-criteria detection, referred to as an alarm decision depends on multiple attributes of a forest fire. The multi-criteria detection is implemented by the artificial neural network algorithm. Meanwhile, we have developed a prototype of the proposed system consisting of the solar batter module, the fire detection module and the user interface module.

## Keywords

forest fire detection; artificial neural network; wireless sensor network

## 1 Introduction

Wireless sensor networks (WSNs) have been the focus of research over the past few years because of their potential in environmental monitoring, target tracking, and object detection [1]. WSNs have also been studied in the context of detecting forest fires, which threaten forest resources and human life. WSNs are not costly and can detect forest fires in real time, unlike current detection methods based on human observation and unlike spot weather forecasts or even satellite monitoring. WSNs can also provide information about environmental conditions within the forest, which is useful for predicting forest fires [2]. Moreover, forest fire detection and prediction is associated with specific location information provided by individual sensor nodes.

Although some practical experiments have been conducted using WSNs to collect sensed data from a forest fire [3]–[5], there are still some challenges to using WSNs for this purpose. A fire detector may sound an alarm based on a simple threshold, which gives rise to false alarms even though the sensing unit of the fire detector may be highly sensitive. False alarms occur for two main reasons:

- A photoelectric smoke sensing unit is sensitive to white aerosol particles from a smoldering fire but also to dust [6].
- Environmental conditions in the forest often severely disturb

the normal behavior of the sensing unit. Sunlight and artificial light are primary sources of interference with the flame-sensing unit.

Limited power supply to sensor nodes makes it difficult to detect fires over a long period of time. The potential energy sources for sensor nodes can be classified according to whether they store energy within the sensor nodes (e.g., in a battery), distribute power to the sensor node through a wire, or scavenge available ambient power (e.g. using a solar battery on the sensor node). Considering the volume of the sensor node, manner of deployment, and forest conditions, the solar battery is one of the most promising sources of energy for detecting forest fires over a long period of time. However, existing works on solar batteries for sensor nodes, e.g., [8]–[13], overlook the problem of intermittent sunlight in the forest.

In this paper, we propose a forest fire detection system that includes an artificial neural network algorithm implemented in a WSN. Overall, the main contributions of this paper are as follows:

- The multi-criteria detection depends on multiple attributes of a forest fire and is introduced into WSNs to increase the accuracy of detecting a forest fire.
- An artificial neural network algorithm is used to fuse sensing data that corresponds to multiple attributes of a forest fire into an alarm decision.
- We introduce the principle of the proposed system as well

as a prototype comprising TelosB sensor nodes and a solar battery to power the WSN.

## 2 System Description

For the sake of clarity, we consider a WSN with only one base station and hundreds of sensor nodes. Because a WSN with multiple base stations can be regarded as multiple WSNs (each comprising one base station and corresponding sensor nodes), the proposed system can also be implemented if the WSN has multiple base stations. Therefore, there are  $n$  sensor nodes in the WSN, each denoted  $s_j$ ,  $1 \leq j \leq n$ . A forest fire  $f$  has  $l$  attributes, each denoted  $r_i^f$ ,  $1 \leq i \leq l$ . Attribute  $r_i^f$  can be sensed by the sensing unit  $u_i$ . A  $u_i$  on a  $s_j$  is denoted  $u_i^j$ . The output sensing data of  $u_i^j$  is denoted  $o_i^j$ . For simplicity, we assume that  $s_j$  has  $l$  types of sensing units covering  $l$  attributes of the forest fire. We use a multilayer back-propagation artificial neural network to fuse sensing data  $o_i^j$ . The total number of layers in the artificial neural network is denoted  $m$ . The input vector of the  $k$ th layer,  $1 \leq k \leq m$ , is denoted  $A^{k-1}$ . The output vector of the  $k$ th layer is denoted  $A^k$ . Therefore,  $A^0$  and  $A^m$  represent the input and output of the artificial neural network, respectively. The alarm decision is denoted  $ad$ .

## 3 Proposed Forest Fire Detection Method

In our proposed system, detection is made more accurate by using multiple criteria, which means the  $ad$  is based on multiple criteria of the forest fire. Multi-criteria detection is implemented by the artificial neural network algorithm. Because of the artificial neural network, the proposed system has low overhead and has self-learning capabilities; that is, it trains itself to build up the relations between sensing data and correct  $ad$ .

### 3.1 Multi-Criteria Detection

In a system that depends on one attribute of a forest fire to raise alarms, there is a high probability of false alarms because of inherent system drawbacks or external disturbances. To overcome such drawbacks and counter external disturbances, the system must take into account the multiple attributes of a forest fire. This is referred to as multi-criteria detection (Definition 1). With multi-criteria detection, multiple attributes of a forest fire are sensed by different types of sensing unit. Therefore, a sensing unit that has been interfered with cannot raise a false alarm. Together, multiple sensing units confirm an alarm. Multi-criteria detection increases the accuracy of detecting a forest fire.

**Definition 1 (Multi-criteria detection).** Multi-criteria detection is represented as a function with multiple arguments  $r_1^f, r_2^f, \dots, r_l^f$ , which refer to the attributes of forest fire  $f$ , and one  $ad$ , given by:

$$ad = f(r_1^f, r_2^f, \dots, r_l^f) \quad (1)$$

The attributes  $r_1^f, r_2^f, \dots, r_l^f$  could be any combination of the attributes of a forest fire. The directly sensed attributes of a forest fire are flame and heat, which are sensed by the flame sensing unit and heat sensing unit. The flame emits visible light, but the forest fire also emits a lot of radiation, the spectral distribution of which is the radiation intensity with respect to different wavelengths and is not uniform. In theory, the radiation intensity is determined by the temperature of the fire. The radiation intensity from a blackbody with respect to the wavelength and temperature is described by Planck's radiation law (2), where  $h$  is Planck's constant,  $c$  is the speed of light,  $\lambda$  is the wavelength,  $k$  is Boltzmann's constant, and  $T$  is the temperature [14].

$$I = \frac{2hc^2}{\lambda^5 (\exp[hc/\lambda kT] - 1)} \quad (2)$$

Therefore, radiation intensity can be the basis for detecting a forest fire given that the typical temperature of a forest fire is  $600^\circ\text{C} - 1000^\circ\text{C}$  [15]. The ultraviolet sensing unit and infrared flame sensing unit work by detecting radiation intensity. Other attributes that can be used to identify a forest fire include combustion products. It is well known that a forest fire gives off bursts of carbon dioxide, carbon monoxide, water vapor, and dust.

### 3.2 Artificial Neural Network Algorithm

We use the multi-layer back-propagation artificial neural network for multi-criteria detection. Although data fusion in WSNs has been covered in much of the literature [16]–[18], the topic has not been considered in the context of forest fires. A multi-layer back-propagation artificial neural network is widely used to emulate the non-linear relationship between its input and output. However, computation in this kind of network is not complex because the network is a combination of neurons dealing with simple functions. Moreover, multi-layer back-propagation artificial neural network is capable of self-learning, which means it can train itself to build up relations between the inputs and desired targets.

#### 3.2.1 Making an Alarm Decision

Without loss of generality, we assume that the multi-layer back-propagation artificial neural network is implemented on  $s_j$  with  $l$  types of sensing units that cover  $l$  attributes of the forest fire. Sensing data  $o_i^j$  of  $u_i^j$  on  $s_j$  corresponds to  $r_i^f$  of the forest fire.

$$A^0 = [a_1^0, \dots, a_l^0]^T \quad (3)$$

For clarity, let all  $o_i^j$ ,  $1 \leq i \leq l$  comprise a column vector  $A^0$  (3), where  $a_i^0 = o_i^j$ . Vector  $A^0$  is the input to the multiple layer artificial neural network.

## Forest Fire Detection Using Artificial Neural Network Algorithm Implemented in Wireless Sensor Networks

Yongsheng Liu, Yansong Yang, Chang Liu, and Yu Gu

Specifically,  $A^0$  is the input to the first layer of the multi-layer artificial neural network. In the first layer,  $A^0$  is multiplied by weight matrix  $W^1$  with dimension  $s^1 \times l$  and bias vector  $B^1$ , including  $s^1$  neurons in the first layer. The intermediate computation result of the first layer is denoted  $N^1$  and is given by:

$$N^1 = W^1 A^0 + B^1 \quad (4)$$

Then,  $N^1$  is sent to transfer function  $F^1$ , which may be a linear or nonlinear. That is,  $F^1$  may be a hard-limit function or sigmoid function depending on the specific problem it needs to solve. In general, transfer functions in the multi-layer artificial neural network are easy to compute. Transfer function  $F^1$  operates on every element of  $N^1$ . The result of transfer function  $F^1$ , denoted  $A^1$ , is the output of the first layer:

$$A^1 = F^1(N^1) = \begin{bmatrix} F^1(n_1^1) \\ \vdots \\ F^1(n_s^1) \end{bmatrix} \quad (5)$$

The fusion of sensing data proceeds in the second layer of the multi-layer artificial neural network. The output  $A^1$  of the first layer becomes the input of the second layer. The calculation process of the second layer is similar to that of the first layer except the second layer has its own  $W^2$ ,  $B^2$ , and  $F^2$ . In general, the calculation of the  $i$ th layer is given by:

$$A^i = F^i(W^i A^{i-1} + B^i), \quad 1 \leq i \leq m-1 \quad (6)$$

where  $m$  is the number of layers in the artificial network.

For a decision to be made on whether there is a forest fire or not, the output of the  $m$ th layer,  $A^m$  (7), is confined to one element.

$$ad = A^m = F^m(W^m A^{m-1} + B^m) \quad (7)$$

This is done by letting the  $m$ th layer contain only one neuron. If the alarm decision is confined to a Boolean value, we need to choose the transfer function, the output of which is a Boolean value, for the  $m$ th layer, such as the hard limit function.

An alarm decision is made by inputting the attributes of a forest fire into the multi-layer back-propagation artificial neural network, as shown in Theorem 1.

Theorem 1. The  $ad$  of the multi-criteria detection is computed by the recursive (8) given sensing data  $A^0 = [a_1^0, \dots, a_l^0]^T$  corresponding to  $l$  attributes of forest fire  $f$ .

$$\begin{cases} ad = F^m(W^m A^{m-1} + B^m) \\ A^i = F^i(W^i A^{i-1} + B^i), \quad 1 \leq i \leq m-1 \end{cases} \quad (8)$$

### 3.2.2 Self-Learning Capability

Given sensing data that corresponds to multiple attributes of a forest fire and given correct alarm decisions, the multi-layer back-propagation artificial neural network trains itself to build

relationships between the sensing data and correct alarm decisions. However complex the relationship, it is easy for the multi-layer back-propagation artificial neural network to fulfil the task.

Essentially, self-learning means having the output of the multi-layer back-propagation artificial neural network approximate the target output by adjusting the weight matrixes and biases. This adjustment is made in order to minimize the mean-square error (MSE) between the output and target output. Suppose  $q$  inputs are denoted  $A_i^0$ ,  $1 \leq i \leq q$ . Corresponding to  $A_i^0$ , the output is denoted  $A_i^m$ , and the target output is denoted  $T_i^m$ . Thus, the MSE for the  $i$ th iterated adjustment is:

$$MSE(i) = E[(T_i^m - A_i^m)^T (T_i^m - A_i^m)] \quad (9)$$

For clarity, the adjustment of the weight matrixes and biases is expressed by Theorem 2.

Theorem 2. In the self-learning, the  $i$ th iterated adjustment of the weight matrixes and biases is conducted according to (10) and (11), where  $\alpha$  is a constant for the learning rate, and  $\phi(j)$  is computed by the recursive (12) where  $D(j) = \text{diag}[(F^j)'(n_1^j), \dots, (F^j)'(n_s^j)]$ .

$$W^j(i) = W^j(i-1) - \alpha \phi(j)(A^{j-1})^T, \quad 1 \leq j \leq m \quad (10)$$

$$B^j(i) = B^j(i-1) - \alpha \phi(j), \quad 1 \leq j \leq m \quad (11)$$

$$\begin{cases} \phi(j) = D(j)(W^{j+1})^T \phi(j+1), \quad 1 \leq j \leq m-1 \\ \phi(m) = -2D(m)(T_i^m - A_i^m) \end{cases} \quad (12)$$

After self-learning, the multi-layer back-propagation artificial neural network builds up a mathematical relationship between the sensing data and correct alarm decisions. Then, the artificial neural network can make an accurate alarm decision.

## 4 Implemented Prototype

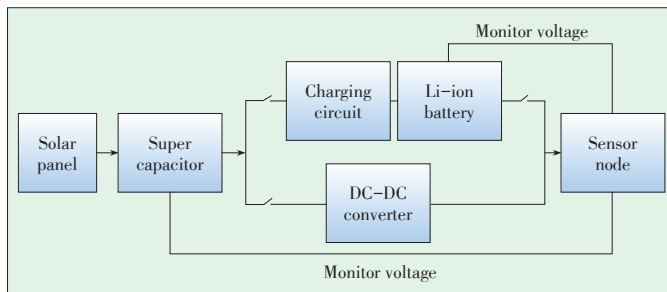
We have developed a prototype of the forest fire detection system using an artificial neural network in a WSN. The system mainly comprises three parts: the solar battery, fire-detection module, and user interface.

### 4.1 Solar Battery

To consistently power the unattended sensor nodes deployed in a forest where only intermittent sunlight is available, we develop a solar battery (Fig. 1). The energy from the solar panel is buffered by the super capacitor. When the energy in the super capacitor reaches a threshold, the super capacitor starts to recharge the Li-ion battery. Because of the intermittent sunlight in the forest, the energy produced by the solar panel is not enough to recharge the battery. If not buffered in the super capacitor, this energy is wasted. On the other hand, the charge-discharge cycles of the Li-ion battery are limited. It is better to

## Forest Fire Detection Using Artificial Neural Network Algorithm Implemented in Wireless Sensor Networks

Yongsheng Liu, Yansong Yang, Chang Liu, and Yu Gu



▲ Figure 1. The solar battery architecture.

charge a Li-ion battery until it is full; otherwise, the life of the battery decreases. On the contrary, the super capacitor has almost infinite charge-discharge cycles and is ideal for frequently pulsing applications.

Here we discuss implementation of the solar battery in detail. The solar panel of the battery is  $110 \times 95$  mm and comprises eight cells connected in parallel and generating 550 mA at 2 V. Theoretically, the maximum energy generated in one hour can sustain a sensor node for 26 days, i.e., 1100 mAh/ ( $0.53 \text{ mA} \times 3.3 \text{ V} \times 24 \text{ h}$ ), provided that the sensor nodes work on a 10% duty cycle with an average current of 0.53 mA. Energy from the solar panel is buffered by two 150 F 2.5 V super capacitors wired in parallel. A 3.7 V 700 mAh Li-ion battery is used to continually save energy. The fully charged Li-ion battery can power a sensor node working on a 10% duty cycle for 55 days, i.e.,  $700 \text{ mAh}/(0.53 \text{ mA} \times 24 \text{ h})$ . We chose MAX1674 and ISL6292 integrated circuits as the DC-DC converters, which have a conversion efficiency of around 90%.

#### 4.2 Fire Detection Module

The fire detection module is responsible for multi-criteria detection. The module comprises five TelosB sensor nodes, four of which monitor the forest fire. That is, they convert the attributes of a forest fire into sensing data. The multi-layer back-propagation artificial neural network is implemented on each individual sensor node because the sensor node is endowed with four types of sensing units. However, for the purpose of analysis, raw sensing data besides the fire alarm are transmitted to users. The last sensor node acts as the base station, collecting sensing data and the fire alarm from the other four sensor nodes. For simplicity, four sensor nodes communicate with the base station directly in one-hop communication. Each TelosB sensor node has a 16 bit 8 MHz microcontroller, an RF transceiver compliant with IEEE 802.15.4, and four sensing units. These sensing units sense temperature ( $-40^\circ\text{C} - 123.8^\circ\text{C}$ ), relative humidity (RH), infrared light (320 nm–1100

nm), and visible light (320 nm–730 nm). Hence, each sensor node can monitor the four attributes of a forest fire.

The architecture of the artificial neural network is shown in Fig. 2.

The back-propagation artificial neural network in the fire detection module is a two-layer network. There are four neurons in the first layer, because of the four sensing units in a TelosB sensor node, and one neuron in the second layer. The transfer function for the first layer is log-sigmoid function ( $f1$  in Fig. 2) and is given by:

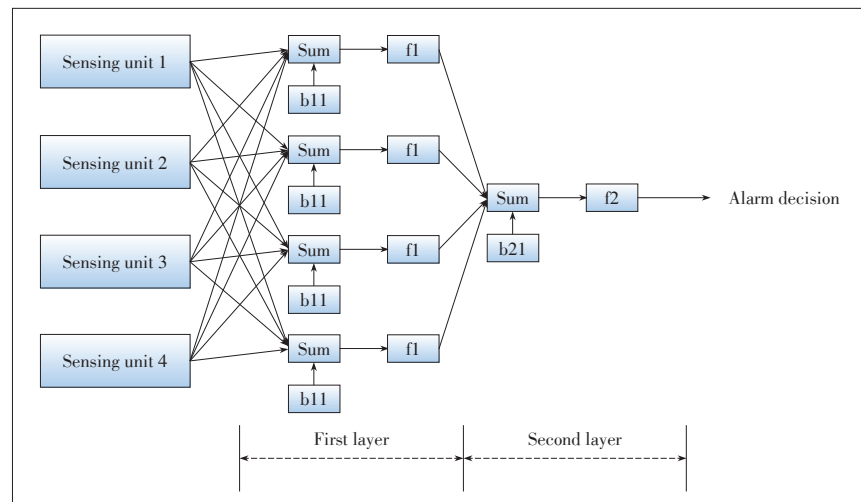
$$f(x) = 1/(1 + e^{-x}) \quad (13)$$

The transfer function for the second layer is a linear function ( $f2$  in Fig. 2) and is given by:

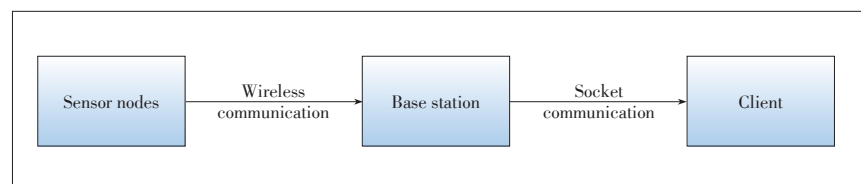
$$f(x) = x \quad (14)$$

#### 4.3 User Interface Module

The user interface module is responsible for displaying the raw sensing data to the user. First, the sensing data and fire alarm are transmitted from the base station to the user. The data flow is shown in Fig. 3. Sensing data from sensor nodes are transmitted to the base station by wireless communication. The base station is a gateway between WSNs and the Internet and forwards the sensing data to a user client. The medium between the base station and user client is the Internet. Therefore, the user may be located far away from the fire-detection system. Socket communication is facilitated by Java. Next, the



▲ Figure 2. The back propagation artificial neural network.



▲ Figure 3. Data flow.



## Forest Fire Detection Using Artificial Neural Network Algorithm Implemented in Wireless Sensor Networks

Yongsheng Liu, Yansong Yang, Chang Liu, and Yu Gu

user interface module displays the sensing data to the user. The graphical interface draws curves for each typed of sensing data over time. The graphical interface is refreshes according to the arrival of new sensing data. Therefore, the curves of the graphical interface are synchronous with the sensing units on sensor nodes. Each type of sensing data is displayed by a tab in the graphical interface.

## 5 Conclusion

A forest fire can threaten forest resources and human life. This threat can be mitigated by timely and accurate alarms. WSNs are widely used for environmental monitoring; therefore, we use a WSN for forest fire detection. To increase the accuracy of the detection system, we propose multi-criteria detection for forest fires. In this paper, multi-criteria detection is implemented by the artificial neural network algorithm. To power the sensor nodes in the forest where only intermittent sunlight is available, we develop a solar battery module. We developed a prototype of the proposed system comprising solar battery module, fire detection module, and user interface module.

## References

- [1] I. Akyildiz, W. Su, Y. Sankarasubramanian, and E. Cayirci, "A survey on sensor networks," *IEEE Communications Magazine*, vol. 40, no. 8, pp. 102–114, 2002.
- [2] B. Son, Y. Her, and J. Kim, "A design and implementation of forest-fire surveillance system based on wireless sensor network for south korea mountains," *International Journal of Computer Science and Network Security*, vol. 6, no. 9, pp. 124–130, 2006.
- [3] D. Doolin and N. Sitar, "Wireless sensors for wildfire monitoring," in *Proceedings of SPIE*, vol. 5765, no. 2, 2005, pp. 477–484.
- [4] C. Hartung, R. Han, C. Seielstad, and S. Holbrook, "Firewxnet: A multitiered portable wireless system for monitoring weather conditions in wildland fire environments," in *Proceedings of the 4th international conference on Mobile systems, applications and services*, Uppsala, Sweden, 2006.
- [5] M. Hefeeda and M. Bagheri, "Wireless sensor networks for early detection of forest fires," in *MASS '07*, Pisa, Italy, 2007, pp. 1–6.
- [6] G. Pfister, "Multisensor/multicriteria fire detection: a new trend rapidly becomes state of the art," *Fire Technology*, vol. 33, pp. 115–139, 1997.
- [7] S. Roundy, M. Strasser, and P. Wright, *Powering ambient intelligent network*, Germany: Springer, 2005, pp. 271–299.
- [8] M. Minami, T. Morito, and H. Morikawa, "Solar biscuit: A batteryless wireless sensor network system for environmental monitoring applications," in *the 2nd international Workshop on Networked Sensing Systems*, San Diego, USA, 2005.
- [9] P. Dutta, J. Hui, and J. Jeong, "Trio: enabling sustainable and scalable outdoor wireless sensor network deployments," in *Information Processing in Sensor Networks*, Nashville, TN, USA, April 19–21, 2006, pp. 407–415.
- [10] V. Raghunathan, A. Kansal, J. Hsu, J. Friedman, and M. Srivastava, "Design considerations for solar energy harvesting wireless embedded systems," in *Information Processing in Sensor Networks*, UCLA, Los Angeles, USA, April 25–27, 2005.
- [11] X. Jiang, J. Polastre, and D. Culler, "Perpetual environmentally powered sensor networks," in *Information Processing in Sensor Networks*, UCLA, Los Angeles, USA, April 25–27, 2005.
- [12] P. Corke, P. Valencia, P. Sikka, T. Wark, and L. Overs, "Long-duration solar-powered wireless sensor networks," in *Proceedings of the 4th Workshop on Embedded Networked Sensors*, Cork, Ireland, June 25–26, 2007, pp. 33–37. doi: DOI: 10.1145/1278972.1278980.
- [13] J. Taneja, J. Jeong, and D. Culler, "Design, modeling, and capacity planning for micro-solar power sensor networks," in *Information Processing in Sensor Networks*, St. Louis, USA, April 22–24, 2008, pp. 407–418.
- [14] S. S. Gyltner and K. Stetter, "A fire detection system and method for early detection of fire," *International Publication Number WO 2009/080581 A1*, World Intellectual Property Organization, 2009.
- [15] E. Valendik and I. Kosov, "Effect of thermal radiation of forest fire on the environment," *Contemporary problems of Ecology*, vol. 1, no. 4, pp. 399–433, 2008. doi: 10.1134/S1995425508040012.
- [16] G. Xing, R. Tan, B. Liu, J. Wang, X. Jia, and C.-W. Yi, "Data fusion improves the coverage of wireless sensor networks," in *Proceedings of the 15th annual international conference on Mobile computing and networking*, Beijing, China, 2009, pp. 157–168.
- [17] L. Freitas, A. Coimbra, V. Sacramento, S. Rosseto, and F. Costa, "Sol: a data fusion protocol in wireless sensor networks for controlled environment," in *IEEE INFOCOM Workshops*, Rio de Janeiro, Brazil, 2009, pp. 1–2. doi: 10.1109/INFCOMW.2009.5072191.
- [18] H. Luo, H. Tao, H. Ma, and S. Das, "Data fusion with desired reliability in wireless sensor networks," *IEEE Transactions on Parallel and Distributed Systems*, vol. 22, no. 3, pp. 501–513, 2011. doi: 10.1109/TPDS.2010.93.

Manuscript received: 2015-04-22

## Biographies

**Yongsheng Liu** (liuys170@chinaunicom.cn) is an engineer at the Network Technology Research Institute, China Unicom. His research interests include network security, wireless sensor networks, and IP and bearer technology. He is also a member of China Communications Standards Association (CCSA) and has proposed some drafts related to Multiprotocol Label Switching (MPLS) and Internet service quality.

**Yansong Yang** (yangys30@chinaunicom.cn) is head of the IP and Bearer Technology Division at the Network Technology Research Institute of China Unicom. He has been engaged design and consultation for the IP network for many years.

**Chang Liu** (liuc131@chinaunicom.cn) works at the Network Technology Research Institute of China Unicom. His current research interests are network modeling and IP and bearer technology.

**Yu Gu** (yugu.bruce@gmail.com) received the BEng and PhD degrees from the University of Science and Technology of China in 2004 and 2010. From February 2006 to August 2006, he interned at the Wireless Network Group, Microsoft Research Asia, Beijing. From 2007 to 2008, he was a visiting scholar in the Department of Computer Science, University of Tsukuba, Japan. From 2010 to 2012, he was a JSPS Research Fellow in the National Institute of Informatics, Japan. He is now a professor in the School of Computer and Information, Hefei University of Technology, China. His research interests include information science, pervasive computing, and wireless networking, especially wireless sensor network.



# WeWatch: An Application for Watching Video Across Two Mobile Devices

Fuji Ren<sup>1</sup>, Mengni Chen<sup>2</sup>, and Yu Gu<sup>2</sup>

(1. Department of Information Science & Intelligent Systems, University of Tokushima, Tokushima 770-8501, Japan;

2. School of Computing and Information, Hefei University of Technology, Hefei 230009, China)

## Abstract

In recent years, high-resolution video has developed rapidly and widescreen smart devices have become popular. We present an Android application called WeWatch that enables high-resolution video to be shared across two mobile devices when they are close to each other. This concept has its inspiration in machine-to-machine connections in the Internet of Things (IoT). We ensure that the two parts of the video are the same size over both screens and are synchronous. Further, a user can play, pause, or stop the video by moving one device a certain distance from the other. We decide on appropriate distances through experimentation. We implemented WeWatch on Android operating system and then optimize Watch so battery consumption is reduced. The user experience provided by WeWatch was evaluated by students through a questionnaire, and the reviews indicated that WeWatch does improve the viewing experience.

## Keywords

together watching experience; screen adaptation; internet of things; distance estimation; energy efficiency

## 1 Introduction

With the rapid development of the mobile industry and growth in the number of high-resolution videos, screen size has become an important factor in product design. Widescreen mobile devices have become more and more popular, but this has led to many problems; for example, a large screen makes one-handed operation more difficult [1]. Nowadays, researchers are trying to improve the viewing experience on smart phones and tablets. The following example highlights the goals we are trying to achieve:

Henry has an old smart phone with a small, low-resolution screen, so he buys a smart phone with a bigger screen. He is watching a movie when:

- He puts the old phone and new phone side by side to get a bigger screen, and the movie plays across the two screens. In this way, he can enjoy the movie on a larger overall screen.

- Someone knocks at the door. He moves one phone away from the other and the video pauses. When he comes back, he only needs to put the two phones together again to pick up where the movie left off.

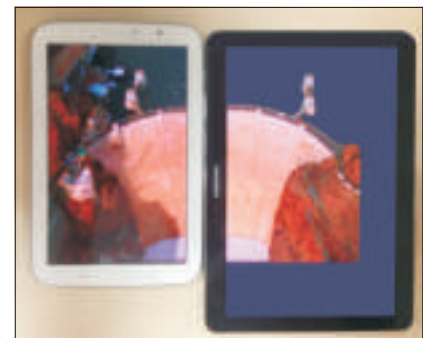
In this paper we propose WeWatch, an application for viewing videos across two devices with different screen sizes and resolutions (**Fig. 1**).

WeWatch provides a better viewing experience than a video player on a single device. It encourages people to use idle devices and share videos. WeWatch has two unique features: screen size adaptation and the use of distance to control video playback.

Previous studies on video adaptation mainly focus on optimally matching the resources and capabilities of diverse client

This work was supported by the National Natural Science Funds of China under Grant No. 61300034, the National High-Tech Research & Development Program of China ("863" Program) under Grant No.2012AA011103, the Key Science and Technology Program of Anhui Province under Grant No.1206c0805039, and a start-up fund for Huangshan Mountain Scholars (Outstanding Young Talents Program of Hefei University of Technology) under Grant No. 405-037070.

Figure 1. Demonstration of WeWatch.



## WeWatch: An Application for Watching Video Across Two Mobile Devices

Fuji Ren, Mengni Chen, and Yu Gu

devices [2]. However, in order to aggregate resources, these client devices need collaboration and synchronization. This is difficult because different devices have different screen sizes and resolutions, and it is also difficult to transform resources so that they match different devices. To solve this problem, we propose an adaptation algorithm that only matches two devices instead of matching both resources and devices. Our adaptation algorithm can match the size of video windows on both devices so that the video only needs be divided into two parts of the same size. When WeWatch is launched on one device, the device transmits its screen size and resolution to the other device, which automatically adjusts itself.

We have devised a special way of using our application: changing the distance between devices. With WeWatch, a video can be paused, played or stopped by moving the devices certain distances from each other. The received signal strength indicator (RSSI) of Wi-Fi is used to measure these distances [3]. Wi-Fi signals are usually used for location-based services [4], [5] but are rarely used for managing applications.

A demo of WeWatch is available online [6]. WeWatch works on two smart devices running Android [7], [8]. We choose this platform because it is popular and open-source.

We have also tested the power consumption of WeWatch and found that it consumes about 40% less power than a normal video player, both in single-screen mode and dual-screen mode. Different parameters have obvious effects on battery consumption. To find the empirical Wi-Fi RSSI values of distances, we determine the relationship between them through real-life simulations. The results help us improve the implementation of the application.

The contributions of this paper are:

- It describes one of the first attempts to combine screens for a better viewing experience. Our scheme does not require any special hardware; it can be implemented on existing mobile devices.
- It describes a new adaptation algorithm that swiftly matches the screen size and resolution of different mobile devices.
- It describes a positioning method, which is used for determining suitable distances for playback control, and a synchronization method for smoother viewing experience.
- It describes a prototype of the screen-sharing system that has been evaluated for energy efficiency and user experience.

## 2 Related Work

The Internet of Things (IoT) comprises interconnected, uniquely identifiable computing devices embedded within the existing Internet infrastructure. Communication will expand to human-to-thing and thing-to-thing communication. Combining devices is a basic concept in the IoT. Much attention has been paid to the IoT in recent years [9]–[11]; however, IoT applications are largely limited to intellectual storage management,

public security, and automation [12], [13]. Not enough attention has been paid to using this new technology in daily life. WeWatch draws on the idea of the IoT to combine two mobile devices and give people a better viewing experience.

The IoT includes RFID technology, sensor network, detection technology, intelligence technology, and nanotechnology [14], [15]. Machine-to-machine connections are an important part of the IoT, and WeWatch combines two smart devices using Wi-Fi ad hoc technology [16], [17].

There are many existing systems and toolkits that enhance user experience on mobile devices [18], [19]. However, most of these are mainly designed for one-way connections, i.e., resources connecting to devices. WeWatch provides a higher level of communication by grouping entities together, i.e., devices connecting to other devices. WeWatch can be used directly between portable devices and does not require Internet access.

Some toolkits are used to develop collaborative mobile applications [20], collaborative and synchronous video annotation platforms [21], and even impromptu assemblies of a logical computer from the best set of wireless components available nearby [22]. We have the same starting point, i.e., to provide convenience through collaborative devices.

A proximeter [23] enables mobile proximity-based content sharing on portable devices. This sharing occurs when consumers of content move within the proximity of the owner of the content. A proximeter also creates opportunities for users to chat with their neighbors through their phones. The proximeter prototype is based on Meamo v4.0, which is an operating system in its infancy. Meamo is only supported by Nokia, and there is a lack of applications for the operating system.

Shu Liu and Yingxin Jiang [24] focused on face-to-face proximity estimation using smartphones and Bluetooth. They explored the relationship between Bluetooth RSSI and distances through a series of experiments. They compared the accuracy of Bluetooth, Wi-Fi and GPS using real-world measurements. However, it is impractical to use Bluetooth to measure the distance between devices.

MobiUS [25] has developed a video application for displaying a high-resolution video across two mobile devices. The application is based on an efficient, collaborative half-frame decoding scheme. Because the collaborative system architecture is tightly coupled, the application only works on devices with the same screen size and resolution.

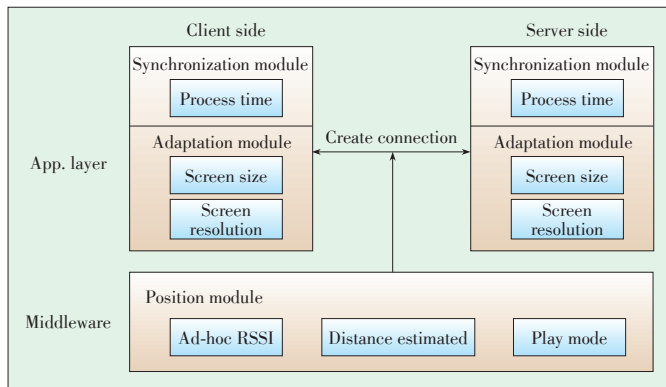
Content adaptation for mobile devices is usually directed towards online multimedia [26] or pictures [27]. With content adaptation, content of different sizes and resolutions can be adapted to different screens. However, researchers have rarely considered the implications of combining screens.

## 3 System Design

We develop WeWatch from both the client side and server side. Our application can decide the role of each device automatically when launched. **Fig. 2** shows the WeWatch architec-

## WeWatch: An Application for Watching Video Across Two Mobile Devices

Fuji Ren, Mengni Chen, and Yu Gu



▲ Figure 2. WeWatch architecture.

ture.

The client and server are linked by Wi-Fi ad hoc networking technologies, which enable direct device-to-device communication. This helps reduce the traffic load in the wireless infrastructure and improve user experience. The role of devices can be easily decided because the hotspot and Wi-Fi cannot be turned on at the same time [28], [29]. Some researchers have examined the trade-off associated with using Wi-Fi ad hoc and infrastructure modes. Their experiments show that mobile devices are stable when communicating directly with each other [30]. With our WeWatch, a user can choose a device to be a hotspot, with other connecting to that hotspot. We separate the ad-hoc function from our application so that a user can exploit it to make new functions.

The client and server sides can send requests to share videos, and these requests are executed after being authenticated by the valid distance from empirical RSSI values.

WeWatch comprises three modules: positioning, adaptation, and synchronization. The positioning module at the client side records the RSSI values and uses these to estimate the distances. Then, it changes the video mode and notices other modules. The adaptation module sends the screen size and resolution between the two devices so that the display across the two screens is the same size. The synchronization module ensures both screens are playing the same video frames at the same time.

### 3.1 Positioning Method

The positioning method used in WeWatch frees our hands from having to click buttons. Specific functions are initiated by dragging one device away from the other, changing the distance between them. Different distances are estimated according to RSSI values. For example, the video is played when the distance between devices is within 10 cm, the video and the video is paused when the distance is more than 10 cm. To quit dual-viewing mode, one of the devices device has to be moved more than 30 cm away. All these operations are reversible.

Device-to-device Wi-Fi ad hoc communication enables the client side to be directly connected to the server side. The cli-

ent side records the signal values sent from the server side. These values are reliable enough to estimate the distance between them. Wi-Fi triangulation is not accurate enough to detect exact position within a very close range [31]; however, we can use it to detect approximate position within a range, e.g., within 10 cm, 10 cm–30 cm, and over 30 cm. These ranges are enough for distinguishing our functions in a video player.

### 3.2 Adaptation Algorithm

Most studies on phone screen interaction are focused on particular equipment—there are no comparative studies of mobile devices with different screen sizes. Screen sizes and resolution are not necessarily related. Some devices have a small, high-resolution screen. For example, the HTC DNA smartphone has a 5-inch,  $1920 \times 1080$  pixel screen, which is higher than some computers. The high resolution in a small screen means it has more pixel dots per inch (dpi). Therefore, we need to analyze them.

To provide a good viewing experience over two screens, we design a novel sharing algorithm that involves two groups of parameters: one from the target screen and the other from the current screen. With Android, the real screen size cannot be read directly and must be calculated using the pixel and dpi values of screen. To facilitate adaptation, the pixels and dpi of the target screen's width and height are sent to the current device. Current device use these received data and corresponding parameters of itself to finish adaptation.

Because the dpi of the width and height are different, they need to be calculated separately.  $W_{ratio}$  is the ratio of the dpi of the width of the target screen  $T$  to that of the current screen  $C$ :

$$W_{ratio} = T_{wdpi} / C_{wdpi} \quad (1)$$

$H_{ratio}$  is the ratio of the dpi of the height of the target screen to that of the current screen:

$$H_{ratio} = T_{hdpi} / C_{hdpi} \quad (2)$$

The width and height pixels shown of the current screen are estimated according to the ratios in (1) and (2), respectively, and pixels from the target screen. The adaptation models are:

$$C_{width} = W_{ratio} \times T_{width} \quad (3)$$

$$C_{height} = W_{ratio} \times T_{height} \quad (4)$$

where  $C_{width}$  is the width of the current screen, and  $C_{height}$  is the height of the current screen. The window of the video player is modified according to these new pixel values. In this way, the two parts of a video are the same size.

### 3.3 Synchronization Method

We synchronize the two devices by immediately sharing the current time of the video between the devices. In this way, the video frames are accurately coordinated across the two

## WeWatch: An Application for Watching Video Across Two Mobile Devices

Fuji Ren, Mengni Chen, and Yu Gu

screens. The current time of the video is sent from one device to the other, which adjusts itself to the same time. Although the data is transmitted very quickly, the timing of the video is slightly asynchronous, and delay in the video may be obvious. WeWatch pauses the video at both sides until the time is synchronized.

Synchronization is controlled by signals from the positioning module. We synchronize according to the three distance ranges mentioned in subsection 3.1. There are three video modes: combined, pause, and full screen. When the devices are within 10 cm of each other, each device plays half the frame of the video, and data is transmitted. When the devices are 10 cm–30 cm from each other, the video is paused and data is not transmitted, but the video is still split between the two screens. When the devices are more than 30 cm from each other, the video is shown in full-screen mode on both devices, and the two devices are disconnected from each other.

## 4 Performance Evaluation

We ran WeWatch on two tablets: Samsung GT-N5110 and Samsung SM-P601. The former had Android 4.1 and an 8-inch  $1280 \times 800$  pixel WXGA screen. The latter had Android 4.3 and a 10.1-inch  $2560 \times 1600$  pixel screen.

We had three primary expectations: real-time synchronous playback, screen size adaptation, and video controlled by distance. Because WeWatch need to open Wi-Fi and the screen should be light all the time, we need to consider the energy efficiency in the real world.

### 4.1 RSSI vs. Distance

Most works on Wi-Fi ranging through RSSI focuses on routing issues and are based on simulations [32]. The performance of peer-to-peer communication using real-world settings has not been adequately studied. Therefore, we measure the relationship between RSSI values and distances through experimentation.

We run our experiments on an office desk, a common place where people watch videos. **Fig. 3** shows Wi-Fi RSSI for distances 0 cm–30 cm. We calculate the average RSSI from 300 values for each distance. Overall, the RSSI decreases as distance increases. The RSSI does not conform exactly to the theoretical values we had predicted, which decrease smoothly. There is an anomalous increase in the mean RSSI over 5 cm–10 cm. This anomaly occurs again over 25 cm–30 cm. This may be because the Wi-Fi signals are disturbed or shielded in such a closed environment. From our experiments, we find that 10 cm and 30 cm are two critical distances, and it is appropriate to use their RSSIs to divide distance. In this way, the video player can be controlled by distance.

### 4.2 Power Comparison

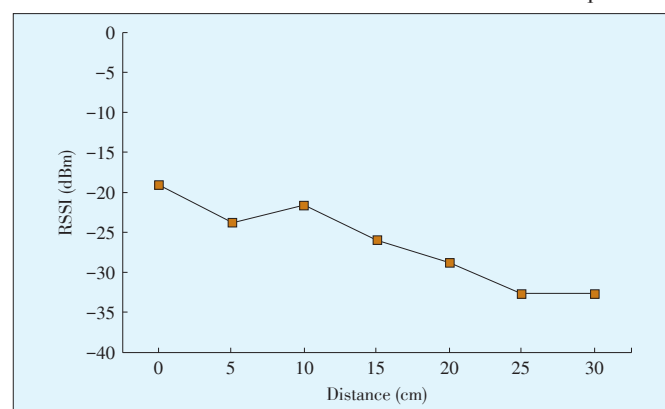
In mobile devices, battery power is very limited, and this is

an important consideration when developing mobile applications. Before we determine how often the Wi-Fi signals should be collected, we compare the normal play function in WeWatch with that of the tablet's own video player. When no data is being transmitted in WeWatch, the player lasts more than three hours longer than the Samsung player (**Fig. 4a**). A possible reason for this is that WeWatch only has common functions, and we do not open any extra background programs. Then we evaluate the video-sharing function. A data connection consumes a lot of power, so the device last two hours less than before. We change the frequency of signal collection from 200 ms to 1 s and measure power consumption with an application that logs the battery level. Then, we analyze the data on a computer (**Fig. 4b**). Each time, we close the other applications on the same tablet, run the application, and record the battery level every hour.

The energy consumption using each method is clear in our experiments. The tablet's own video player consumes the most power. WeWatch consumes less power than the tablet's own video player when the WeWatch update interval is 200 ms. When this interval is changed to 1 s, WeWatch can last more than half an hour. As this update interval is increases, WeWatch's power consumption decreases. In terms of user experience, the difference between 200 ms and 1 s update intervals is not perceptible to the human eye. So we optimize WeWatch by collect the RSSI every second. We also conducted an experiment on power consumption where we turned off all applications and the screen was dark. The tablet was in standby mode for about one week. The result showed that the screen consumes the most energy.

### 4.3 User Study

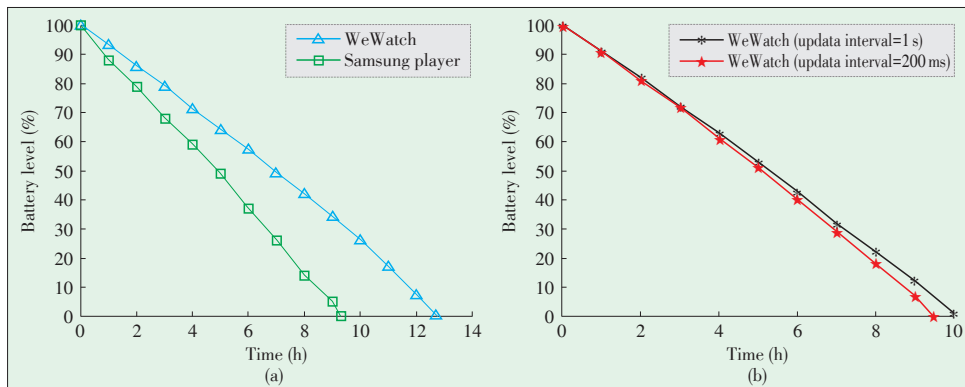
Current applications can detect user habits and usage context [33], [34]. This capability affects user experience and the user's preferences for their device. The motivation of our study is to improve user viewing experience. We gave our system to 27 students to try. In general, predicting user experience is quite difficult because there are so many factors affecting the interaction of users with devices. We formulated a question-



▲ **Figure 3.** RSSI versus distance.

## WeWatch: An Application for Watching Video Across Two Mobile Devices

Fuji Ren, Mengni Chen, and Yu Gu



▲ Figure 4. Energy consumption.

naire (Fig. 5) that would help us evaluate the user experience of WeWatch. Fig. 6 shows the results of this questionnaire.

More than 50% of participants gave WeWatch a score of nine points or higher out of a possible ten points because they appreciated the WeWatch concept. Some of these participants commented that the app was novel and truly improved the viewing experience. All participants viewed our application favorably, i.e., gave it a score of at least 6 points, but some commented that we still have a lot of work to do to improve the demonstration.

The question many asked is how to eliminate the physical frame between the screens of the two devices. The frames of different devices are often different widths and colors, and this detracts from the dual-screen viewing experience. This problem will be addressed over the next few years. Concept mobile devices with no frame have already been showcased. For example, SHARP released a new frameless screen at CES 2014 [35], and we believe the no-frame products will be mainstream soon. Participant in our trial also suggested using distance control to download and transmit videos across devices and introducing greater flexibility in the direction that devices can be moved from each other in order to use these functions.

## 5 Conclusion

In this paper, we have presented an Android application called WeWatch that combines two to improve the video viewing experience. The basis of this idea is IoT, i.e., making devices connect to one another and become an Internet. WeWatch users can place two devices close to each other to create a bigger screen over which synchronized videos can be played. Functions such as play, pause and stop are controlled by moving the devices towards or away from each other. The app architecture comprises positioning module, adaptation algorithm, and synchronization module. We installed WeWatch on two tablets and tested it. To properly control the video player, we used a distance-estimation model based on realistic data and analyzed the appropriate distance ranges to be set. We experimented with WeWatch to determine how much energy it con-

sumed, and we compared this with another video player application. We then compared the battery life with different update intervals in WeWatch to optimize energy efficiency.

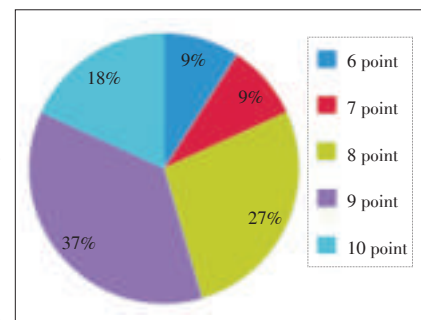
We studied dual-screen viewing across two devices because this is the most basic case. WeWatch only focuses on left and right adaptation. In the short-term, we plan to extend this so that playback can be controlled through vertical movements of a device and enable videos to be matched from all four sides of the screen. In this way, we can extent WeWatch to more screens. In the long term, we intend

Questionnaire about WeWatch

1. WeWatch achieve the basic functions of a player, like play, pause, and fast-forward?  
☐ YES ☐ NO
2. The resolution and quality of video is higher after play across two devices?  
☐ YES ☐ NO
3. The synchronization of video is precision and has no time delay?  
☐ YES ☐ NO
4. WeWatch can improve the watching experience?  
☐ YES ☐ NO
5. Controlled the play/pause of video by distance is convenient?  
☐ YES ☐ NO
6. Separate two device more than 10cm, the together-watching mode will change to normal player, is this function useful?  
☐ YES ☐ NO
7. The functions of WeWatch are easy to understand and remember?  
☐ YES ☐ NO
8. If you want to review WeWatch what score would you give it out of 10?  
\_\_\_\_\_
9. Would you recommend WeWatch to a friend?  
☐ YES ☐ NO
10. How can we improve WeWatch? Write down your ideas and suggestions.  
\_\_\_\_\_  
\_\_\_\_\_

▲ Figure 5. WeWatch questionnaire.

Figure 6.  
Results of questionnaire  
(score given out of 10, with  
10 being the highest score.  
No participants scored  
WeWatch lower than 6  
out of 10).





## WeWatch: An Application for Watching Video Across Two Mobile Devices

Fuji Ren, Mengni Chen, and Yu Gu

to expand WeWatch so that it can support real-time video transmission across three or more devices.

### References

- [1] S. Kristoffersen and F. Ljungberg, "‘Making place’ to make IT work: empirical explorations of HCI for mobile CSCW," in *International ACM SIGGROUP Conference on Supporting Group Work*, New York, USA, 1999, pp. 276–285.
- [2] R. Mohan, J. R. Smith, and C.-S. Li, "Adapting multimedia Internet content for universal access," *IEEE Transactions on Multimedia*, vol. 1, no. 1, pp. 104–114, Mar. 1999. doi: 10.1109/6046.748175.
- [3] J. Krumm and K. Hinckley, "The Nearme wireless proximity server," in *UbiComp '04: Ubiquitous Computing*, Nottingham, UK, Sept. 2004, pp. 283–300. doi: 10.1007/978-3-540-30119-6\_17.
- [4] V. M. Olivera, J. M. C. Plaza, and O. S. Serrano, "WiFi localization methods for autonomous robots," *Robotica*, vol. 24, no. 4, pp. 455–461, Jul. 2006. doi: 10.1017/S0263574705002468.
- [5] B. Roberts and K. Pahlavan, "Site-specific RSS signature modeling for WiFi localization," in *IEEE Global Telecommunications Conference*, Hawaii, USA, Dec. 2009, pp. 1–6. doi: 10.1109/GLOCOM.2009.5425740.
- [6] *WeWatch Demo* [Online]. Available: [v.youku.com/v\\_show/id\\_XNzQwNjAyNzcy.html](http://v.youku.com/v_show/id_XNzQwNjAyNzcy.html)
- [7] E. Oliver, "A survey of platforms for mobile networks research," *ACM SIGMOBILE Mobile Computing and Communications Review*, vol. 12, no. 4, pp. 56–63, 2008. doi: 10.1145/1508285.1508292.
- [8] M. Butler, "Android: changing the mobile landscape," *IEEE Pervasive Computing*, vol. 10, no. 1, pp. 4–7, 2011. doi: 10.1109/MPRV.2011.1.
- [9] ITU. (2005, Nov. 17). *ITU internet reports 2005: the internet of things* [Online]. Available: [www.itu.int/osg/spu/publications/internetofthings](http://www.itu.int/osg/spu/publications/internetofthings)
- [10] L. Atzori, A. Iera, and G. Morabito, "The internet of things: a survey," *Computer Networks*, vol. 54, no. 15, pp. 2787–2805, Oct. 2010.
- [11] L. Tan and N. Wang, "Future internet: the internet of things," in *3rd International Conference on Advanced Computer Theory and Engineering (ICACTE)*, Chengdu, China, Jun. 2010, pp. 376–380.
- [12] L. Zeng, "The internet of things technological application in the region of fire control," *Computer Programming Skills & Maintenance*, no. 16, pp. 118–119, Aug. 2012.
- [13] L. Cai, "Intelligent logistics in the era of the internet of things," *Logistics Sci-Tech*, vol. 33, no. 12, 2010.
- [14] Q. Sun, J. Liu, S. Li, et al., "Internet of things: summarize on concepts, architecture and key technology problem," *Journal of Beijing University of Posts and Telecommunications*, vol. 33, no. 3, pp. 1–9, 2010. doi: 10.13190/jbupt.201003.1.038.
- [15] B. Zhang, X. Yang, J. Li, et al., "Overview on internet of things," in *17th Annual Conference of China Information Theory Society*, Xi'an, China, 2010.
- [16] C. K. Toh, *Ad Hoc Mobile Wireless Networks: Protocols and Systems*. Upper Saddle River, USA: Prentice Hall, 2001.
- [17] C. de M. Cordeiro and D. P. Agrawal, *Ad Hoc and Sensor Networks: Theory and Applications*, 2nd ed. Singapore: World Scientific Publishing Company, 2011.
- [18] S. R. Subramanya and B. K. Yi, "Enhancing the user experience in mobile phones," *Computer*, vol. 40, no. 12, pp. 114–117, Dec. 2007. doi:10.1109/MC.2007.420.
- [19] H. Wigeliuss and H. Väättäjä, "Dimensions of context affecting user experience in mobile work," *12th IFIP TC 13 International Conference*, Uppsala, Sweden, Aug. 2009, pp. 604–617. doi: 10.1007/978-3-642-03658-3\_65.
- [20] S. Bendel and D. Schuster, "WatchMyPhone—providing developer support for shared user interface objects in collaborative mobile applications," in *IEEE International Conference on Pervasive Computing and Communications Workshops*, Lugano, Switzerland, Mar. 2012, pp. 166–171. doi: 10.1109/PerComW.2012.6197471.
- [21] G. Zhai, G. C. Fox, M. Pierce, et al., "eSports: collaborative and synchronous video annotation system in grid computing environment," in *Seventh IEEE International Symposium on Multimedia*, Irvine, USA, Dec. 2005, pp. 95–103. doi: 10.1109/ISM.2005.55.
- [22] R. Want, T. Pering, S. Sud, and B. Rosario, "Dynamic composable computing," *9th Workshop on Mobile Computing Systems and Applications*, Napa Valley, USA, Feb. 2008, pp. 17–21. doi: 10.1145/1411759.1411765.
- [23] B. Xing, K. Seada, and N. Venkatasubramanian, "Proximeter: enabling mobile proximity-based content sharing on portable devices," in *IEEE International Conference on Pervasive Computing and Communications*, Galveston, USA, Mar. 2009, pp. 1–3. doi: 10.1109/PERCOM.2009.4912802.
- [24] S. Liu, Y. Jiang, and A. Striegel, "Face-to-face proximity estimation using bluetooth on smartphones," *IEEE Transactions on Mobile Computing*, vol. 13, no. 4, pp. 811–823, Apr. 2014. doi: 10.1109/TMC.2013.44.
- [25] G. Shen, Y. Li, and Y. Zhang, "Mobius: enable together-viewing video experience across two mobile devices," in *5th international conference on Mobile Systems, Applications and Services*, San Juan, Puerto Rico, Jun. 2007, pp. 30–42. doi: 10.1145/1247660.1247667.
- [26] R. Mohan, J. R. Smith, and C.-S. Li, "Adapting multimedia Internet content for universal access," *IEEE Transactions on Multimedia*, vol. 1, no. 1, pp. 104–114, Mar. 1999. doi: 10.1109/6046.748175.
- [27] H. Liu, X. Xie, W.-Y. Ma, and H.-J. Zhang, "Automatic browsing of large pictures on mobile devices," in *11th ACM International Conference on Multimedia*, Berkeley, USA, Nov. 2003, pp. 148–155. doi: 10.1145/957013.957045.
- [28] T. Camp, J. Boleng, and V. Davies, "A survey of mobility models for ad hoc network research," *Wireless Communications and Mobile Computing*, vol. 2, no. 5, pp. 483–502, Aug. 2002. doi: 10.1002/wcm.72.
- [29] S. Basagni, M. Conti, S. Giordano, and I. Stojmenovic, *Mobile Ad Hoc Networking*. Hoboken, USA: Wiley-IEEE Press, 2004.
- [30] B. Xing, K. Seada, and N. Venkatasubramanian, "An experimental study on Wi-Fi ad-hoc mode for mobile device-to-device video delivery," in *IEEE INFOCOM Workshops 2009*, Rio de Janeiro, Brazil, Apr. 2009, pp. 1–6. doi: 10.1109/INFCOMW.2009.5072111.
- [31] J. Figueiras and S. Frattasi, *Mobile Positioning and Tracking*. Hoboken, USA: Wiley, 2010.
- [32] C. Sweet, V. Devarapalli, and D. Sidhu. (2004). *IEEE 802.11 performance in an ad-hoc environment* [Online]. Available: [www.csee.umbc.edu/~sweet/papers/80211adhoc.pdf](http://www.csee.umbc.edu/~sweet/papers/80211adhoc.pdf)
- [33] R. L. Wakefield and D. Whitten, "Mobile computing: a user study on hedonic/utitarian mobile device usage," *European Journal of Information Systems*, vol. 15, pp. 292–300, Jun. 2006. doi: 10.1057/palgrave.ejis.3000619.
- [34] S. Consolvo, L. Armstein, and B. R. Franza, "User study techniques in the design and evaluation of a ubicomp environment," *4th International Conference on Ubiquitous Computing*, Göteborg, Sweden, Sept. 2002, pp. 73–90. doi: 10.1007/3-540-45809-3\_6.
- [35] CES. (2014). *2014 international CES* [Online]. Available: <http://www.cesweb.org/>

Manuscript received: 2015-03-05

## Biographies

**Fuji Ren** (ren@is.tokushima-u.ac.jp) is a professor in the Faculty of Engineering of the University of Tokushima, Japan. He received his BE and ME degrees from Beijing University of Posts and Telecommunications, China in 1982 and 1985. He received his PhD degree in 1991 from Hokkaido University, Japan. His research interests include information science, artificial intelligence, language understanding and communication, and affective computing. He is a member of IEICE, CAAI, IEEJ, IPSJ, JSAI, AAMT, and a senior member of IEEE. He is a fellow of the Japan Federation of Engineering Societies. He is the president of the International Advanced Information Institute.

**Mengni Chen** (chengmn\_222@163.com) received her BE degree from Beijing University of Technology, China in 2012. She is a graduate student at School of Computer and Information, Hefei University of Technology, China. Her research interests include intelligence computing and wireless communication technology.

**Yu Gu** (yugu.bruce@gmail.com) received his DE degree from the Department of Computer Science, University of Science and Technology of China (USTC) in 2010. He received his BE degree in 2004, from the Special Classes for the Gifted Young, USTC. From February 2006 to August 2006, he was an intern at Wireless Network Group, Microsoft Research Asia, China. From December 2007 to December 2008, he was a visiting scholar at the Department of Computer Science, University of Tsukuba, Japan. From November 2010 to October 2012, he was a JSPS research fellow with the National Institute of Informatics, Japan. Now he is a professor of the School of Computer and Information, Hefei University of Technology, China. He is a member of the IEEE. His research interests include pervasive computing, resource management, and wireless communication networks.



# A Parameter-Detection Algorithm for Moving Ships

Yaduan Ruan, Juan Liao, Jiang Wang, Bo Li, and Qimei Chen

(School of Electronic and Engineering, Nanjing University, Nanjing 210093, China)

## Abstract

In traffic-monitoring systems, numerous vision-based approaches have been used to detect vehicle parameters. However, few of these approaches have been used in waterway transport because of the complexity created by factors such as rippling water and lack of calibration object. In this paper, we present an approach to detecting the parameters of a moving ship in an inland river. This approach involves interactive calibration without a calibration reference. We detect a moving ship using an optimized visual foreground detection algorithm that eliminates false detection in dynamic water scenarios, and we detect ship length, width, speed, and flow. We trialed our parameter-detection technique in the Beijing-Hangzhou Grand Canal and found that detection accuracy was greater than 90% for all parameters.

## Keywords

video analysis; interactive calibration; foreground detection algorithm; traffic parameter detection

## 1 Introduction

Waterway transport is important in China because it is low cost [1], [2]. Compared with road transport, waterways are more susceptible to changes in natural conditions. A dry season lowers water levels and narrows channels. A rainy season raises water levels and lowers the clearance for ships passing under bridges. There are fewer restrictions on ships as there are on vehicles. Additionally, because of the profit motive, high-tonnage ships are often navigated through low-grade channels at high speed, which causes congestion within the channel and increases the likelihood of a collision. Therefore, the size, speed, and flow of ships need to be monitored and regulated [3]. At present, there the only way of determining whether a ship is oversized is to stop the ship and take manual measurements, and speed and flow are measured by visual estimation. Automated video surveillance has been used on freeways but has drawbacks when used on waterways. For example, there are no marking lines that can be used for calibration. Such lines help transform data from the image plane to real ground plane. In a channel, ripples hamper efforts to detect the ship's size and ship that are sheltering each other when close together. In [4], the authors propose a method for extracting the ship's edge and generating a minimum bounding rectangle that approximates the ship's size at the pixel level. However, it does

not give the real size of the ship. In [5], the authors propose a method for photographing the side and top of a ship and using column scanning to obtain the ship's length and width at the pixel level. Then, the real size can be calculated according to the image resolution. However, this method is only suitable for stationary ships and a static background. In [6], the authors use background modeling to extract ships and a perspective transformation model to calculate the real size of the ships. However this method assumes that the axis of the ship is parallel or perpendicular to the river boundary, which is not always the case.

All these detection methods are easy to realize and are reliable in real time; however, they are too ideal to be used in complex river scenarios where there are no reference objects for auto-calibration. In this paper, we introduce an interactive calibration method for mapping image coordinates to real-world coordinates. A visual background extractor algorithm (ViBe) is used for accurate foreground detection and precise extraction of ships in an aquatic scenario. Then the size, speed, and flow are measured using detection models. This method, which has been used in China's shipping network, predicts ship size, speed, and flow with 90% of the accuracy of field measurements.

## 2 Algorithm Framework

The existing parametric detection algorithm for a moving ship is not suitable in complex scenarios. Because it lacks effective camera calibration, it cannot accurately calculate the

This work was supported by Fund of National Science & Technology monumental projects under Grants NO.61401239, NO.2012-364-641-209.

# A Parameter-Detection Algorithm for Moving Ships

Yaduan Ruan, Juan Liao, Jiang Wang, Bo Li, and Qimei Chen

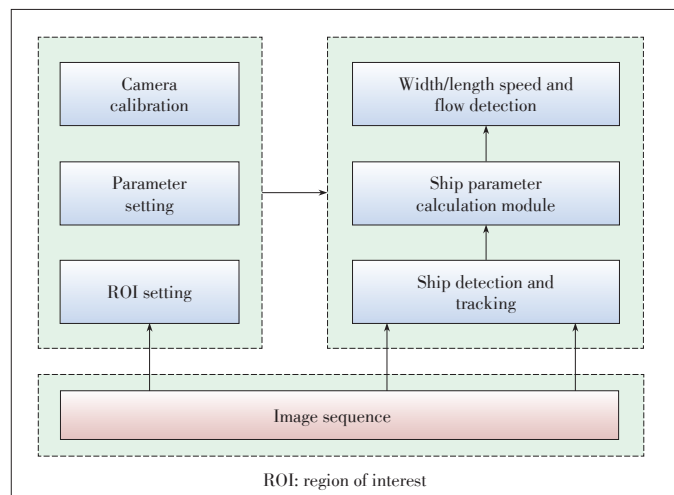
parameters for a moving ship. To obtain accurate traffic parameters, we propose a new parameter-detection algorithm for inland river scenarios. The basic framework of this algorithm is shown in **Fig. 1**.

In the pre-processing stage, the region of interest needs to be set to remove redundant information while monitoring the scenario, threshold values need to be determined to provide criteria for ship classification, and interactive grid calibration is required to translate the image-plane coordinate system into the real-world coordinate system. Then, we use an optimized ViBe algorithm to extract the moving ship, we track every ship using a Kalman filter [7], and we record the center point of every ship in each frame image. We obtain the navigation path through these center points by using the least squares function. Finally, the parameters, including width, length, speed and flow, are calculated.

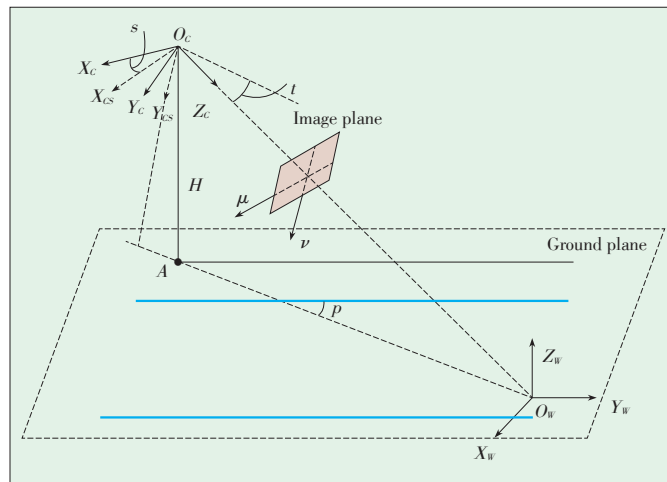
## 3 Interactive Calibration

Camera calibration is the basis of intelligent video analysis (IVA). Parameters of moving objects, such as size and speed, need to be translated into a physical value by calibration. Because there are no reference objects in our river scenario, we use an interactive method that involves a handler and terminal interface for calibration. This allows us to translate the image coordinates into real-world coordinates and calculate physical sizes in real time without any reference objects.

**Fig. 2** shows the transformation relations between the image plane coordinates  $u-v$  and real-world 3D coordinates  $X_w-Y_w-Z_w$ . These relations are specified by the camera-imaging model, and three coordinates are defined. Of these,  $X_w-Y_w-Z_w$  and camera coordinates  $X_c-Y_c-Z_c$  describe the three-dimensional space, and  $u-v$  describes the camera image plane. The origin of  $u-v$  is the center of the camera image, and the origin of  $X_w-Y_w-Z_w$  is the point where the optical axis of the camera intersects the ground plane.



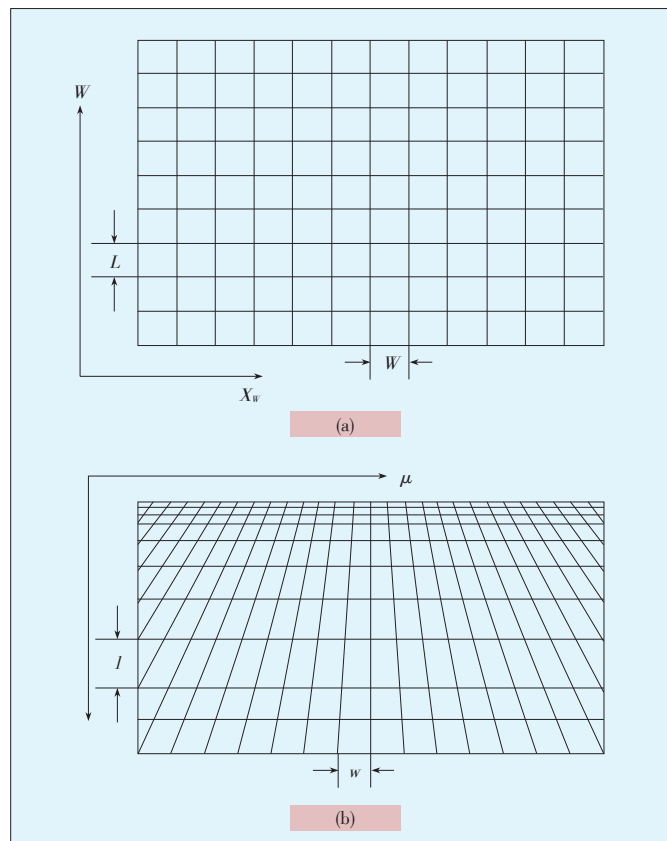
▲ Figure 1. Algorithm framework.



▲ Figure 2. The camera imaging model.

To obtain the transform relations between the  $u-v$  and  $X_w-Y_w-Z_w$ , four parameters must be obtained by camera calibration. These parameters are: focal length  $f$ , height of the camera  $H$ , pitch angle of the camera  $t$ , and deviation angle  $p$ .

Therefore, we introduce an interactive calibration technique that does not require a calibration reference. We superimpose a virtual regular grid on the ground, as in **Fig. 3a**, but allowing for perspective, this appears as in **Fig. 3b**. We can build the



▲ Figure 3. Grid image.

transform relations from the ground grid to the image grid when obtaining the four required parameters. According to [8], translation between the  $u$ - $v$  and  $X_w$ - $Y_w$ - $Z_w$  is given by:

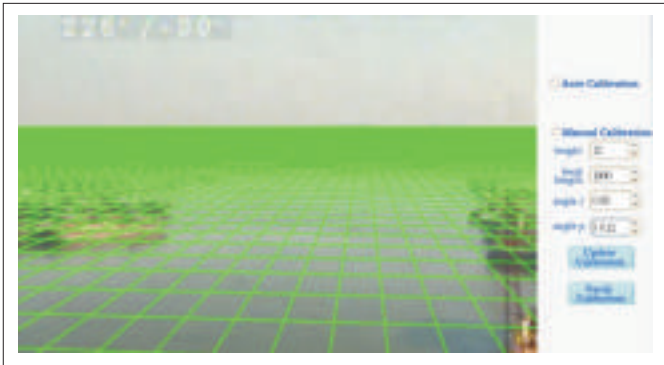
$$\begin{aligned} u &= \frac{-f \left[ \cos(p) \cos(s) X_w - \sin(p) \cos(s) Y_w + \sin(t) \sin(p) \sin(s) X_w + \sin(t) \cos(p) \sin(s) Y_w \right]}{\left[ \cos(t) \sin(p) X_w + \cos(t) \cos(p) Y_w + (H/\sin(t)) \right]} \\ v &= \frac{-f \left[ \cos(p) \sin(s) X_w - \sin(p) \sin(s) Y_w - \sin(t) \sin(p) \cos(s) X_w - \sin(t) \cos(p) \cos(s) Y_w \right]}{\left[ \cos(t) \sin(p) X_w + \cos(t) \cos(p) Y_w + (H/\sin(t)) \right]} \end{aligned} \quad (1)$$

If  $W = 1$  m and  $L = 2$  m, a corresponding grid can be generated as long as  $H$ ,  $t$ ,  $s$ , and  $f$  have been given initial values. We describe the grid image as  $g(H, t, s, f)$ . If any of these four parameters changes,  $g(H, t, s, f)$  changes. **Fig. 4** shows the grid image on the interactive calibration interface. The handler adjusts the four parameters until the grid fits the river plane and obtains the parameters.

#### 4 Ship Extraction and Tracking

Before a ship can be tracked and its behavior analyzed, it first must be extracted. In [10], a Universal Visual Background Extractor (ViBe) represents background features of each pixel with neighboring observed samples and uses a stochastic updating policy to diffuse the current pixel value into its neighboring pixels. In [11], the authors compare the applicability and effectiveness of several background modeling algorithms, including Mixture of Gaussian (MOG), codebook, and ViBe. With ViBe, the decision threshold and randomness parameter are fixed for all pixels, which is too inflexible when there are variations in the background. To make background model more adaptable to dynamic backgrounds, the decision threshold is dynamically adjusted according to the degree of background changes in each pixel. The main steps in ship extraction and tracking are as follows.

First, a nonparametric background model is built. A single frame at time  $t$  is denoted  $I_t$ , and  $B_t(i, j)$  of pixel  $(i, j)$  observed at time  $t$  is defined by a collection of  $N$  recently observed pixel



▲ **Figure 4.** Interaction calibration.

values:

$$\begin{aligned} B_t(i, j) &= \{b_1(i, j), b_2(i, j), \dots, b_N(i, j)\} \\ &= \{I_{t-N}(i, j), I_{t-N+1}(i, j), \dots, I_{t-1}(i, j)\} \end{aligned} \quad (2)$$

Second, the decision threshold  $R(i, j)$  of each pixel is adaptively set according to the degree of variation of the background, which is measured by the mean of a collection of  $N$  minimum Euclidean distances, defined as follows:

$$D_t(i, j) = \{d_{t-N}(i, j), \dots, d_k(i, j), \dots, d_{t-1}(i, j)\} \quad (3)$$

where  $d_k(i, j) = \min_k \text{dist}[I_t(i, j), B_k(i, j)]$  is the minimum Euclidean distance between the pixel values of pixel  $(i, j)$  and  $N$  background values. The mean value of  $D_t(i, j)$  is estimated using:

$$d_{\min}(i, j) = \frac{1}{N} \sum_k D_k(i, j) \quad (4)$$

As in (4), the greater the number of background changes, the greater the value of  $d_{\min}(i, j)$ . Using  $d_{\min}(i, j)$ , the decision threshold  $R_t(i, j)$  of pixel  $(i, j)$  is:

$$R_t(i, j) = \begin{cases} R_t(i, j)(1 - \alpha_1) & \text{if } R_t(i, j) > \eta d_{\min}(i, j) \\ R_t(i, j)(1 + \alpha_2) & \text{else} \end{cases} \quad (5)$$

where  $\alpha_1$ ,  $\alpha_2$  and  $\eta$  are fixed parameters. The decision threshold  $R_t(i, j)$  can dynamically adapt to background changes. For static backgrounds,  $R_t(i, j)$  slowly approximates to a constant  $\eta d_{\min}(i, j)$ . However, for dynamic backgrounds,  $R_t(i, j)$  increases in order to not integrate background pixels into the foreground.

Third, we compare the pixel value  $I_t(i, j)$  of pixel  $(i, j)$  at time  $t$  with  $N$  background values of  $B_t(i, j)$ . The pixel  $(i, j)$  is a foreground pixel if the distance between  $I_t(i, j)$  and  $N$  background values of  $B_t(i, j)$  is:

$$F_t(i, j) = \begin{cases} 1 & \text{if } \text{num}\{\text{dist}[I_t(i, j), B_t(i, j)] < R_t(i, j)\} < 2 \\ 0 & \text{else} \end{cases} \quad (6)$$

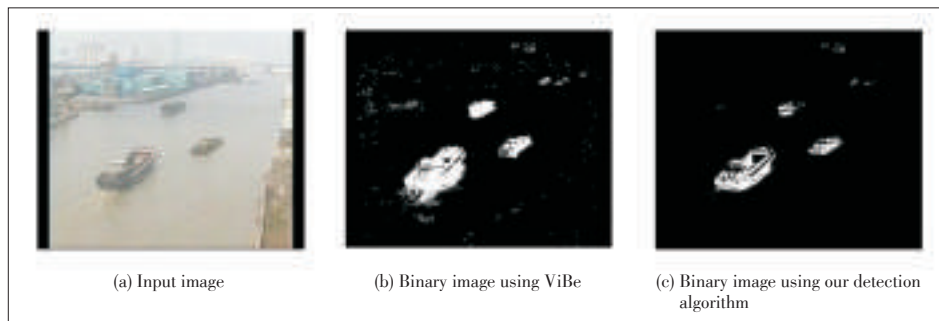
where  $\text{dist}\{\cdot\}$  is the Euclidean distance between  $I_t(i, j)$  and  $B_t(i, j)$ , and  $\text{num}\{\cdot\}$  is the number of background values satisfying the condition  $\text{dist}\{\cdot\} < R_t(i, j)$ . The foreground segmentation mask is denoted  $F_t$ . If  $F_t(i, j) = 1$ ,  $(i, j)$  in the current frame is a foreground pixel. If  $F_t(i, j) = 0$ , the corresponding pixel belongs to the background.

Fourth, noise is filtered out using morphological operations, and virtual targets are removed through area features. From **Fig. 5**, it can be found that our method removes the interference of water ripples and extracts the contour of the ship more clearly than ViBe.

Fifth, the background model  $B_t(i, j)$  should be updated in real time to adapt to the changing background. If the pixel value of  $(i, j)$  at time  $t$  matches its background model  $B_t(i, j)$ , the pixel is classified as background and is used to randomly update  $B_t$ .

## A Parameter-Detection Algorithm for Moving Ships

Yaduan Ruan, Juan Liao, Jiang Wang, Bo Li, and Qimei Chen



▲ Figure 5. Ship detection.

$(i, j)$ . We randomly choose a background value  $b_k(i, j)$  ( $k \in 1, \dots, N$ ) and replace it with the current pixel value  $I(i, j)$ , which has a probability  $\varphi$ .

Sixth, a Kalman filter is used when tracking ship to guarantee accuracy and continuity.

## 5 Traffic Parameter Detection

Here, we introduce our approach to calculating ship parameters: length and width, speed, and flow.

### 5.1 Length and Width

We extract a contour of the binary image of a moving ship by using background subtraction algorithm with a Canny operator [12]. Frame by frame, the center of a ship's contour is pinpointed and these points are recorded as the navigation path. The least squares approach is used to draw a straight line (main line) from these center points. As shown in Fig. 6, the main line and ship's contour intersect at two points, and the distance between the two points is the ship's length. We draw the line so that it crosses through the center point and is perpendicular to the main line. The main line and ship's contour intersect at another two points, and the distance between these two points is the ship's width.

### 5.2 Speed

Here, we calculate the ship's average speed through a detected region. The average speed is determined by two horizontal parallel lines in the image. When a ship passes over one of two parallel lines, we record the time and ship's center point. Once the ship has touch the other line, the time and ship's center point are recorded again. By comparing the two records, we can determine the time difference  $T$  and distance  $S$  between the two center points. The ship's average speed  $V$  is given by  $V = S/T$ .

### 5.3 Flow

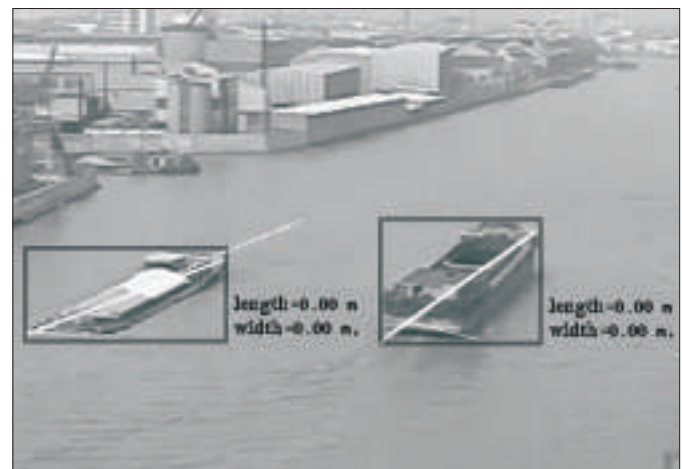
Flow detection involves understanding the dynamic image sequence. The

traditional approach to flow detection is to place a gate line in the surveillance image and add up the number of ships whose centers cross the gate line. Large ships often cover smaller ones at the gate line when the ships are close together, which causes flow detection errors. To solve this problem, we use two horizontal gate lines in the image. These gate lines are used together to count ships. Fig. 7 shows what happens when two adjacent separate from

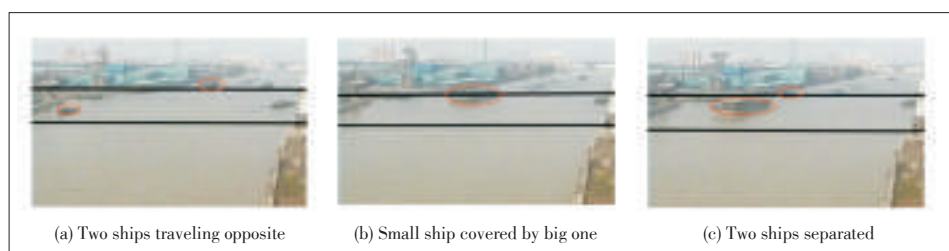
each other. The small ship is moving upriver and the larger ship is moving downriver. The larger ship covers the smaller one when they come to the upper gate line. The smaller ship misses by upper gate line but has been recorded by the lower gate line. Therefore, the flow is determined correctly.

## 6 Experimental Results

We trialed our parameter-detection algorithm in an inland river in Nantong, Jiangsu province. The test sequence was obtained on September 17, 2013. The camera calibration parameters were:  $H = 34$ ,  $f = 700$ ,  $t = 0.32$ , and  $p = 0.39$ . Ship length and width, speed, and flow were detected using our algorithm (Tables 1 to 3, respectively), and the accuracy was measured against the actual ship parameters. As shown in Tables 1 to 3,



▲ Figure 6. Navigation path of moving ships.



▲ Figure 7. Occlusion between two ships.

## A Parameter-Detection Algorithm for Moving Ships

Yaduan Ruan, Juan Liao, Jiang Wang, Bo Li, and Qimei Chen

▼ Table 1. Length and width detection

Ship name	Detected length (m)	Actual length (m)	Accuracy	Detected width (m)	Actual width (m)	Accuracy
Xin hang huo	39	36.8	94.02%	6.8	6.8	100%
Su yan huo	44	41.5	93.92%	6.8	7.5	90.67%
Wan hong qi	52	54.5	95.24%	9.5	10.2	93.14%
Tong hai ji	32	30.0	97.99%	5.8	5.7	98.25%
E zhou huo	41.0	41.0	100.0%	7.5	7.6	98.68%
Wuhu 1069	39.0	36.0	91.67%	7.1	6.8	95.59%

▼ Table 2. Speed detection

Detected speed (m/s)	Actual speed (m/s)	Accuracy
2.1	2	95.0%
3.9	4	97.5%
5.7	6	95.0%
7.9	8	98.75%

▼ Table 3. Flow detection

	Detected flow	Actual flow	Accuracy
Up	23	21	90.1%
Down	60	65	92.3%
Total	83	87	96.0%

the accuracy of our algorithm was greater than 90%. Our algorithm is therefore more accurate than previous manual methods of determining ship parameters and is better for waterway traffic management and emergency rescue.

## 7 Conclusion

Intelligent video image processing can be used to determine ship size, speed, flow, and other parameters. We can make full use of video resources of inland waterways and access to ship and channel information in order to make better management decisions. In this paper, we introduced a human-machine camera calibration technique and optimized the ViBe algorithm to create a model for determining ship parameters such as length, width, speed, and flow. The experimental results showed that our algorithm can obtain these parameters in real-time with an accuracy of more than 90%. This means the algorithm can be implemented in real applications and also has important theoretical value for the development of intelligent waterway transportation.

## References

- [1] A. Caris, S. Limbourg, C. Macharis, et al., "Integration of inland waterway transport in the intermodal supply chain: a taxonomy of research challenges," *Journal of Transport Geography*, vol. 41, pp. 126 – 136, 2014. doi: 10.1016/j.jtrangeo.2014.08.022.

- [2] L. Guo, *The Research of Collection of Traffic Information Based on Information Fusion*. Hefei, China: Press of University of Science and Technology of China, 2007.
- [3] V. Bugarski, T. Bačkalic, and U. Kuzmanov, "Fuzzy decision support system for ship lock control," *Expert Systems with Applications*, vol. 40, no. 10, pp. 3953–3960, 2013. doi: 10.1016/j.eswa.2012.12.101.
- [4] J. Wang, *Wavelet Analysis and its Application in the Measuring of Size of the Boat Image*. Nanjing, China: Press of HoHai University, 2006.
- [5] J. Wang, *The Research of Intelligent detection method and Application based on Image Fusion technology*. Nanjing, China: Press of HoHai University, 2009.
- [6] X. Zhang, L. Xu, and A. Shi, "Visual measurement system for traffic flow of inland waterway," *Journal of Image and Graphics*, vol. 16, no. 7, pp. 1219–1225, 2011.
- [7] S. Kluge, K. Reif, and M. Brokate, "Stochastic stability of the extended Kalman filter with intermittent observations," *IEEE Transactions on Automatic Control*, vol. 55, no. 2, pp. 514–518, 2010. doi: 10.1109/TAC.2009.2037467.
- [8] R. Dong, B. Li and Q. Chen, "An automatic calibration method for PTZ camera in expressway monitoring system," *World Congress on Computer Science and Information Engineering*, Los Angeles, USA, 2009, pp. 636–640.
- [9] O. Barnich and M.V. Droogenbroeck, "ViBe: A universal background subtraction algorithm for video sequences," *IEEE Transaction on Image Processing*, vol. 20, no. 6, pp. 1709–1724, 2011. doi:10.1109/TIP.2010.2101613.
- [10] X. Fang, *The Research on Background Modeling Algorithm of Moving Target in Ship Video Sequences*. Wuhan, China: Press of Wuhan University of Technology, 2013.
- [11] E. Li, B. Zhang, and X. Zhou, "The Research on Adaptive Canny edge detection algorithm," *Science of Surveying and Mapping*, vol. 33, no. 6, pp. 119–121, 2008.
- [12] R. Biswas and J. Sil, "An improved canny edge detection algorithm based on type - 2 fuzzy sets," *Procedia Technology*, vol. 4, pp. 820–824, 2012. doi: 10.1016/j.protec.2012.05.134.

Manuscript received: 2015-03-29

## Biographies

**Yaduan Ruan** (ruanyaduan@163.com) received the PhD degree from Nanjing University in 2014. She is a lecturer at School of Electronic Science and Engineering, Nanjing University. Her research interests include image processing and machine learning.

**Juan Liao** (liaojuan308@163.com) received the BS and MS degrees from Anhui University of Science and Technology in 2008 and 2011. She is currently a PhD candidate at Nanjing University. Her research interests include computer vision and image processing.

**Jiang Wang** (jiangnju\_edu@sina.com) received the BS degree from Nanjing University in 2012. He is an MS degree candidate at Nanjing University. His research interests include computer vision and image processing.

**Bo Li** (liboe@nju.edu.cn) received the PhD degree in signal and information processing from Nanjing University in 2009. He is an associate professor at Nanjing University. His research interests include computer vision and machine learning.

**Qimei Chen** (chenqimei@nju.edu.cn) received the MS degree from Tsinghua University, Beijing, in 1982. He is a professor at Nanjing University. His research interests include visual surveillance, image and video processing.



# Inter-WBAN Coexistence and Interference Mitigation

Bin Liu<sup>1</sup>, Xiaosong Zhao<sup>1</sup>, Lei Zou<sup>1</sup>,  
and Chang Wen Chen<sup>2</sup>

(1. Key Laboratory of Electromagnetic Space Information, Chinese Academy of Sciences, University of Science and Technology of China, Hefei 230027, China;

2. Dept. of Computer Science and Engineering, The State University of New York at Buffalo, NY 14260-1604, USA)

## 1 Introduction

The world's population is aging, and increased health care expenses are affecting the quality of life of elderly people. Thus, inexpensive health care solutions are urgently needed. Recently, wireless body area networking (WBAN) has been proposed as one such solution. Physiological information, such as electrocardiography (ECG) signals, blood pressure readings, and body posture signals, can be acquired by a WBAN and sent to a remote medical center for analysis and treatment [1]. This has the potential to relieve the pressure on public medical resources and increase convenience for patients. A WBAN could reduce the number of times a patient with a chronic disease needs to visit the hospital.

A WBAN also has other applications, such as somatic and virtual reality [2], sports training and fitness analysis, and military applications [3], [4].

A WBAN comprises a coordinator node and several sensor nodes deployed on the body, within the body, or around the body. These nodes usually form a network with a star topology and single-hop communication. Sensor nodes collect information from the human body and transmit it to the coordinator node for processing. A typical WBAN architecture is shown in Fig. 1.

The body-centric, health-related, mobile nature of WBAN

## Abstract

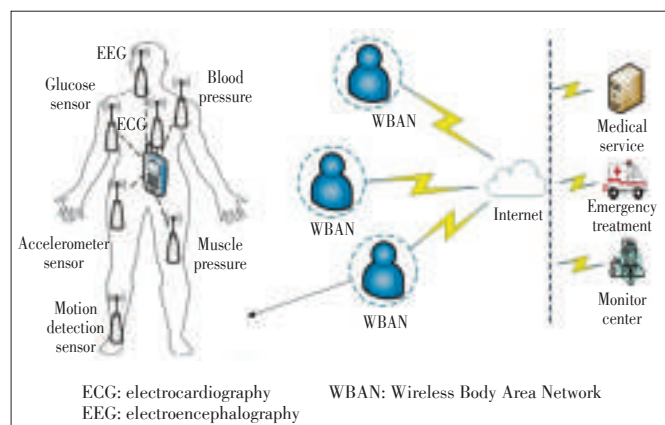
With promising applications in e-health and entertainment, wireless body area networks (WBANs) have attracted the interest of both academia and industry. If WBANs are densely deployed within a small area, serious problems may arise between the WBANs. In this paper, we discuss issues related to the coexistence of WBANs and investigate the main factors that cause inter-WBAN interference. We survey inter-WBAN interference mitigation strategies and track recent research developments. We also discuss unresolved issues related to inter-WBAN interference mitigation and propose future research directions.

## Keywords

wireless body area network (WBAN); inter-WBAN interference mitigation; e-health

means there are some special requirements that need to be considered when designing a WBAN system. First, energy efficiency needs to be reflected in the system design because sensor nodes only have limited-capacity batteries that are often inconvenient to recharge or replace (especially for implanted sensors). Second, traffic in a WBAN primarily comprises vital signs; therefore, latency and throughput need to be guaranteed. Finally, a WBAN is heterogeneous because there are diverse nodes located in different positions, and these nodes have different QoS requirements. There are also the differences between WBAN users. Therefore, is necessary to design protocols that enable the data rate to be scaled and services to be differentiated for different sensor nodes and WBANs.

Common wireless technologies may not be suitable for use in a WBAN. For example, Bluetooth [5] only supports a limited



▲ Figure 1. Typical WBAN architecture.

This work is supported by the National Natural Science Foundation of China under Grant No. 61202406 and the USTC Grand Master Professor Funds under Grant No. ZC9850290097.



number of terminal nodes and single-hop communication. It also consumes a lot of power [6]. Zigbee [7] does not sufficiently guarantee QoS or mobility [6]. The IEEE 802.15.6 Task Group published the WBAN standard in 2012. The purpose of this Task Group was to establish a communication standard optimized for sensors operating on, in or around both human and animal bodies. The standard ensures reliability, QoS, energy efficiency, high data rate, and no interference in a variety of WBAN applications [1]. Many researchers have also investigated WBAN-related topics, including model architecture [8], PHY and MAC layer design [9], [10], adaptive route protocol [11], and interference mitigation [12], [13].

Attached to the body, a WBAN moves as the hosts does. In a hospital or nursing home, coexistence of WBANs may cause problems. Adjacent WBANs may use the same channel simultaneously because of limited frequency and dense distribution. Without scheduling or coordination between adjacent WBANs, intra-WBAN packet delivery may suffer. WBANs may also need to compete with other wireless networks for spectrum if both networks use the same spectrum band, e.g., unlicensed 2.4 GHz ISM. Problems arising from the coexistence of WBANs and other wireless networks can be simplified by regarding the WBAN as a uniformly distributed disturbance point because a WBAN is much smaller than other wireless networks. Some research on the coexistence of WBANs and other wireless networks has been done recently [14]–[16]. Problems arising from coexisting WBANs are more complex due to the fact that the scale of communication of different WBANs is similar and different inter- and intra-WBANs may have heterogeneous characteristics. Such problems hamper the widespread deployment of WBANs.

In this paper, we focus on problems arising from the coexistence of multiple WBANs and discuss related interference-mitigation solutions. We also discuss research trends and unresolved issues related to inter-WBAN coexistence.

In section 2, we describe inter-WBAN interference problems in detail. In section 3, we introduce and compare inter-WBAN interference mitigation solutions. In section 4, we discuss related open research issues. In section 5, we summarize and conclude the paper.

## 2 Problems Arising from the Coexistence of WBANs

Problems with coexisting WBANs occur for three main reasons:

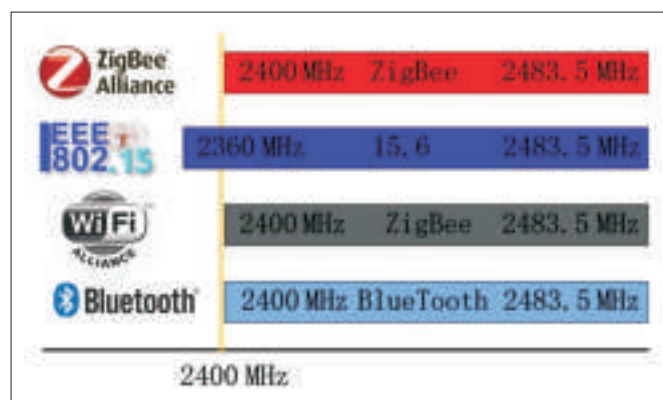
- 1) a large number of WBAN users gathered together. Although WBANs usually only have a short communication range, they may still come close to each other in certain places, such as metro stations, hospitals, nursing homes, or retirement villages. If the WBANs are not scheduled properly, transmission collision may occur.
- 2) limited wireless resources. Most WBANs use the 2.4 GHz

ISM band, which is also used by Wi-Fi, Bluetooth, and Zigbee networks (**Fig. 2**). The problem is compounded because Wi-Fi APs have been widely deployed both in public places and at home. Therefore, there are insufficient collision-free channel resources to satisfy demand.

- 3) random mobility. In crowded and resource-limited environments, reuse of frequency channels is inevitable. However, the random mobility of WBAN users breaks down the spatial isolation of co-channel WBANs.

The distance between WBANs and the distribution intensity of WBANs are both important factors affecting the degree of interference between two WBANs. In [17], Muhammad *et al.* conducted experiments on the change in packet loss rate (PLR) in a WBAN in relation to the distance of the WBAN from other interfering WBANs. They found that the distance between WBANs noticeably affects the PLR in each WBAN. In [18], the relationship between the number of interfering WBANs and packet error rate (PER) was analyzed. The authors found that densely distributed interference sources congest the channel and cause high PER. Thus, closer inter-WBAN distance and denser distribution increases interference between WBANs and degrades communication.

Body movements and clothing give rise to a shadowing effect, i.e., lack of signal reflection, in a WBAN. The antenna angle greatly affects the received signal strength (RSS), which is given by the received signal-to-interference-plus-noise ratio (SINR) [19]. An unsuitable transmission angle may create serious interference for other WBANs. In addition, the topology of a WBAN affects the degree of interference for other WBANs. For example, WBAN users form a line when queuing in a station or a ring when sitting around a table. In [20], Wang *et al.* studied WBANs with a hexagonal lattice structure within an inter-WBAN mesh structure. Geometric probability was then used to model and analyze interference arising from coexistence of WBANs. In [21], the power-law distribution model of the crowd was introduced to simulate the structure of multiple WBANs, and the distance-based distribution function of interference probability was proposed to estimate the probability of inter-WBAN interference.



▲ Figure 2. Wireless frequency occupancy around 2.4 GHz.

### Inter-WBAN Coexistence and Interference Mitigation

Bin Liu, Xiaosong Zhao, Lei Zou, and Chang Wen Chen

Apart from the previously mentioned external factors, there are some factors within a WBAN that significantly affect inter-WBAN interference. In [22], De Silva *et al.* investigated the relationship between packet delivery rate (PDR), packet transmission rate, and number of interfering networks. They found that PDR decreases to as low as 65% for a transmission rate of 100 packets/s in a mission-critical WBAN situation. This reduced to 60% when there were eight WBANs in the surrounding environment. In [23], Sarra *et al.* investigated transmission power, frequency of data transmission, and packet size in a WBAN when there was both heavy and light interference from the surrounding environment. They found that decreasing the packet size or frequency of data transmission can improve the expected transmission (ETX) and increase PDR. Increasing transmission power also increases the SINR. In [18], the authors investigated SINR, BER, and probability of collision for TDMA, FDMA and CDMA access schemes when there was inter-piconet coexistence. The authors confirmed that interference from coexisting WBANs significantly degrades the performance of WBANs within the system. The experimental results showed that TDMA and FDMA are better choices than CDMA for mitigating interference when there are coexisting WBANs.

## 3 Solutions for Mitigating Interference Caused by Coexisting WBANs

As with intra-WBAN multiple access, inter-WBAN coexistence can be achieved by separating WBANs in the frequency, time, or spatial domains. In the following subsections, we discuss frequency allocation, time scheduling and co-channel interference mitigation. Some other interference-mitigation strategies are also discussed.

### 3.1 Channel Assignment

In general, each WBAN should choose a wireless channel for intra-WBAN data transmission. Reasonable channel allocation is the most straightforward way of avoiding inter-WBAN interference. A WBAN is assigned a channel that is different from an adjacent conflicting WBAN. In most scenarios, there is no centralized managing entity; therefore, channels need to be assigned in a distributed way.

In [1], distributed channel-hopping mechanisms were described. Channel hopping is controlled by the hopping sequence, which is generated by the generator polynomial based on the Galois linear feedback shift register (LFSR). The WBAN coordinator may then change its operating channel periodically according to the Channel Hopping State and Next Channel Hop fields in its beacons without exchanging information. In [18], [24], [25], some other random channel-allocation strategies can be found. These random channel hopping or allocation schemes are easy to implement and are well suited to an environment with a small number of WBANs. However, when WBANs are densely distributed and channel resources are lim-

ited, randomized channel-assignment schemes lead to a high probability of channel conflict and significantly degrade performance.

Some other channel-assignment solutions use only self-measured interference indicators, such as received signal strength indication (RSSI) and received signal - to - interference ratio (SIR), which can only be regarded as rough indicators of interfering WBANs. In [26], the authors propose an interference-aware channel switching (inter - ACS) algorithm that senses whether WBANs are experiencing interference according to the SIR. Depending on the degree of SIR detected by the coordinator, various  $n$ -hop channels are assigned to WBANs. This results in better performance than that achieved using uniform or random channel allocation.

SIR-based methods are not well suited to crowd scenarios, in which more information about other interfering WBANs needs to be acquired to better allocate channels. In a distributed situation, messages need to be exchanged between WBANs so that WBANs know the interference information of adjacent WBANs. In [27], Deylami *et al.* proposed a distributed dynamic coexistence management (DCM) mechanism to improve the performance of coexisting WBANs. In DCM, each WBAN listens the channel and extracts beacon information from other WBANs when it suffers beacon loss. If there is an insufficient gap for coexistence, the WBAN switches to another channel. In [28] and [29], Movassaghi *et al.* designed a scheme based on the interference region (IR) for eliminating inter-WBAN interference. In this scheme, each WBAN records the information of interfering nodes in the IR and shares this information with all the other WBANs in its vicinity. A channel-reuse strategy similar to that in cellular networks is then used. With this strategy, distant WBANs can use the same channel, and orthogonal sub-channels are assigned to WBANs that are close to each other and experiencing interference.

If more information is exchanged between WBANs, channel assignment can be modeled as a graph coloring problem. Network topology is modeled as a graph  $G = (V, E)$ , where the vertex set  $V$  represents an individual WBAN, and the edge of set  $E$  of  $G$  shows that the two connected vertices (WBANs) conflict with each other if allocated the same channel. The colors of the graph show the channel resources. Hence, channel allocation can then be transformed into a graph coloring problem with fastest speed and least colors. In [30], a Random Incomplete Coloring (RIC) algorithm with low time complexity and high spatial reuse was proposed. In this algorithm, quick inter-WBAN scheduling (IWS) is achieved through random-value coloring, and the reuse efficiency of channel resources is guaranteed by incomplete coloring. In [31], a combination of cooperative scheduling and graph coloring was proposed to eliminate inter-WBAN interference. The main idea of this scheme is that adjacent WBAN pairs form a cluster that can allocate channels using the same method as that in [28] and further distribute resources between clusters by using the graph coloring

method. With graph coloring methods, perfect superframe synchronization is assumed. However, such synchronization cannot be guaranteed because of the randomness of WBANs. Furthermore, interference should also be detected while building the graph model.

By passing messages between WBANs, the channel-assignment scheme ensures a higher channel reuse rate. The main problem with this scheme is that effective channel allocation cannot be guaranteed in some scenarios, such as when WBANs are densely distributed or when frequency spectrum is scarce. Furthermore, frequent interference detection and information exchange consumes wireless resources and energy. Therefore, the channel-assignment scheme is only appropriate when there is a relatively large frequency spectrum to be allocated or when there is a relatively small number of coexisting WBANs.

### 3.2 Time Rescheduling

The TDMA-based scheme is usually used for intra-WBAN communication to avoid sensor collision. In such a scheme, non-overlapping time slots are allocated to different sensors for transmission. Similarly, inter-WBAN interference can also be mitigated by time rescheduling. When an individual WBAN occupies the channel only part of the time, e.g., during the channel sensing period or inactive period of superframe in [1], [5] and [7], the other WBANs can temporarily access the channel to transmit data. This is a more efficient way of utilizing the channel.

In [32]–[37], the authors use time rescheduling to mitigate inter-WBAN interference. In [32], the authors propose a BAN-BAN interference mitigation (B2IRS) beacon-enabled strategy in which the coordinator of the WBAN collects information about adjacent WBANs at the end of superframe active time. In this way, multiple WBANs do not access the channel at the same time. In [33], Kim *et al.* proposed an asynchronous inter-network interference avoidance scheme called AIIA. This scheme was implemented in the coordinator of the WBAN and maintained a table containing the time scheduling information about adjacent WBANs. Thus, every WBAN could transmit in a conflict-free time slot according to the information table. In [34], information was exchanged between proximal coordinators of WBANs in order to arrange the transmission sequence of WBANs according to application priority. In [35] and [36], Mahapatro *et al.* focused on the fairness between WBANs when there was an insufficient number of time slots. If all WBANs accessed the channel in a round-robin way according to their time slot requirements, WBANs with fewer nodes would have a long wait. The authors then proposed a scheme in which WBAN containing fewer nodes could occupy more time slots and found that average wait times between WBANs remained the same. In time-rescheduling solutions, complete and up to date information about adjacent WBANs is prerequisite. In [37], Wen *et al.* used a CSMA-like mechanism to trans-

mit the beacon without collision caused by an incomplete neighbor list.

Some other contention-based time rescheduling approaches are found in [38]–[42]. In [38], [39], the listening strategy is similar to that in [32]; however the channel is sensed when the beacon needs to be sent. A Poisson distribution model is established to generate the probability of channel sensing. Then, the beacon is sent to reserve the channel once the channel is idle. However, if the channel is busy, there needs to be a wait period before resensing. In [40]–[41], Dong *et al.* modified the inter-WBAN time-scheduling scheme to uniformly access the channel when there is no cooperation between WBANs. At the same time, an opportunistic relaying (OR) strategy was introduced to select the minimum interference link inside a WBAN. This enhances coexistence between WBANs. However, this scheme was not practical because links were selected according to channel measurements rather than a prediction scheme, and an increase in the number of relays had the potential to sacrifice system performance.

Time scheduling requires complex arrangement strategies to avoid inter-WBAN interference. With scheduling-based methods of inter-WBAN interference mitigation, frequent coordination consumes a lot of energy. With contention-based methods of inter-WBAN interference mitigation, broadcasting information before accessing the channel consumes a lot of energy. In addition, it is also a challenge for a WBAN to obtain transmission information about other WBANs in the vicinity in a timely way. The key issue for effective time scheduling is timely updating of information. Therefore, time-scheduling methods may be more appropriate when the inter-WBAN topology is changing slowly.

### 3.3 Co-Channel Interference Mitigation

Generally speaking, resource management strategies, such as channel assignment and time rescheduling, are the most straightforward ways of reducing interference between coexisting WBANs. Each WBAN can work in an orderly manner based on the established resource allocation strategy. However, sometimes there may be problems with resource management because WBANs are densely deployed and the inter-WBAN topology changes quickly. In this case, we can only adjust the transmission power to improve the performance of coexisting densely distributed WBANs. Interference between WBANs may still exist, and a proper method should be used to mitigate it.

Adjusting the transmission power is a natural way of improving the performance of coexisting densely distributed WBANs. However, although decreasing the transmission power of one WBAN mitigates the interference experienced by that WBAN, it also degrades the performance of that WBAN. Game theory is usually introduced to trade off performance for energy consumption in a cooperative or non-cooperative manner. The importance of performance or energy consumption can be adjust-

## Inter-WBAN Coexistence and Interference Mitigation

Bin Liu, Xiaosong Zhao, Lei Zou, and Chang Wen Chen

ed by setting the fixed or adaptive weighting factor in the application-based utility function. According to Nash Equilibrium (NE), anyone who changes their strategy alone without consideration of the strategies of other participants will benefit less [43]. That is, each rational participant is not motivated to change their strategy unilaterally if they seek the maximum possible benefit.

In [21] and [43]–[46], the authors describe power-control game for inter-WBAN interference mitigation. In [21], [43], [45], and [46], a power control game involving a trade-off between throughput and power consumption was proposed to mitigate interference arising from coexisting WBANs. The existence of and uniqueness of the NE solution was discussed. Fast-convergence algorithms such as Harmonic Mean (HM) [43]; Proactive Power Update (PAPU) [46]; and Best Response Iteration [21], [45] have been proposed to converge to the unique NE. In [44], Wu *et al.* created a decentralized inter-user interference suppression (DISG) algorithm for a WBAN. They proposed a power-control game based on the SINR and power use to choose a suitable channel and transmission power. After proving the existence of the NE, the authors derived the condition that would guarantee the uniqueness of the NE and introduced the No-Regret Learning algorithm to optimize the NE.

Most of works referring to the power-control game for WBANs only consider the single link inside the WBAN, which is impractical because a WBAN comprises many sensors with various QoS requirements, link gains, etc. The convergence speed of the power-updating algorithm must keep up with any change in the inter-WBAN topology; otherwise, the solution obtained in the current iteration is only optimal for the earlier period, not the current period.

In [47], Kazemi *et al.* do not use game theory to mitigate interference arising from coexistence of WBANs. Instead, they propose a power controller based on reinforcement learning (RL) that exploits environmental information such as received interference, previous transmission power, and SINR. In [48], the authors propose a fuzzy power controller (FPC) that exploits the SINR, transmission power, and interference power level. An FPC uses genetic algorithms (GAs) to optimize parameters and can maximize throughput and minimize power consumption by updating the optimal transmission power according to the current environment.

As well as power-adjustment strategies, adaptive strategies can be used to mitigate inter-WBAN interference. In [13], Yang *et al.* proposed a scheme that included adaptive modulation, adaptive data rate, and adaptive duty cycle. They also introduced the interference mitigation factor (IMF), which is used to quantitatively analyze the effectiveness of their proposed scheme.

Co-channel interference-suppression methods such as power control based on game theory, power controller, and adaptive schemes are passive ways of mitigating inter-WBAN interference. Passively mitigating inter-WBAN interference involves

constantly adjusting the transmission strategy according to the communication environment rather than actively altering the communication environment. This means compromising on performance when there is severe interference. In such situations, resource allocation strategies are ineffective.

### 3.4 Other Strategies

There are also other strategies for mitigating inter-WBAN interference [1], [21], [22]. In [1], beacon-shifting strategies are introduced to protect the most important part of intra-WBAN communication, i.e., transmission of the beacon, and make it easier for WBANs to coexist. The coordinator of a WBAN can transmit its beacon at different offsets relative to the start of the beacon periods in order to avoid repeated beacon collisions. The coordinator can also schedule allocation conflicts that occur as a result of coexistence. The offsets are decided by the unique beacon shifting sequence chosen by the coordinator.

Some auxiliary information can also be used to mitigate inter-WBAN interference. In [21], the authors use social interaction detection to estimate the distance of interference. In [22], De Silva *et al.* designed a fixed sensor network to predict potential interference. An interference prediction module was used to obtain the location of WBANs and RSSI, and the likelihood of interference was predicted according to the distance and RSSI level. Finally, a resource arbitrator was assigned channels that were different to those of the relevant WBANs in order to avoid potential interference.

### 3.5 Summary and Discussion

Tables 1 and 2 summarize different inter-WBAN interference mitigation solutions. These proposed solutions are all designed for different particular scenarios. When there are sufficient resources and a slowly changing network topology, resource-allocation methods such as channel assignment and time rescheduling are the most straightforward methods for mitigating inter-WBAN interference. However, in some scenarios, such as densely deployed WBANs, limited frequency resource

▼ Table 1. Summary of solutions for inter-WBANs coexistence and interference mitigation problem

Methods	Specific classification	Index of literature
Channel assignment	Random assignment	[1], [18], [24], [25]
	SIR-based assignment	[26]
	Message-exchanging-based assignment	[27]–[31]
Time rescheduling	Scheduled-based strategy	[32]–[37]
	Contention-based strategy	[38]–[42]
Co-channel interference mitigation	Game-based power control	[21], [43]–[46]
	Other power control strategies	[47], [48]
	Adaptive schemes	[13]
Other strategies	N/A	[1], [21], [22]
SIR: signal-to-interference ratio		



▼ **Table 2. Comparison of solutions for inter-WBANs coexistence and interference mitigation problem**

Methods	Advantage	Disadvantage	Application scenario
Channel assignment	Simple, effective, positive	Limited resources	Sufficient frequency resource, sparse deployment of WBANs
Time rescheduling	Simple, effective, positive	Sensitive to topology and energy consumption	Stable network topology, sparse deployment of WBANs
Co-channel interference mitigation	Adaptive, passive	Inefficient	Basically all environment
WBAN: wireless body area network			

and frequently changing network topology, resource allocation may not be appropriate because of the lack of channels and insufficient assigning time. Co-channel interference mitigation is suitable in such scenarios. With co-channel interference mitigation, the transmission strategy is adjusted according to the environment so that performance degradation is minimized. The density of WBAN deployment, rate of topology change, and number of time and frequency resources all affect the choice of inter-WBAN interference mitigation solution. Although we have classified these solutions as channel assignment, time rescheduling, and co-channel interference mitigation, they are not mutually exclusive. Co-channel interference mitigation solutions can complement resources-allocation solutions. To further improve existing solutions, there are some unresolved issues that need to be addressed.

## 4 Open Research Issues

### 4.1 Link Diversity

In [21], [44]–[46], intra-WBAN communication is modeled as a single link for simplified analysis. However, the links from intra-WBAN sensors to the coordinator are different because sensors are positioned differently and the body is moving. Hence, link diversity inside the WBAN needs to be considered when dealing with inter-WBAN interference.

### 4.2 Unequal QoS Requirements

Another aspect that is often overlooked is varied QoS requirements for sensors inside the WBAN and for different WBAN users. Intra-WBAN sensors may have different requirements in terms of transmission latency, data rate, priority and PLR, and the amount of interference they experience. Thus, the WBAN should not be regarded as a homogeneous network when designing an interference-mitigation solution. There are also personalized WBANs to serve individual needs, and these tend to have different performance demands. These different demands should not be ignored as well.

### 4.3 Mobility

A characteristic of a WBAN is random mobility. This is the

combination of sensor mobility, due to body movements, and WBAN mobility, due to daily activities. Sensor mobility results in a change of intra-WBAN topology and internal link gain, which may lead to a failure of convergence of the power control game in a co-channel interference mitigation solution. Unconscious movements change the inter-WBAN topology and cause problems with the resource management strategy for inter-WBAN coexistence. For example, two WBAN users who are initially far apart may be assigned the same channel according to a certain resource-allocation strategy. When the users move close to each other, a collision occurs. Mobility creates some serious challenges for current interference mitigation solutions. However, in order to make the deployment of WBANs more widespread, more attention has to be paid to mobility. In [1], [40], [49], [50], the authors have made some preliminary attempts to analyze mobility in relation to mitigation of inter-WBAN interference.

### 4.4 Auxiliary Information

A WBAN is a body-centric network and the human behavior and neighboring environment would affect inter-WBAN coexistence. For example, the density of WBANs is very different in a coffee shop or subway station. The social relations between WBAN users may also affect the distance between WBANs. Though some efforts made in [21], [22] have considered the environmental support, the social attributes of WBAN are still not be utilized sufficiently and need further investigated.

## 5 Conclusion

This paper presented a deep analysis of the inter-WBAN coexistence issue and provided a broad overview of the inter-WBAN coexistence and interference mitigation strategies. The solutions to solve the coexistence problem, including channel assignment strategies, time rescheduling strategies, co-channel interference mitigation strategies, etc., were summarized in this work. Some constructive suggestions were also proposed for the study of inter-WBAN coexistence problem in the future.

### References

- [1] IEEE. (2012). *802.15.6-2012—IEEE standard for local and metropolitan area networks—part 15.6: wireless body area networks* [Online]. Available: standards.ieee.org/findstds/standard/802.15.6-2012.html
- [2] D. M. Barakah and M. Ammad-uddin, "A survey of challenges and applications of wireless body area network (WBAN) and role of a virtual doctor server in existing architecture," in *2012 Third International Conference on Intelligent Systems, Modelling and Simulation (ISMS)*, Kota Kinabalu, Malaysia, 2012, pp. 214–219. doi: 10.1109/ISMS.2012.108.
- [3] S. Ullah, H. Higgins, B. Braem, *et al.*, "A comprehensive survey of wireless body area networks," *Journal of Medical Systems*, vol. 36, no. 3, pp. 1065–1094, Jun. 2012. doi: 10.1007/s10916-010-9571-3.
- [4] M. Chen, S. Gonzalez, A. Vasilakos, *et al.*, "Body area networks: a survey," *Mobile Networks and Applications*, vol. 16, no. 2, pp. 171–193, Apr. 2011. doi: 10.1007/s11036-010-0260-8.
- [5] IEEE. (2010). *802.15.1-2005—IEEE standard for information technology—local and metropolitan area networks—specific requirements—part 15.1a: wireless medium access control (MAC) and physical layer (PHY) specifications for wireless personal area networks (WPAN)* [Online]. Available: standards.ieee.org/findstds/



## Inter-WBAN Coexistence and Interference Mitigation

Bin Liu, Xiaosong Zhao, Lei Zou, and Chang Wen Chen

- standard/802.15.1-2005.html
- [6] E. Georgakakis, S. A. Nikolidakis, D. D. Vergados, and C. Douligeris, "An analysis of bluetooth, zigbee and bluetooth low energy and their use in WBANs," *Wireless Mobile Communication and Healthcare*, vol. 55, pp. 168–175, 2011. doi: 10.1007/978-3-642-20865-2\_22.
  - [7] IEEE. (2011). 802.15.4-2011—IEEE standard for local and metropolitan area networks--part 15.4: low-rate wireless personal area networks (LR-WPANs) [Online]. Available: standards.ieee.org/findstds/standard/802.15.4-2011.html
  - [8] L. Januszkiwicz, "Simplified human body models for interference analysis in the cognitive radio for medical body area networks," in *8th International Symposium on Medical Information and Communication Technology (ISMICT)*, Firenze, Italy, Apr. 2014, pp. 1–5. doi: 10.1109/ISMICT.2014.6825246.
  - [9] R. Chavez-Santiago, K. E. Nolan, O. Holland, et al., "Cognitive radio for medical body area networks using ultra wideband," *IEEE Wireless Communications*, vol. 19, no. 4, pp. 74–81, Aug. 2012. doi: 10.1109/MWC.2012.6272426.
  - [10] I. Kirbas, A. Karahan, A. Sevin, and C. Bayilmis, "isMAC: an adaptive and energy-efficient MAC protocol based on multi-channel communication for wireless body area networks," *KSI Transactions on Internet and Information Systems*, vol. 7, no. 8, pp. 1805–1824, Aug. 2013. doi: 10.3837/tiis.2013.08.004.
  - [11] B. R. Gonchikar, V. Geetha, and R. Kunabeva, "An adaptive routing mechanism for wireless body area network (WBAN)," *International Journal of Innovative Research and Development*, vol. 3, no. 6, Jun. 2014.
  - [12] H. Mounsla, A. Jarray, A. Karmouch, and A. Mehaoua, "Cost-effective reliability- and energy-based intra-WBAN interference mitigation," in *IEEE Global Communications Conference (GLOBECOM)*, Austin, USA, Dec. 2014, pp. 2399–2404. doi: 10.1109/GLOCOM.2014.7037167.
  - [13] W. Yang and K. Sayrafian-Pour, "Interference mitigation using adaptive schemes in body area networks," *International Journal of Wireless Information Networks*, vol. 19, no. 3, pp. 193–200, Sept. 2012. doi: 10.1007/s10776-012-0192-2.
  - [14] T. Hayajneh, G. Almashaqbeh, S. Ullah, and A. V. Vasilakos, "A survey of wireless technologies coexistence in WBAN: analysis and open research issues," *Wireless Networks*, vol. 20, no. 8, pp. 2165–2199, Nov. 2014. doi: 10.1007/s11276-014-0736-8.
  - [15] N. Torabi and V. C. M. Leung, "Realization of public m-health service in license-free spectrum," *IEEE Journal of Biomedical and Health Informatics*, vol. 17, no. 1, pp. 19–29, Jan. 2013. doi: 10.1109/JTHB.2012.2227117.
  - [16] Y. Kim, S. Lee, and S. Lee, "Coexistence of ZigBee-based WBAN and WiFi for health telemonitoring systems," *IEEE Journal of Biomedical and Health Informatics*, vol. PP, no. 99, Jan. 2015. doi: 10.1109/JBHI.2014.2387867.
  - [17] M. U. Memon, L. X. Zhang, and B. Shaikh, "Packet loss ratio evaluation of the impact of interference on zigbee network caused by Wi-Fi (IEEE 802.11b/g) in e-health environment," in *IEEE 14th International Conference on e-Health Networking, Applications and Services (Healthcom)*, Beijing, China, Oct. 2012, pp. 462–465. doi: 10.1109/HealthCom.2012.6379462.
  - [18] A. Zhang, D. B. Smith, D. Miniutti, et al., "Performance of piconet co-existence schemes in wireless body area networks," in *IEEE Wireless Communications and Networking Conference (WCNC)*, Sydney, Australia, Apr. 2010, pp. 1–6. doi: 10.1109/WCNC.2010.5506746.
  - [19] L. W. Hanlen, D. Miniutti, D. Smith, et al., "Co-channel interference in body area networks with indoor measurements at 2.4 GHz: distance-to-interferer is a poor estimate of received interference power," *International Journal of Wireless Information Networks*, vol. 17, no. 3–4, pp. 113–125, Dec. 2010. doi: 10.1007/s10776-010-0123-z.
  - [20] W. Xuan and C. Lin, "Interference analysis of co-existing wireless body area networks," in *IEEE Global Telecommunications Conference (GLOBECOM 2011)*, Houston, USA, Dec. 2011, pp. 1–5. doi: 10.1109/GLOCOM.2011.6133624.
  - [21] Z. Zhang, H. Wang, C. Wang, and H. Fang, "Interference mitigation for cyber-physical wireless body area network system using social networks," *IEEE Transactions on Emerging Topics in Computing*, vol. 1, no. 1, pp. 121–132, Jun. 2013. doi: 10.1109/TETC.2013.2274430.
  - [22] B. de Silva, A. Natarajan, and M. Motani, "Inter-user interference in body sensor networks: preliminary investigation and an infrastructure-based solution," in *Sixth International Workshop on Wearable and Implantable Body Sensor Networks*, Berkeley, USA, Jun. 2009, pp. 35–40. doi: 10.1109/BSN.2009.36.
  - [23] E. Sarra, H. Mounsla, S. Benayoune, and A. Mehaoua, "Coexistence improvement of wearable body area network (WBAN) in medical environment," in *IEEE International Conference on Communications (ICC)*, Sydney, Australia, 2014, pp. 5694–5699. doi: 10.1109/ICC.2014.6884229.
  - [24] W. Lee, S. H. Rhee, Y. Kim, and H. Lee, "An efficient multi-channel management protocol for wireless body area networks," in *International Conference on Information Networking*, Chiang Mai, Thailand, Jan. 2009, pp. 1–5.
  - [25] C. Ren, H. Yu, C. Ma, et al., "An energy-efficient spectrum handoff and access mechanism for the WBAN system," in *IEEE/CIC International Conference on Communications in China—Workshops (CIC/ICCC)*, Xi'an, China, Aug. 2013, pp. 125–130. doi: 10.1109/ICCCChinaW.2013.6670580.
  - [26] J. Mahapatro, S. Misra, M. Manjunatha, and N. Islam, "Interference-aware channel switching for use in WBAN with human sensor interface," in *4th International Conference on Intelligent Human Computer Interaction (IHCI)*, Kharagpur, India, Dec. 2012, pp. 1–5. doi: 10.1109/IHCI.2012.6481814.
  - [27] M. N. Deylami and E. Jovanov, "A distributed scheme to manage the dynamic coexistence of IEEE 802.15.4-based health-monitoring WBANs," *IEEE Journal of Biomedical and Health Informatics*, vol. 18, no. 1, pp. 327–334, Jan. 2014. doi: 10.1109/JBHI.2013.2278217.
  - [28] S. Movassaghi, M. Abolhasan and D. Smith, "Smart spectrum allocation for interference mitigation in wireless body area networks," in *IEEE International Conference on Communications (ICC)*, Sydney, Australia, Jun. 2014, pp. 5688–5693. doi: 10.1109/ICC.2014.6884228.
  - [29] S. Movassaghi, M. Abolhasan, D. Smith, and A. Jamalipour, "AIM: adaptive internetwork interference mitigation amongst co-existing wireless body area networks," in *IEEE Global Communications Conference (GLOBECOM)*, Austin, USA, Dec. 2014, pp. 2460–2465. doi: 10.1109/GLOCOM.2014.7037177.
  - [30] S. H. Cheng and C. Y. Huang, "Coloring-based inter-wban scheduling for mobile wireless body area networks," *IEEE Transactions on Parallel and Distributed Systems*, vol. 24, no. 2, pp. 250–259, Feb. 2013. doi: 10.1109/TPDS.2012.133.
  - [31] S. Movassaghi, M. Abolhasan, and D. Smith, "Cooperative scheduling with graph coloring for interference mitigation in wireless body area networks," in *IEEE Wireless Communications and Networking Conference (WCNC)*, Istanbul, Turkey, Apr. 2014, pp. 1691–1696. doi: 10.1109/WCNC.2014.6952484.
  - [32] P. R. Grassi, V. Rana, I. Beretta, and D. Sciuto, "B2IRS: a technique to reduce BAN-BAN interferences in wireless sensor networks," in *Ninth International Conference on Wearable and Implantable Body Sensor Networks (BSN)*, London, UK, May 2012, pp. 46–51. doi: 10.1109/BSN.2012.30.
  - [33] E. Kim, S. Youm, T. Shon, and C. Kang, "Asynchronous inter-network interference avoidance for wireless body area networks," *The Journal of Supercomputing*, vol. 65, no. 2, pp. 562–579, 2013. doi: 10.1007/s11227-012-0840-4.
  - [34] A. Jamthe, A. Mishra, and D. P. Agrawal, "Scheduling schemes for interference suppression in healthcare sensor networks," in *IEEE International Conference on Communications (ICC)*, Sydney, Australia, Jun. 2014, pp. 391–396. doi: 10.1109/ICC.2014.6883350.
  - [35] J. Mahapatro, S. Misra, M. Manjunatha, and N. Islam, "Interference mitigation between WBAN equipped patients," in *Ninth International Conference on Wireless and Optical Communications Networks (WOCN)*, Indore, India, Sept. 2012, pp. 1–5. doi: 10.1109/WOCN.2012.6331909.
  - [36] J. Mahapatro, S. Misra, M. Mahadevappa, and N. Islam, "Interference-aware MAC scheduling and admission control for multiple mobile WBANs used in healthcare monitoring," *International Journal of Communication Systems*, vol. 28, no. 7, pp. 1352–1366, May 2015. doi: 10.1002/dac.2768.
  - [37] S. Wen, G. Yu, and W. Wai-Choong, "A lightweight inter-user interference mitigation method in body sensor networks," in *IEEE 8th International Conference on Wireless and Mobile Computing, Networking and Communications (WiMob)*, Barcelona, Spain, Oct. 2012, pp. 34–40. doi: 10.1109/WiMOB.2012.6379098.
  - [38] K. Seungku, K. Seokhwan, K. Jin-Woo, and E. Doo-Seop, "Flexible beacon scheduling scheme for interference mitigation in body sensor networks," in *9th Annual IEEE Communications Society Conference on Sensor, Mesh and Ad Hoc Communications and Networks (SECON)*, Seoul, South Korea, Jun. 2012, pp. 157–164. doi: 10.1109/SECON.2012.6275772.
  - [39] S. Kim, S. Kim, J. Kim, and D. Eom, "A Beacon Interval Shifting Scheme for Interference Mitigation in Body Area Networks," *Sensors*, vol. 12, no. 8, pp. 10930–10946, Aug. 2012. doi: 10.3390/s120810930.
  - [40] D. Jie and D. Smith, "Cooperative body-area-communications: Enhancing coexistence without coordination between networks," in *IEEE 23rd International Symposium on Personal Indoor and Mobile Radio Communications (PIMRC)*, Sydney, Australia, Sept. 2012, pp. 2269–2274. doi: 10.1109/PIMRC.2012.6362733.
  - [41] D. Jie and D. Smith, "Opportunistic relaying in wireless body area networks: coexistence performance," in *IEEE International Conference on Communications (ICC)*, Budapest, Hungary, 2013, pp. 5613–5618.
  - [42] Z. Xie, G. Huang, J. He, and Y. Zhang, "A clique-based WBAN scheduling for mobile wireless body area networks," *Procedia Computer Science*, vol. 31, pp. 1092–1101, 2014. doi: 10.1016/procs.2014.05.364.
  - [43] Z. Lei, L. Bin, C. Chang, and W. C. Chang, "Bayesian game based power con-

## Inter-WBAN Coexistence and Interference Mitigation

Bin Liu, Xiaosong Zhao, Lei Zou, and Chang Wen Chen

trol scheme for inter-WBAN interference mitigation," in *IEEE Global Communications Conference (GLOBECOM)*, Austin, USA, Dec. 2014, pp. 240–245. doi: 10.1109/GLOCOM.2014.7036814.

- [44] G. Wu, J. Ren, F. Xia, *et al.*, "A game theoretic approach for interuser interference reduction in body sensor networks," *International Journal of Distributed Sensor Networks*, vol. 2011, article ID 329524, 2011. doi: 10.1155/2011/329524.
- [45] M. Nazir and A. Sabah, "Cooperative cognitive WBAN: from game theory to population dynamism," in *3rd International Congress on Ultra Modern Telecommunications and Control Systems and Workshops (ICUMT)*, Budapest, Hungary, Oct. 2011, pp. 1–6.
- [46] R. Kazemi, R. Vesilo, E. Dutkiewicz, and F. Gengfa, "Inter-network interference mitigation in wireless body area networks using power control games," in *International Symposium on Communications and Information Technologies (IS-CIT)*, Tokyo, Japan, Oct. 2010, pp. 81–86. doi: 10.1109/ISCIT.2010.5664908.
- [47] R. Kazemi, R. Vesilo, E. Dutkiewicz, and P. L. Ren, "Design considerations of reinforcement learning power controllers in wireless body area networks," in *IEEE 23rd International Symposium on Personal Indoor and Mobile Radio Communications (PIMRC)*, Sydney, Australia, Sept. 2012, pp. 2030–2036. doi: 10.1109/PIMRC.2012.6362688.
- [48] R. Kazemi, R. Vesilo, and E. Dutkiewicz, "A novel genetic-fuzzy power controller with feedback for interference mitigation in wireless body area networks," in *IEEE 73rd Vehicular Technology Conference (VTC Spring)*, Yokohama, Japan, May 2011, pp. 1–5. doi: 10.1109/VETECS.2011.5956462.
- [49] Z. Chen and M. L. Sichitiu, "N-body: social based mobility model for wireless ad hoc network research," in *7th Annual IEEE Communications Society Conference on Sensor Mesh and Ad Hoc Communications and Networks (SECON)*, Boston, USA, Jun. 2010, pp. 1–9. doi: 10.1109/SECON.2010.5508280.
- [50] M. Nabi, M. Geilen, and T. Basten, "MoBAN: a configurable mobility model for wireless body area networks," in *4th International ICST Conference on Simulation Tools and Techniques*, Barcelona, Spain, Mar. 2011, pp. 168–177. doi: 10.4108/icst.simutools.2011.245511.

Manuscript received: 2015-03-26

## Biographies

**Bin Liu** (flowice@ustc.edu.cn) is an associate professor in the School of Information Science and Technology, University of Science and Technology of China (USTC). He received his BS and MS degrees in electrical engineering from USTC in 1998 and 2001. He received his PhD degree in electrical engineering from Syracuse University, USA in 2006. He was selected in Program for New Century Excellent Talents in Universities of China 2009. His research interests include signal processing and communications in wireless sensor and body area networks.

**Xiaosong Zhao** (zhaoxiaosong124@sina.com) is a Master's degree student at the School of Information Science and Technology, USTC. He received his BE degree in electronic information engineering from Chongqing University, China in 2013. His research interests include inter-WBAN interference mitigation and data mining.

**Lei Zou** (zoule@mail.ustc.edu.cn) is a doctoral student in information and communication engineering at USTC. He received his BE degree in electronic engineering from USTC in 2011. His research interests include coexistence of wireless devices and interference mitigation, particularly related to WBANs.

**Chang Wen Chen** is a professor of Computer Science and Engineering at the State University of New York at Buffalo, USA. Previously, he was Allen S. Henry Endowed Chair Professor at Florida Institute of Technology from 2003 to 2007, a faculty member at the University of Missouri - Columbia from 1996 to 2003 and at the University of Rochester, Rochester, NY, from 1992 to 1996. He has been the Editor-in-Chief for *IEEE Trans. Multimedia* since 2014. He has also served as the Editor-in-Chief for *IEEE Trans. Circuits and Systems for Video Technology* from January 2006 to December 2009 and an Editor for Proceedings of IEEE, IEEE T-MM, IEEE JSAC, IEEE JETCAS, and IEEE Multimedia Magazine. He is a recipient of Sigma Xi Excellence in Graduate Research Mentoring Award in 2003, Alexander von Humboldt Research Award in 2009, and SUNY-Buffalo Exceptional Scholar—Sustained Achievements Award in 2012. He is an IEEE Fellow and an SPIE Fellow.

## Roundup

## Call for Papers

### ZTE Communications Special Issue on Optical Wireless Communications

Optical wireless communication, which serves as an important alternative to the radio-frequency communication, shows great potential to a lot of applications, such as indoor communication, secure communication, and battlefield communication. It has attracted increasing research interests from both academia and industrial fields. Moreover, optical wireless communication has been applied to the indoor communication and positioning system. The upcoming special issue of *ZTE Communication* will focus on the cutting-edge research and application on the communication system and related signal processing in optical wireless communication. The expected publication date will be in Mar. 2016. It includes (but not limited to) the following research directions:

- Coded modulation;
- Channel modeling and estimation;
- Ultra-density transceiver technology;
- Signal detection and estimation in the non-Gaussian noise;
- Design and implementation on the transceiver architecture;
- Interference signal processing;
- Integrated communication and positioning;
- UV optical wireless communications;

- Underwater, free-space, and vehicle-to-vehicle optical wireless communication;
- Optical wireless communication system optimization.

#### Paper Submission

Please directly send to cgong821@ustc.edu.cn and copy to all guest editors, and use the email title "ZTE-OWC-Paper-Submission".

#### Tentative Schedule

Paper submission due: 9/30/2015;  
Review complete: 11/30/2015;  
Final manuscript due: 12/31/2015.

#### Guest Editors

**Prof. Xiaodong Wang**, Columbia University (xw2008@columbia.edu)

**Prof. Chen Gong**, University of Science and Technology of China (cgong821@ustc.edu.cn)

**Prof. Xuan Tang**, CAS Quanzhou Institute of Equipment Manufacturing (xtang@fjirsm.ac.cn)

# A Visual Lossless Image -Recompression Framework

Ping Lu<sup>1</sup>, Xia Jia<sup>1</sup>, Hengliang Zhu<sup>2</sup>, Ming Liu<sup>1</sup>,  
Shouhong Ding<sup>2</sup>, and Lizhuang Ma<sup>2</sup>

(1. ZTE Corporation, Shenzhen 518057, China;

2. Shanghai Jiao Tong University, Shanghai 200240, China)

## Abstract

In this paper, we propose a novel image recompression framework and image quality assessment (IQA) method to efficiently recompress Internet images. With this framework image size is significantly reduced without affecting spatial resolution or perceptible quality of the image. With the help of IQA, the relationship between image quality and image evaluation scores can be quickly established, and the optimal quality factor can be obtained quickly and accurately within a pre-determined perceptual quality range. This process ensures the image's perceptual quality, which is applied to each input image. The test results show that, using the proposed method, the file size of images can be reduced by about 45%–60% without affecting their visual quality. Moreover, our new image -recompression framework can be used in to many different application scenarios.

## Keywords

image recompression; image quality assessment; user experience; visual lossless

## 1 Introduction

**B**ecause of rapid growth in the number of images in the network and user demands for better image quality and faster loading, image-compression technology has become a research focus. Many commercial applications have been designed to improve user experience and save cost by reducing the size of color images. Many companies have developed image -compression algorithms and have achieved a higher compression ratio without obvious loss of visual quality. Google has developed its own web image format [1], and Mozilla has developed mozjpeg [2] image -com-

pression format.

The Joint Photographic Experts Group (JPEG) standard [3] and JPEG 2000 standard [4] reduce the size of images without obviously affecting image quality. Most images currently on the Internet are JPEG images, and the JPEG baseline algorithm has been used widely in many digital -imaging applications. JPEG lossless compression saves device storage memory and transmission bandwidth [5]. Our work mainly focuses on recompressing JPEG images in order to further reduce their size [6].

Image quality is very important. In general, most people are less interested in how lossy compression is implemented; their main concern is that the visual quality of the compressed image is reasonable. Most people are willing to trade off fine image quality for the ability to save more images in a limited space. We use the Image Quality Assessment (IQA) method to preserve the perceptual quality of images. This method can be used to accurately predict the quality of a compressed image prior to compression.

## 2 Related Works

Many objective IQA algorithms have been proposed to evaluate image quality [7]. The goal of research on objective IQA is to develop quantitative measures for automatically evaluating image quality. Depending on whether the image is an original or whether a reference image is used, objective image quality metrics can be classified as full -reference, reduced -reference, or no -reference. We use full -reference IQA in our proposed recompression system. Over the past decade, researchers have proposed various utility IQAs, including mean squared error (MSE), peak signal -to -noise ratio (PSNR), structural similarity (SSIM) index, information content weighted SSIM (IW -SSIM) index, and feature similarity (FSIM) index.

Early image -quality metrics that were widely used are MSE and PSNR. These metrics are determined by averaging the squared intensity differences of distorted and reference image pixels and were popular because they are simple to calculate and have clear physical meanings.

In 2004, Wang *et al.* [8] proposed SSIM, a state -of -the -art IQA model. SSIM is based on the hypothesis that the human visual system (HVS) is highly adapted to extract structural information from a visual scene. This metric involving structural similarity can provide a good approximation of the perceived image quality. Wang *et al.* [9] then proposed a multiscale extension of SSIM (MS -SSIM) that performed better than SSIM. Wang and Li [10] further improved on MS -SSIM by introducing a new information content -weighting quality -score pooling strategy. The resulting IW -SSIM performed better than MS -SSIM.

In 2011, Shoham *et al.* proposed a perceptual image quality measure called Block -Based Coding Quality (BBCQ) [11]. This metric evaluates the pixel -wise error using PSNR, added artifactual edges along coding block boundaries, and texture

This research work was supported in part by China "973" Program under Grant No.2014CB340303.

distortion. In BBCQ, a weighted geometric average is used to combine these three measures.

Lin Zhang *et al.* proposed the FSIM index [12]. This new metric uses phase congruency and gradient magnitude to construct the local similarity map. The authors suggest that phase congruency and gradient magnitude play an important role in characterizing local image quality.

We have designed and implemented an image -recompression framework in which image recompression does not perceptibly reduce image quality. This framework is robust and efficient in many different applications. Experimental results show that the framework adaptively recompresses massive color JPEG images and that the loss associated with this recompression is imperceptible to the human eye.

### 3 Application Descriptions

Our framework for efficient image recompression (**Fig. 1**) is intended to save as much bandwidth and storage as possible in applications involving massive Internet images.

## 4 Architecture and Design

### 4.1 Overview

Our proposed image -recompression system is based on IQA. It accepts an input image, typically in JPEG format, and outputs a recompressed JPEG image. This recompressed image is perceptually identical to the input image, but the file size is smaller. In our framework, image recompression can also be customized for different applications.

The image -recompression framework has six components: input image, initial recompression, quality measure, system control, image recompression, and output image (**Fig. 2**).

### 4.2 Components

The first component is the input image, which initializes the system. The framework computes the original quality factor of this image. The second component is initial recompression, during which the fixed quality factor is used to recompress the input image.

The third component is the quality measure, which is used to determine the quality of the recompressed image relative to the input image. This measure is based on gradient and texture similarity quality (GPT -IQA) and is more practical and accurate than other perceptual image quality measures. GPT -IQA has a range of 0 to 1, with 1 indicating an identical image and 0 indicating the worst image. GPT -IQA is based on gradient similarity, PSNR similarity, and texture distortion similarity. These three measures are combined by using an arithmetic mean, given by:

$$S_{GPT} = \text{Mean}(\text{graSim} \times \text{psnrSim} \times \text{tdSim}) \quad (1)$$

where  $S_{GPT}$  is the GPT -IQA score and  $\text{graSim}$ ,  $\text{psnrSim}$  and  $\text{tdSim}$  are the three measurement factors for GPT -IQA. We first divide the input image into many tiles, the sizes of which depend on the input image resolution. Then, the three factors are determined for each image tile. This metric evaluates the difference in quality between the original image and reference image.

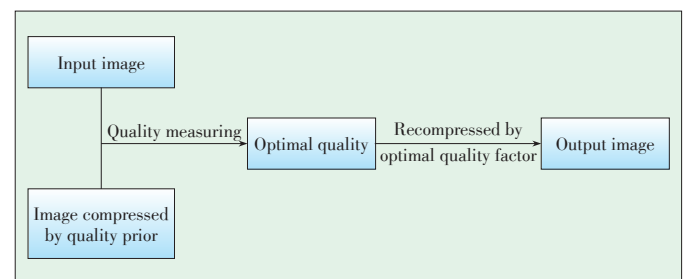
The fourth component is the system controller, which controls image recompression. The distribution of the quality factor and metric fit a sigmoid function. In **Fig. 3**, we use the two quality -score pairs to construct the sigmoid function. The first pair is the original quality factor and a score of 1; the second pair is a fixed quality factor and calculated score. Then we can obtain the optimal compression quality factor from the predetermined perceptual quality score. We can also obtain an optimal compression level for different applications by modifying this score.

The fifth and sixth components are image recompression and output image. The optimal target compression quality factor determined by the system controller is used to recompress the input image, and the final image is then output.

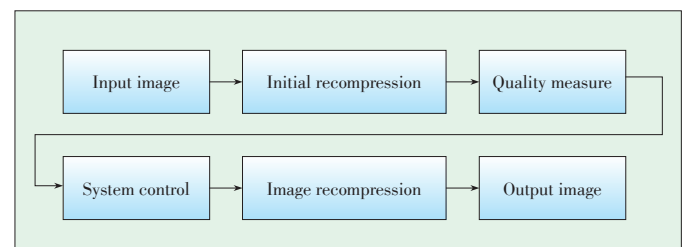
### 4.3 Image Quality Assessment

Previous work indicates that gradient magnitudes and texture significantly affect image quality. Therefore, we propose using an IQA method based on gradient similarity and texture similarity to measure image quality. We also add PSNR to make the results more closely resemble a subjective evaluation.

An image gradient is a directional change in the intensity or color in an image. Image gradients may be used to extract information from images, and calculation of the image gradient well -covered topic in image processing. Gradient operators can be expressed by convolution masks. In this paper, we use Prewitt



▲ Figure 1. Image recompression framework.



▲ Figure 2. Image recompression process.



### A Visual Lossless Image -Recompression Framework

Ping Lu, Xia Jia, Hengliang Zhu, Ming Liu, Shouhong Ding, and Lizhuang Ma

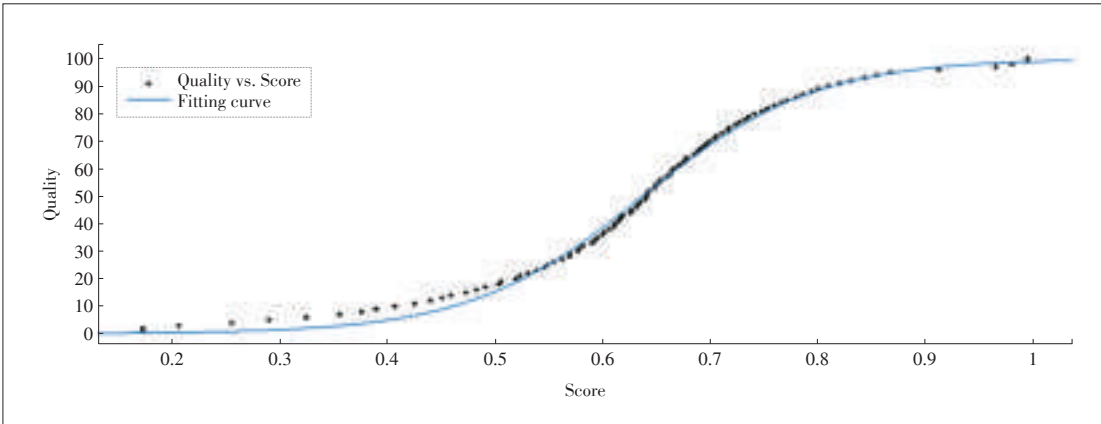


Figure 3. Quality and score curve fitting.

operator as the gradient operator. The gradient magnitude is given by:

$$G_x = \frac{1}{3} \begin{bmatrix} 1 & 0 & -1 \\ 1 & 0 & -1 \\ 1 & 0 & -1 \end{bmatrix} * \text{img} \quad (2)$$

$$G_y = \frac{1}{3} \begin{bmatrix} 1 & 1 & 1 \\ 0 & 0 & 0 \\ -1 & -1 & -1 \end{bmatrix} * \text{img} \quad (3)$$

$$G = \sqrt{G_x^2 + G_y^2} \quad (4)$$

We compare the similarity between image  $X$  and  $Y$ . The similarity measure for  $G(X)$  and  $G(Y)$  is:

$$\text{graSim} = [2G(X) \times G(Y) + \varepsilon] / [G^2(X) + G^2(Y) + \varepsilon] \quad (5)$$

where  $\varepsilon$  is a positive constant that depends on the dynamic range of image's gradient magnitude values.

We use local texture similarity and local PSNR to compare differences between the source and test images. Statistics are computed within a local  $8 \times 8$  window that moves pixel-by-pixel over the entire image [13]. One problem with this method is that the resulting statistics often exhibit undesirable "blocking" artifacts. In this paper, we use an  $11 \times 11$  Gaussian weighting function  $W = \{w_i | i = 1, 2, \dots, N\}$ , with standard deviation of 1.5 samples, normalized to unit  $\sum_i w_i = 1$ . The estimates of local statistics PSNR and texture  $\sigma(X)$ ,  $\sigma(Y)$ , of images  $X$  and  $Y$  are then:

$$d^2 = \sum_{i=1}^N w_i (x_i - y_i)^2 \quad (6)$$

$$\text{psnr} = 10 \log_{10} \left( \frac{(2^k - 1)^2}{d^2} \right) \quad (7)$$

$$\mu_1 = \sum_{i=1}^N w_i \times x_i \quad (8)$$

$$\mu_2 = \sum_{i=1}^N w_i \times y_i \quad (9)$$

$$\sigma_1^2 = \sum_{i=1}^N w_i (x_i - \mu_1)^2 \quad (10)$$

$$\sigma_2^2 = \sum_{i=1}^N w_i (x_i - \mu_2)^2 \quad (11)$$

Then PSNR similarity and texture similarity are given by:

$$\text{psnrSim} = \min(\text{psnr}/\text{THR}_{\text{psnr}}, 1) \quad (12)$$

$$\text{texSim} = (2\sigma_1\sigma_2 + T) / (\sigma_1^2 + \sigma_2^2 + T) \quad (13)$$

Finally, we pool the three measures to obtain a similarity score for images  $X$  and  $Y$  (1).

#### 4.4 Optimal Quality Factor

Generally, for satisfactory recompression, the optimal target compression level can be figured out by continuous iterations. However, immoderate iterations often severely limit recompression performance. To reduce the number of iterations and increase recompression efficiency, we focus on an optimal compression level.

Using our image quality measure with its default parameters, we first analyze the relationship between the image quality factor and GPT-IQA similarity score. We observe more than 10,200 Internet images and construct a perceptual similarity prior, i.e., the quality-score distribution of one image can be fitted to a sigmoid function, defined as:

$$f(x) = 100 / (1 + e^{-ax+b}) \quad (14)$$

where  $x$  is the similarity score, and  $f(x)$  is the compressed quality factor. Given  $(x_1, f(x_1))$  and  $(x_2, f(x_2))$ , the unknown coefficients are:

$$a = \frac{\ln\left(\frac{100}{f(x_1)} - 1\right) - \ln\left(\frac{100}{f(x_2)} - 1\right)}{x_2 - x_1} \quad (15)$$

$$b = \ln\left(\frac{100}{f(x_1)} - 1\right) + ax_1 \quad (16)$$



For the above distribution function, we have to first compute two of quality -score pairs. When  $s = 1$ ,  $Q(s)$  approximates the source compression level of the input image. We can efficiently avoid one of those two pairs by estimating its compression quality from the source image. Given the quantization matrix of the source image  $M_s$  and the baseline matrix  $M_b$ , we can estimate the compression quality using their linear transformations, given by:

$$Q(1) \approx \min_q \sum_i \frac{|M_q(i) - M_s(i)|}{M_b(i)} \quad (17)$$

where  $q$  is the image quality and  $M_q$ , is its quantization matrix based on  $M_b$ . According to (17), we can initialize one of the quality - score pairs,  $s_1 = 1.0$ ,  $Q(s_1)$ . Moreover, given  $Q = 60$ , we can determine that  $s_2$ ,  $Q(s_2) = 50$ .

After obtaining the two quality -score pairs, we can produce the corresponding optimal quality factor. Given the score threshold  $S_t$ , the optimal quality factor is:

$$Q(s_t) = 100 / (1 + e^{-a(s_t - b)}) \quad (18)$$

#### 4.5 Algorithm

**Algorithm 1** shows the steps of image -recompression.

##### Algorithm 1. Image Recompression

Input: An image and required parameters

1. Get file size and other information of input image. If image size is very small or the image is not a normal image, then directly copy it.
2. Get quantization tables and source quality factor of the input image. If source quality factor is less than 60, then copy it.
3. Judge whether the quantization tables are standard quantization tables, if not, save the image according to its quantization tables.
4. Compress the input image by  $Q_{low}$ , and compare the resulting image with input image through GPT\_IQA method to get quality score  $S_{low}$ .
5. Predict parameters  $a$  and  $b$  of Sigmoid function from quality-score pairs  $(Q_{init}, S_{init})$  and  $(Q_{low}, S_{low})$ .
6. Get optimal quality factor  $Q_{opt}$  according to the sigmoid function and threshold quality score  $S_{threshold}$ . If  $Q_{opt}$  is between  $Q_{low}$  and  $Q_{init}$ , turn to step (8), else turn to step (7).
7. Get  $Q_{opt}$  as the average value of  $Q_{low}$  and  $Q_{init}$ .
8. Recompress the input image by  $Q_{opt}$ .

Output: recompressed image

## 5 Experiments and Evaluation

We investigated the potential of GPT-IQA in our image -recompression framework. Our experiments were run on a PC with Intel®Xeon® CPU w3530 at 2.80 GHz and using Windows 7.

### 5.1 Proposed IQA and Other IQAs

There are many publicly available image datasets in the IQA community, including TID2013 [14], TID2008 [15], CSIQ

[16], and LIVE [17]. In our experiment, we chose the CSIQ as our test dataset. Two commonly used performance metrics are used to evaluate the IQA metrics: Spearman rank -order correlation coefficient (SROCC) and Kendall rank -order correlation coefficient (KROCC), which can measure the prediction monotonicity of an IQA metric. To prove that our method is more accurate than existing IQA for assessing JPEG image quality, we determine the quality of every compressed JPEG image and then obtain the SROCC and KROCC (**Table 1**).

▼ **Table 1. Comparison of different IQAs**

Metric	IQA			
	BBCQ	SSIM	FSIM	Proposed
SROCC	0.9596	0.9546	0.9654	0.9642
KROCC	0.8235	0.8167	0.8386	0.8326
BBCQ: Block -Based Coding Quality FSIM: feature similarity index IQA: image quality assessment KROCC: Kendall rank -order correlation coefficient SROCC: Spearman rank -order correlation coefficient SSIM: structural similarity index				

In Table 1, our method and FSIM are better than the other two IQAs. However, our method is faster than FSIM in obtaining the optimal quality factor, and our proposed IQA only needs to calculate image's quality score twice, whereas FSIM needs to calculate it more times.

### 5.2 Compression Time and Ratio for Different Types of Images

Different types of images have different structures; therefore, compressing all types of images to the same ratio is not ideal. **Table 2** shows the different compression ratios for different types of images. The average picture compression time is less than 10 ms for images with a resolution of less than  $400 \times 400$  pixels. The average compression time is 23.734 ms for images of objects with a resolution of less than  $640 \times 480$  pixels. The average compression time is 157.091 ms for images of paintings with a resolution of less than  $2300 \times 2300$  pixels.

We can compress images of buildings more than images of objects because most images of buildings have fewer colors and their structures are more regular.

In **Fig. 4**, there are no perceptible differences between the pictures before and after compression. Thus the compression is lossless. The compressed image file is much smaller than the original image file, but the quality of the recompressed image remains high. Therefore, the lossless image -compression algorithm performs very well.

## 6 Conclusion

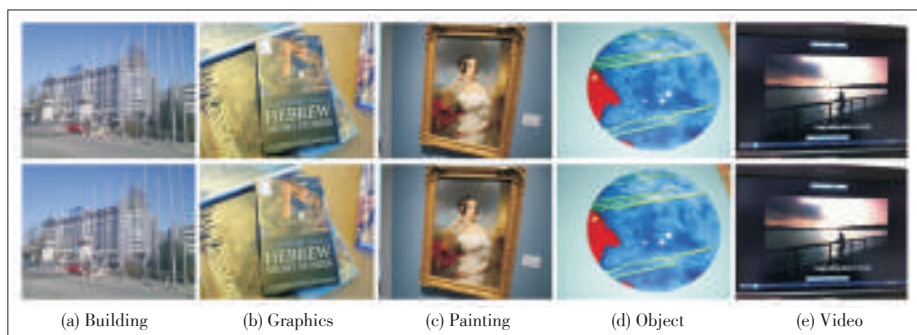
In this paper, we proposed a new IQA method for recompressing JPEG images. The loss associated with this recompression is imperceptible to the human eye. We obtain the optimal quality factor quickly and accurately within a predetermined perceptual quality range. The experimental results show

## A Visual Lossless Image -Recompression Framework

Ping Lu, Xia Jia, Hengliang Zhu, Ming Liu, Shouhong Ding, and Lizhuang Ma

▼ Table 2. Different compression ratios for different types of images

Image type	Number of images	Resolution (pixels)	Avg. original size (MB)	Avg. compressed size (MB)	Avg. compression ratio	Avg. compression time (ms)
Building	1076	< 400 × 400	61.8	27.5	0.555	6.596
Graphics	988	< 400 × 400	38.4	19.3	0.497	3.712
Painting	364	< 2300 × 2300	402.0	190.0	0.527	157.091
Object	3014	< 640 × 480	384.0	204.0	0.469	23.734
Video	1611	< 400 × 400	51.6	25.8	0.500	6.935



▲ Figure 4. The compression results of different types of images. Original image is on the top and the compressed image is on the bottom.

that our framework reduces the size of massive images by about 45%–60%, with a loss of quality that is imperceptible to the human eye. File size is significantly reduced without affecting the perceptual image quality. This improves user experience, saves storage, and saves transmission bandwidth.

### References

- [1] Wikipedia. (2015, May 4). *WebP* [Online]. Available: <http://en.wikipedia.org/wiki/WebP>
- [2] Josh Aas. (2014, Jul. 20). *Mozilla advances JPEG encoding with mozjpeg 2.0* [Online]. Available: <https://blog.mozilla.org/research/2014/07/15/mozilla-advances-jpeg-encoding-with-mozjpeg-2-0/>
- [3] G. K. Wallace. "The JPEG still picture compression standard." *Communications of the ACM*, vol. 34, no. 4, pp. 30–44, 1991. doi: 10.1145/103085.103089.
- [4] M. Rabbani and R. Joshi. "An overview of the JPEG 2000 still image compression standard." *Signal Processing: Image Communication*, vol. 17, no. 1, pp. 3–48, Jan. 2002. doi: 10.1016/S0923-5965(01)00024-8.
- [5] W. B. Pennebaker and J. L. Mitchell. *JPEG: Still Image Data Compression Standard*. New York, USA: Van Nostrand Reinhold, 1993.
- [6] S. Ding, F. Huang, Z. Xie, et al., "A novel customized recompression framework for massive internet images," in *Computational Visual Media Conference*, Beijing, China, Nov. 2012, pp. 9–16. doi: 10.1007/978-3-642-34263-9\_2.
- [7] Z. Wang and A. C. Bovik. *Modern Image Quality Assessment*. USA: Morgan & Claypool Publishers, Mar. 2006.
- [8] Z. Wang, E. P. Simoncelli, and A. C. Bovik. "Multiscale structural similarity for image quality assessment," in *Conference Record of the Thirty-Seventh Asilomar Conference on Signals, Systems and Computers*, Pacific Grove, USA, Nov. 2004, vol. 2, pp. 1398–1402. doi: 10.1109/ACSSC.2003.1292216.
- [9] Z. Wang and Q. Li. "Information content weighting for perceptual image quality assessment," *IEEE Transactions on Image Processing*, vol. 20, no. 5, pp. 1185–1198, May 2011. doi: 10.1109/TIP.2010.2092435.
- [10] T. Shoham, D. Gill, and S. Carmel. "A novel perceptual image quality measure for block based image compression," in *Proc. SPIE 7867*, San Francisco, USA, Jan. 2011, pp. 786709–786715. doi: 10.1117/12.872231.
- [11] L. Zhang, D. Zhang, X. Mou, and D. Zhang. "FSIM: a feature similarity index for image quality assessment," *IEEE Transactions on Image Processing*, vol. 20, no. 8, pp. 2378–2386, Aug. 2011. doi: 10.1109/TIP.2011.2109730.

- [12] Z. Wang. "Rate scalable foveated image and video communications," Ph.D. thesis, Dept. of ECE, The University of Texas at Austin, Austin, USA, Dec. 2001.
- [13] Z. Wang and A. C. Bovik. "A universal image quality index," *IEEE Signal Processing Letters*, vol. 9, no. 3, pp. 81–84, Mar. 2002. doi: 10.1109/97.995823.
- [14] N. Ponomarenko, O. Lereameiev, V. Lukin, et al., "Color image database TID2013: peculiarities and preliminary results," in *4th European Workshop on Visual Information Processing*, Paris, France, Jun. 2013, pp. 106–111.
- [15] N. Ponomarenko, V. Lukin, A. Zelensky, et al., "TID2008—a database for evaluation of full-reference visual quality assessment metrics," *Advances of Modern Radioelectronics*, vol. 10, pp. 30–45, 2009.
- [16] E. C. Larson and D. M. Chandler. "Most apparent distortion: full-reference image quality assessment and the role of strategy," *Journal of Electronic Imaging*, vol. 19, no. 1, pp. 001006:1–001006:21, Jan. 2010. doi: 10.1117/1.3267105.
- [17] H. R. Sheikh, M. F. Sabir, and A. C. Bovik. "A statistical evaluation of recent full reference image quality assessment algorithms," *IEEE Transactions on Image Processing*, vol. 15, no. 11, pp. 3440–3451, Nov. 2006. doi: 10.1109/TIP.2006.881959.

Manuscript received: 2015-03-16

## Biographies

**Ping Lu** (lu.ping@zte.com.cn) received the ME degree in automatic control theory and applications from South East University. He is the chief executive of the Cloud Computing & IT R&D Institute of ZTE Corporation. His research interests include augmented reality and multimedia services technologies.

**Xia Jia** (jia.xia@zte.com.cn) received the MS degree from Dalian University of Technology in 2001. She is a leader of Multimedia Technology Research Team at the Cloud Computing & IT R&D Institute of ZTE Corporation. Her research interests include computer vision and its application field.

**Hengliang Zhu** (hengliang\_zhu@163.com) received the MS degree from Fujian Normal University, China in 2010. He is now a PhD candidate in the Department of Computer Science and Engineering, Shanghai Jiao Tong University, China. His current research interests include image and video editing, computer vision, computer graphics, and digital media technology.

**Ming Liu** (liu.ming83@zte.com.cn) received the BE and MS degrees from Harbin Engineering University, China in 2008 and 2011. He is now a senior engineer at the Cloud Computing & IT R&D Institute of ZTE Corporation. His research interests include augmented reality, visual search, and deep learning.

**Shouhong Ding** (dingsh1987@yahoo.com.cn) received the BS and MS degrees from Dalian University of Technology, China in 2008 and 2011. He is currently a PhD candidate in the Department of Computer Science and Engineering, Shanghai Jiao Tong University, China. His current research interests include image and video editing, computer vision, computer graphics, and digital media technology.

**Lizhuang Ma** (ma\_lz@cs.sjtu.edu.cn) received the PhD degree from Zhejiang University, China in 1991. He is now a full professor and the head of Digital Media Technology and Data Reconstruction Lab at Shanghai Jiao Tong University, China. He is also the chairman of the Center of Information Science and Technology for Traditional Chinese Medicine at Shanghai Traditional Chinese Medicine University. His research interests include computer-aided geometric design, computer graphics, scientific data visualization, computer animation, digital media technology, and theory and applications for computer graphics, CAD/CAM.

# Channel Modeling for Air-to-Ground Wireless Communication

Yingcheng Shi<sup>1</sup>, Di He<sup>1</sup>, Bin Li<sup>2</sup>, and Jianwu Dou<sup>2</sup>

(1. Shanghai Jiao Tong University, Shanghai 200240, China;

2. ZTE Corporation, Shenzhen 518057, China)



## Abstract

In this paper, we discuss several large-scale fading models for different environments. The COST231-Hata model is adapted for air-to-ground modeling. We propose two criteria for air-to-ground channel modelling based on test data derived from field testing in Beijing. We develop a new propagation model that is more suitable for air-to-ground communication than previous models. We focus on improving this propagation model using the field test data.



## Keywords

air-to-ground communication; large-scale fading model

## 1 Introduction

Research on large-scale fading models has a history of about 40 years [1]–[4]. In the 1960s, P. L. Rice and A. G. Longley *et al.* proposed the Rice-Longley model, also called the Irregular Terrain Model (ITM), for forecasting the median transmission fading caused by irregular terrain in free space. With this model, transmission loss could be computed with respect to parameters such as frequency, antenna height, and transmission distance. However, only the effect of irregular terrain was taken into account.

The Durkin-Edwards model promoted the development of large-scale modeling. With this model, loss during transmission could be calculated and loss of barrier due to irregularities could also be predicted. The model could accurately predict the field strength of the signal but not the effect of obstacles, such as buildings and trees, on the signal.

The Okumura model was a milestone in large-scale fading modeling. It is the classic model for large-scale fading and the foundation of research on large-scale fading. During testing, the parameters of Okumura model were continually corrected so that the model had strong applicability. However, if the spread of the signal changed faster than that predicted by the model, there would be large errors. Although the model still has some flaws, it works reasonably well. The Okumura-Hata model is now the most widely used model for large-scale fading.

There are two types of fading model for different frequency ranges: Okumura-Hata and COST231-Hata model. The former is based on the Okumura model and mainly used in macro cell systems where the cell radius is greater than 1 km. It is particularly applicable to cities. However, as urban construction becomes denser, the cell radius is no longer greater than 1 km, and a second model, COST231-Hata, is used.

In our research, we focus on air-to-ground communication, where the frequency is 2.36 GHz and the maximum height of an aircraft is about 3 km. To the best of our knowledge, no one has proposed air-to-ground channel modeling before. However, with the rapid development of 4G and the deregulation of low-altitude airspace, such modeling has become increasingly important. Our research in this area is based on test data.

## 2 Large-Scale Fading Mechanism

When a signal wave encounters rugged terrain, buildings, vegetation or other obstacles along the propagation path, it casts a shadow on the electromagnetic fields [5], [6]. If a mobile station in motion falls under the shadow of an obstacle, shadow fading occurs. Shadow fading is measured in large spatial scales and mainly depends on the propagation environment. Factors such as rolling hills, height distribution of buildings, street direction and position, height of base station antennas, and speed of the mobile station all need to be taken into account when determining the extent of shadow fading.

The relationship between shadow fading and propagation distance is:

$$PL(d) = \overline{PL}(d_0) + 10n \log(d/d_0) + X_\sigma \text{ dB} \quad (1)$$

where  $X_\sigma$  is the zero mean standard deviation for a Gaussian random variable  $\sigma$  dB with its pdf given by:

$$p(M) = \left(1/\sqrt{2\pi}\sigma\right) e^{-(x^2/2\sigma^2)} \quad (2)$$

where  $\sigma$  is calculated using the linear recursive method to minimize the mean squared error of the measured value and estimated value.

### 2.1 Okumura Model

The Okumura model is the most widely used model for predicting city signals in Japan and has become the standard system model. In Tokyo, it is common to use different frequencies,

This research work is supported by the ZTE Corporation and University Joint Research Project under Grant No. CON1307100001, and the National High Technology Research and Development Program of China under Grant No. 2013AA013602.

## Channel Modeling for Air-to-Ground Wireless Communication

Yingcheng Shi, Di He, Bin Li, and Jianwu Dou

antenna height, and distance to select a different series of tests [7]. The experience curve constructs the model and is applicable for a frequency of 150 MHz to 3 GHz, a distance of 1 km–100 km, and an antenna height of 30–1000 m.

A city is assumed to be a quasi-smooth terrain in the Okumura model, so a fixed field strength value is set. For an irregular terrain, there are several correction factors. By obtaining details of the topography and surface of the situation, a more accurate prediction can be made.

In a quasi-smooth terrain, the propagation attenuation values are also called the basic attenuation values. The model gives a quasi-smooth terrain as well as the family of curves of propagation attenuation values in the urban area.

Within a city, wave propagation attenuation depends on the propagation distance, frequency, base station antenna effective height, mobile antenna height and street width, antenna direction, and more. The attenuation can be expressed as:

$$L = L_F + A_{mu}(f, d) - G(h_b, d) - G(h_m, f) - G_{AREA} \text{ dB} \quad (3)$$

where  $L_F$  is the free space loss,  $A_{mu}(f, d)$  is the relative spatial attenuation value,  $G(h_b, d)$  is the base station antenna height gain,  $G(h_m, f)$  is the terminal antenna height gain, and  $G_{AREA}$  is the environmental gain.

The model is derived from test data and does not provide any analysis or interpretation. It makes the most reliable path-loss prediction and is the most accurate solution for cellular systems and terrestrial wireless systems. The deviation in path loss between the prediction and tested data is about 10–14 dB.

### 2.2 Okumura-Hata Model

The frequency range applicable to the Okumura-Hata model is 150–1500 MHz. The formula for urban path loss is:

$$L_{50}(\text{urban}) = 69.55 + 26.16 \log f_c - 13.82 \log h_{re} - \alpha(h_{re}) + (44.9 - 6.95 \log h_{te}) \log dd \text{ dB} \quad (4)$$

where  $f_c$  is the frequency,  $h_{te}$  is the height of transmitting antenna, and  $h_{re}$  is the height of the receiving antenna. The antenna height correction factor is  $\alpha(h_{re})$ .

The Okumura-Hata model makes an accurate prediction in a macro cellular system and also in attenuation.

### 2.3 Cost231-Hata Model

The COST231-Hata model is used on the condition that the carrier frequency is less than 2.5 GHz. This model is a modified Hata model that can be applied in urban macro cell, suburban macro cell, or microcell city situation [8].

For the urban macro cell, the path loss model is:

$$L = 46.3 + 33.9 \lg f - 13.82 \lg h_{te} + 44.9 \lg d - 6.55 \lg h_{te} \lg d - 1.11 h_{te} \lg f + 0.7 h_{te} + 1.56 \lg f + 3.8 \text{ dB} \quad (5)$$

For suburbs, the macro cell environment path loss model is:

$$L = 46.3 + 33.9 \log f - 13.82 \lg h_{te} + 44.9 \lg d - 6.55(\lg h_{te})(\lg d) - 3.2(\lg 11.75 h_{te})^2 + 4.97 \text{ dB} \quad (6)$$

where  $f$  is the frequency of transmitting antenna, and  $d$  is the distance between transmitting antenna and receiving antenna. All the above models are not completely accords with the specific environment of air-to-ground communication.

## 3 Improved Model Based on Measured Data

On February 27, 2014, low-altitude air-to-ground testing of TD-LTE was carried out in Pinggu District, Beijing. There was one aircraft at an altitude of 300 m–600 m. The testing was carried out in a basin surrounded by mountains on three sides. The height of mountain was about 200 m–300 m. The testing environment is shown in **Fig. 1**.

The frequency was 2.36 GHz, there were two transmitting and receiving antennas, the maximum altitude of the aircraft was 600 m, and the speed of aircraft was about 150 km/h. **Fig. 2** shows the flight path of the aircraft.

An air-ground channel model has never been built or appeared in any of the literature before. Building an air-to-ground channel model based on the test data and optimization methods is a creative job.

### 3.1 Improved COST231-Hata Model Based on MMSE Criterion

The reason we choose the COST231-Hata model to optimize the air-to-ground channel model is that COST231-Hata model is suitable for macro cells in rural areas, which is similar to the condition of air-to-ground communication.

In the urban macro cell environment, the general COST231-HATA urban path-loss model is [9]:



▲ Figure 1. Testing environment of air-to-ground communications.



$$L = a_1 + b_1 \lg f - c_1 \lg h_{te} + d_1 \lg d - e_1 \lg h_{te} \lg d - f_1 h_{re} \lg f + g_1 h_{re} \quad (7)$$

where  $L$  is the path loss and  $a_1, b_1, c_1, d_1, e_1, f_1, g_1$  are the corresponding coefficients. Assuming that the total number of received signals is  $N$  and the path loss corresponding to the sampling point  $n$  is  $L(n)$ , the instantaneous frequency is  $f(n)$ .

The minimum mean-square error (MMSE) criterion-based approach is used to optimize the formula coefficients. The objective function can be expressed as:

$$F(a_1, b_1, c_1, d_1, e_1, f_1, g_1) = \frac{1}{N} \sum_{n=1}^N [L(n) - a_1 - b_1 \lg f(n) + d_1 \lg d(n) + e_1 \lg h_{te}(n) \lg d(n) + f_1 h_{re}(n) \lg f(n) - g_1 h_{re}(n)]^2 \quad (8)$$

The partial derivatives of the objective function are expressed as:

$$\frac{\partial F}{\partial a_1} = -\frac{2}{N} \sum_{n=1}^N [L(n) - a_1 - b_1 \lg f(n) + c_1 \lg h_{te}(n) - d_1 \lg d(n) + e_1 \lg h_{te}(n) \lg d(n) + f_1 h_{re}(n) \lg f(n) - g_1 h_{re}(n)] = 0 \quad (9)$$

$\partial F / \partial b_1, \partial F / \partial c_1, \partial F / \partial d_1, \partial F / \partial e_1, \partial F / \partial f_1$ , and  $\partial F / \partial g_1$  take the same process as  $\partial F / \partial a_1$ .

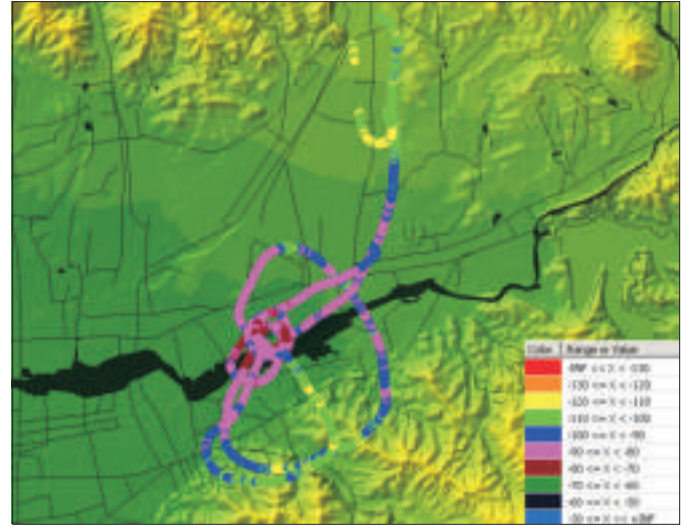
This can be expressed in simplified matrix format:

$$M \cdot \begin{bmatrix} a_1 \\ b_1 \\ c_1 \\ d_1 \\ e_1 \\ f_1 \\ g_1 \end{bmatrix} = \begin{bmatrix} -\sum_{n=1}^N L(n) \\ -\sum_{n=1}^N \lg f(n) \cdot L(n) \\ -\sum_{n=1}^N \lg h_{te}(n) \cdot L(n) \\ -\sum_{n=1}^N \lg d(n) \cdot L(n) \\ -\sum_{n=1}^N \lg h_{te}(n) \cdot \lg d(n) \cdot L(n) \\ -\sum_{n=1}^N \lg h_{re}(n) \cdot \lg f(n) \cdot L(n) \\ -\sum_{n=1}^N h_{re}(n) \cdot L(n) \end{bmatrix} \quad (10)$$

where  $M$  is a  $7 \times 7$  dimensional matrix, and  $\{m_{ij}\} (i, j = 1, 2, \dots, 7)$  are:

$$\begin{aligned} m_{11} &= -N \\ m_{12} &= -\sum_{n=1}^N \lg f(n) \\ m_{13} &= -\sum_{n=1}^N \lg h_{te}(n) \end{aligned} \quad (11)$$

To solve (10), we obtain the optimal solution based on the



▲ Figure 2. Flight path of aircraft.

MMSE criterion:

$$\begin{bmatrix} a_1 \\ b_1 \\ c_1 \\ d_1 \\ e_1 \\ f_1 \\ g_1 \end{bmatrix}_{opt} = \begin{bmatrix} a_{1opt} \\ b_{1opt} \\ c_{1opt} \\ d_{1opt} \\ e_{1opt} \\ f_{1opt} \\ g_{1opt} \end{bmatrix} = M^{-1} \cdot \begin{bmatrix} -\sum_{n=1}^N L(n) \\ -\sum_{n=1}^N \lg f(n) \cdot L(n) \\ -\sum_{n=1}^N \lg h_{te}(n) \cdot L(n) \\ -\sum_{n=1}^N \lg d(n) \cdot L(n) \\ -\sum_{n=1}^N \lg h_{te}(n) \cdot \lg d(n) \cdot L(n) \\ -\sum_{n=1}^N \lg h_{re}(n) \cdot \lg f(n) \cdot L(n) \\ -\sum_{n=1}^N h_{re}(n) \cdot L(n) \end{bmatrix} \quad (12)$$

where  $a_{1opt}, b_{1opt}, c_{1opt}, d_{1opt}, e_{1opt}, f_{1opt}, g_{1opt}$  are the optimal values of  $a_{1opt}, b_{1opt}, c_{1opt}, d_{1opt}, e_{1opt}, f_{1opt}, g_{1opt}$ , respectively. According to the air-to-ground channel testing, parameters such as  $f$  and  $h_{te}$  are decided; we reduce the computational complexity; and (7) can be simplified as:

$$L(n) = a_1 + b_1 \lg d(n) \quad (13)$$

The objective function (7) has only three variables  $a_1, b_1$ :

$$F(a_1, b_1) = \frac{1}{N} \sum_{n=1}^N [L(n) - a_1 - b_1 \lg d(n)]^2 \quad (14)$$

We obtain the optimal coefficient vector:

$$M \cdot \begin{bmatrix} a_1 \\ b_1 \end{bmatrix} = \begin{bmatrix} -\sum_{n=1}^N L(n) \\ -\sum_{n=1}^N \lg d(n) \cdot L(n) \end{bmatrix} \quad (15)$$



## Channel Modeling for Air-to-Ground Wireless Communication

Yingcheng Shi, Di He, Bin Li, and Jianwu Dou

where

$$M = \begin{bmatrix} -N, -\sum_{i=1}^N \lg d \\ -\sum_{i=1}^N \lg d, -\sum_{i=1}^N (\lg d)^2 \end{bmatrix} \quad (16)$$

According to the analysis above, we obtain the result  $[a_1 b_1]_{opt}^*$  using the testing data  $L(n), d(n), h_{te} f$ , and (13) can be expressed with  $[a_1 b_1]_{opt}^*$ .

## 4 Optimization Result

According to the analysis and calculation in the last section, we obtain the coefficients  $a_1$ ,  $b_1$ , and  $c_1$ . In testing,  $f$  and  $h_{te}$  are decided, and we record the location information of each sampling point. The result of optimization in a Matlab simulation is shown in **Fig. 3**.

The formula of air-ground channel fading model corresponding to Fig. 3 is:

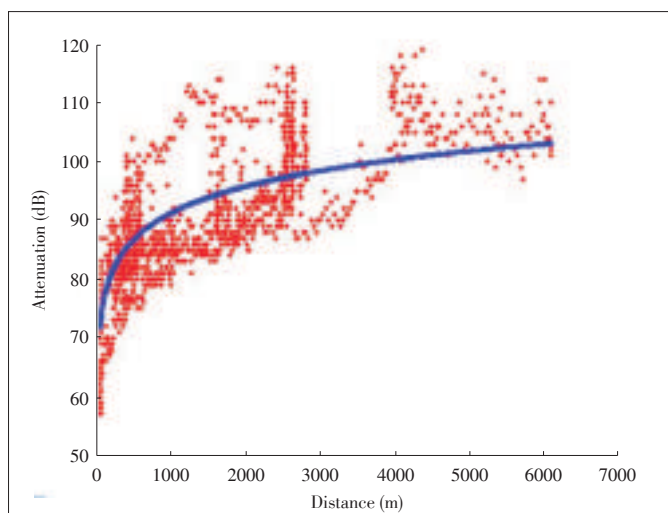
$$PL = 45.7613 + 6.5767 \log(d) \quad (17)$$

Using the distance between transmitting antenna and receiving antenna, we divide the large-scale fading into three different situations (**Table 1**).

▼ **Table 1. Classification of situations**

Situation	Distance (m)
Parked	0–500
Take-off/landing	500–1000
Cruising	>1000

According to the analysis, we give the air-to-ground large-scale fading model formula and the model formula in different



▲ **Figure 3. Air-to-ground channel fading model.**

situations (**Table 2**).

▼ **Table 2. Results of simulation**

Situation	MMSE
Large-scale overall	$PL = 45.7613 + 6.5767 \log(d)$
Parked	$PL = 51.8915 + 5.44 \log(d)$
Take-off/landing	$PL = 3.5069 + 63.4481 \log(d)$
Cruising	$PL = 7.3843 + 11.55161 \log(d)$
MMSE: minimum mean-square error	

The formula for the parked situation (**Fig. 4**) is:

$$PL = 51.8915 + 5.44 \log(d) \quad (18)$$

The formula for the take-off/landing situation (**Fig. 5**) is:

$$PL = 3.5069 + 63.4481 \log(d) \quad (19)$$

The formula for the cruising situation (**Fig. 6**) is:

$$PL = 7.3843 + 11.55161 \log(d) \quad (20)$$

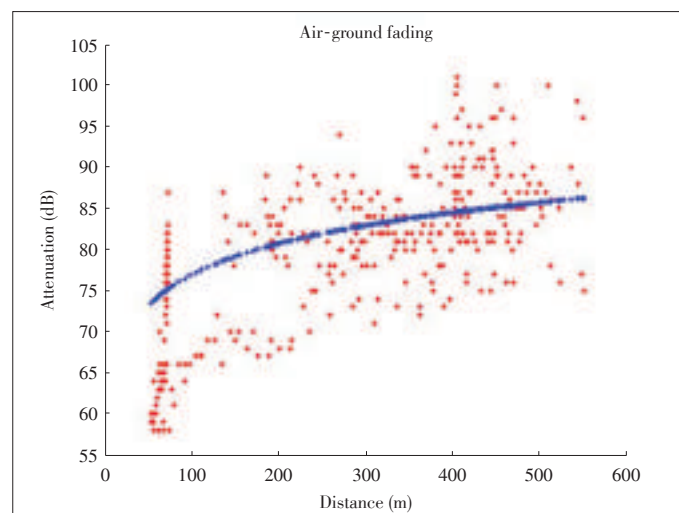
The free-space propagation, which is based on conventional COST231 model, can be expressed as:

$$PL = 32.45 + 20 \log(d)(km) + 20 \log(f)MHz \quad (21)$$

**Fig. 7** shows the proposed advanced COST231 model fits the real data better than the conventional COST231 model in (21). The MMSE of advanced COST231 model is  $7.1157 \times 10^4$  and that of the free-space fading model is  $6.4546 \times 10^5$ . The proposed model is more suitable than free-space fading model.

## 5 Conclusion

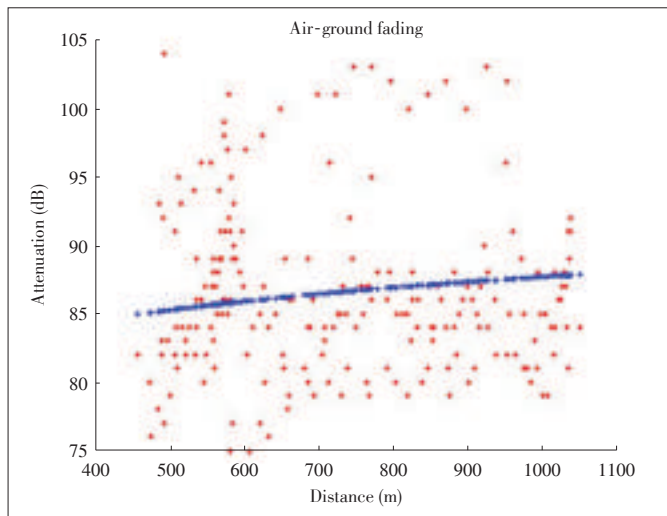
In this paper, we have described an air-to-ground wireless communication channel model for 2.36 GHz based on COST231 - Hata, and actual measured data was used. We di-



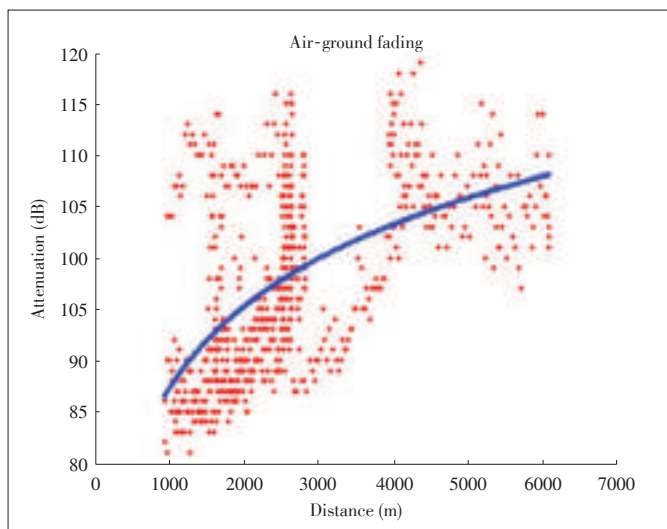
▲ **Figure 4. Simulation of parked situation.**

## Channel Modeling for Air-to-Ground Wireless Communication

Yingcheng Shi, Di He, Bin Li, and Jianwu Dou



▲ Figure 5. Simulation of take-off/landing situation.

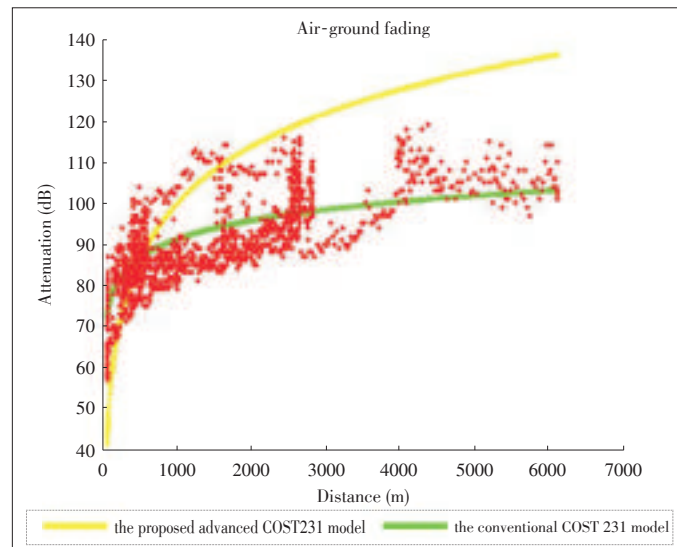


▲ Figure 6. Simulation of cruising situation.

vide it into three situations: parked, take-off/landing, cruising. Based on MMSE/LS criterion, we derived formula of large-scale fading in different situations. Because the data was obtained through real tests, the simulation formula is convincing and helpful for the future research. Therefore, the proposed model describes the air-to-ground situation more accurately.

## References

- [1] Y. R. Zheng and C. Xiao, "Improved models for the generation of multiple uncorrelated Rayleigh fading waveforms," *IEEE Communications Letters*, vol. 6, no. 6, pp. 256–258, Jun. 2002. doi: 10.1109/LCOMM.2002.1010873.
- [2] B. Roturier *et al.*, "Experimental and theoretical field strength evaluation on VHF channel for aeronautical mobiles," AMCP Doc.AMCP/WG-D/7-WP/58, Madrid, Spain, Apr. 1997.
- [3] P. Dent and G. E. Bottomley, "Jakes fading model revisited," *Electronics Letters*, vol. 29, no. 3, pp.1162–1163, Jun. 1993. doi: 10.1049/el:19930777.
- [4] Andrea Goldsmith, *Wireless Communications*. Cambridge, UK: Cambridge University Press, Aug. 2005.
- [5] M. Failli, "Digital land mobile radio communications: final report (14 March



▲ Figure 7. Comparison of improved COST231 model and free-space propagation model.

- 1984–13 September 1988), "Commission of the European Communities, Directorate - General Telecommunications, Information Industries and Innovation, 1989.
- [6] W. C. Y. Lee, *Mobile Cellular Telecommunication System, Analog & Digital*. New York, USA: McGraw Hill, 1995.
- [7] G. Dyer and T. G. Gilbert, "Channel sounding measurements in the VHF A/G radio communications channel," Aeronautical Mobile Communications Panel, Oberpfaffenhofen, Germany, document AMCP/WG-D/8-WP/19, 1997.
- [8] Commission of the European Communities and COST Telecommunications, "Digital mobile radio: COST 231 view on the evolution towards 3rd generations systems", Brussels, Belgium, COST 231 Final report, 1999.
- [9] E. Haas, "Aeronautical channel modelling," *IEEE Transactions on Vehicular Technology*, vol. 51, no. 2, pp. 254–264, Mar. 2002. doi: 10.1109/25.994803.

Manuscript received: 2014-11-13

## Biographies

**Yingcheng Shi** (yingchengshi@sjtu.edu.cn) received the MS degrees from Shanghai Jiao Tong University 2015. His research interests include air-to-ground wireless communications, LTE communications, and D2D communications.

**Di He** (dihe@sjtu.edu.cn) received the PhD degree in circuits and systems from Shanghai Jiao Tong University in 2002. From 2002 to 2004, he was a postdoctoral fellow in the Department of Electrical and Computer Engineering, University of Calgary, Canada. From 2004 to present, he has been an associate professor at Shanghai Jiao Tong University. His research interests include wireless communications (particularly air-to-ground wireless communications), LTE communications, cognitive radio and long-term evolution, nonlinear dynamics and its applications in wireless communications, and satellite communications.

**Bin Li** (li.bin23@zte.com.cn) received the MSc degree in electronics and computer science from University of Southampton, UK, in 2008. Since 2009, he has been a senior engineer of the System Simulation Department at ZTE Corporation. His research interests include signal processing, parameter estimation, and propagation studies of mobile radio channels.

**Jianwu Dou** (dou.jianwu@zte.com.cn) received the PhD degree from Beijing University of Technology in 2001. Since 2001, he has been in charge of research and system design of the radio resource management algorithm in UMTS, TD-SCDMA and LTEv1 at ZTE Corporation. From 2006, he has also been responsible for system simulation of 2G, 3G, 4G, and WLAN as a director of the department at ZTE. His research interests include RRM, system simulation, wireless channel sounding and modelling, data mining, high-frequency physical-layer design, and MTC.

# Terminal-to-Terminal Calling for GEO Broadband Mobile Satellite Communication

Qing Wang, Minjiong Zhu, Jie Zhou, Zhen Gao, and Jinsheng Yang

(School of Electrical Information Engineering, Tianjin University, Tianjin 300072, China)



## Abstract

Satellite and terrestrial components of IMT-Advanced need to be integrated so that the traditional strengths of each component can be fully exploited. LTE/LTE-A is now a recognized foundation of terrestrial 4G networks, and mobile satellite networks should be based on it. Long transmission delay is one of the main disadvantages of satellite communication, especially in a GEO system, and terminal-to-terminal (TtT) design reduces this delay. In this paper, we propose a protocol architecture based on LTE/LTE-A for GEO mobile satellite communication. We propose a detailed call procedure and four TtT modes for this architecture. We describe the division of tasks between the satellite gateway (SAT-GW) and satellite as well as TtT processing in the physical layer of the satellite in order to reduce delay and ensure compatibility with a terrestrial LTE/LTE-A system.



## Keywords

TtT call; LTE/LTE-Advanced; satellite communication system

## 1 Introduction

Integrated terrestrial and satellite communication has been addressed for many years and is at the forefront of R&D within the satellite community [1]. The ITU has made recommendations for the development of the satellite radio interface of IMT-Advanced [2].

The broadband mobile satellite (BMSat) radio interface is mainly used for broadband mobile satellite services that use geostationary (GEO) satellites [3]. BMSat is derived from the terrestrial LTE-Advanced specifications [4]–[6] and enables access to LTE-Advanced core networks.

Because there are differences between terrestrial and satel-

lite channels, LTE-Advanced has to be modified for satellite radio transmission. Some LTE-Advanced specifications can be used without modification for satellite radio transmission whereas others need to be modified. Similarly, some LTE-Advanced specifications are not relevant and some BMSat specifications have no corresponding LTE-Advanced specification. In [7], a kind of narrowband transmission scheme was proposed for allocating limited bandwidth to user equipment (UE). Such a scheme is particularly necessary for a satellite channel, which is power-constrained [7].

In a conventional mobile satellite communication systems using GEO satellites, communication passes through the geostationary satellite twice. This is called a double-hop connection. Such a connection increases the delay between user terminals and reduces link quality. People in areas where land communication networks are not developed benefit from reduced link delay. In [8], four single-hop connection methods were proposed and compared. With these methods, communication frames are transferred between user terminals via satellite only once [8].

A terminal-to-terminal (TtT) call can be established in double-hop mode but can provide single-hop TtT services. There is a long delay associated with a double-satellite-hopped mobile-to-mobile service. Therefore, a single-hopped service can be routed directly through the satellite—from any terminal in any spot beam to any other terminal in any other spot beam. In single-hop mode, two mobile Earth stations (MESs) engaged in a call communicate directly via the satellite. In [9], the authors define a TtT call at a circuit-switched L-L channel on the satellite. However, in a BMSat system based on LTE/LTE-A, differences between the uplink SC-FDMA and downlink OFDM are challenging to TtT call specification design.

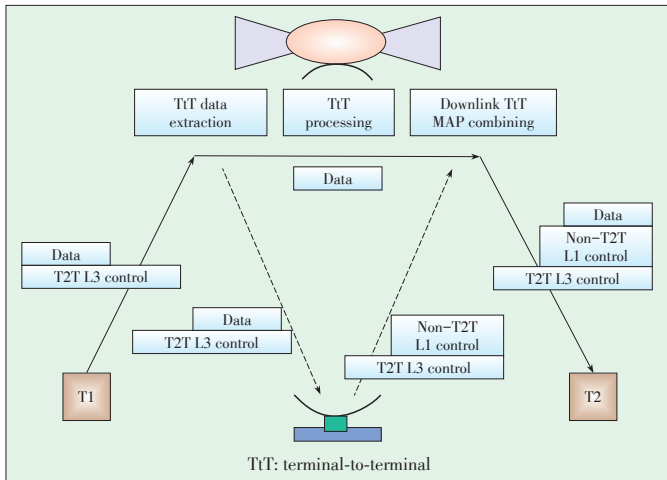
In this paper, we propose a GEO BMSat TtT architecture and related call procedure based on LTE/LTE-A. These are designed to reduce transmission delay and increase terrestrial compatibility. The paper is organized as follows: section 2 describes the concept of a single-hop TtT call. In section 3, the protocols of four TtT modes are described. In section 4, division of tasks between SAT-GW and satellite are defined. In section 5, TtT call singling processing is defined. Section 6 concludes the paper.

## 2 Concept of Single-Hop TtT

The BMSat network should support single-hop voice calls, i.e., TtT calls, between two UEs on the same satellite network. During TtT call processing, the gateway station (GS) establishes a single-hop call between two UEs when circumstances permit. When the TtT call has been established, the voice data is transferred via satellite directly, which avoids the long delay. The satellite gateway (SAT-GW) is responsible for non-TtT data transfer, parameter configuration, and legal interception. The satellite responds by extracting TtT data from the uplink

message, TtT processing, and downlink TtT MAP combining. The TtT concept is shown in **Fig. 1**.

TtT call has following characteristics:



▲ **Figure 1.** TtT concept.

- It uses single-hop mode only for voice services.
- It supports mobility management (handover).
- It supports end-to-end ciphering.
- It supports legal interception.
- It does not use hybrid automatic repeat request (HARQ).
- It uses semi-persistent scheduling.
- It responds to any release requirement immediately during communication.

### 3 TtT Mode

To distinguish TtT data from non-TtT data, a TtT radio bearer (TRB) is used for a TtT call. When establishing a TRB, an Evolved Universal Terrestrial Radio Access Network (E-UTRAN) is used to decide how to transfer the packets of an Evolved Packet System (EPS) bearer across the radio interface. An EPS bearer is mapped one-to-one to a TRB, a TRB is mapped one-to-one to a TtT traffic channel (TTCH) logical channel. Then, radio resource control (RRC) information with TTCH requires ciphering and robust header compression (ROHC). Packet Data Convergence Protocol (PDCP) is configured to compress the header and significantly reduce signaling overhead, as required in LTE [10].

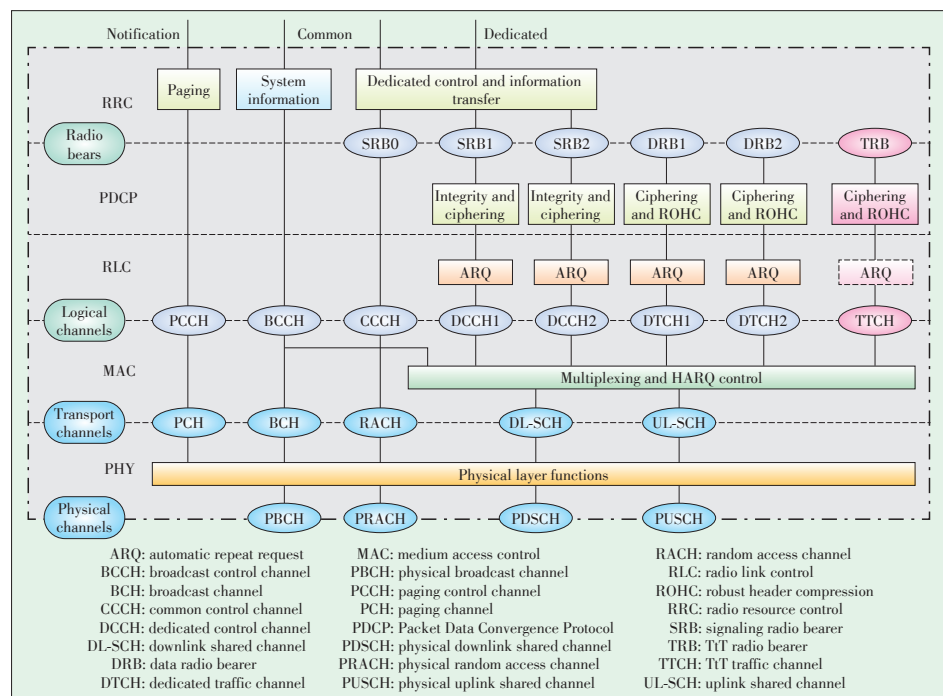
Unacknowledged mode (UM) is used in the radio link control (RLC) layer to provide unidirectional data transfer. This is mainly use by delay-sensitive

and error-tolerant real-time applications. Automatic repeat request (ARQ) is not included in RLC layer for TtT service. Then, in the medium access control (MAC) layer, the TTCH is mapped to

- A downlink shared channel (DL-SCH) or uplink shared channel (UL-SCH) multiplexes with other logical channels and is identified by a TtT logical channel ID (LCID). The DL-SCH or UL-SCH is mapped one-to-one to the corresponding physical downlink shared channel (PDSCH) or physical uplink shared channel (PUSCH). This is TtT mode one, i.e., TtT TTCH in MAC PDU.
- A separate TtT channel (TCH). A MAC protocol data unit (PDU) only bears the TTCH logical channel, and the TCH is mapped to the physical layer in three ways:
  - 1) The TCH is mapped to the PDSCH, which is identified by a TtT radio network temporary identifier (T-RNTI) or by one bit in the physical downlink control channel (PDCCH). This is TtT mode two, i.e., TtT TCH in PDSCH.
  - 2) The TCH is mapped to a separate physical TtT channel (PTCH), which is periodically scheduled in dedicated physical resource blocks (PRBs). This is TtT mode three, i.e., TtT PTCH in dedicated PRBs.
  - 3) TCH is mapped to a separate PTCH, which is periodically scheduled in a dedicated subframe. This is TtT mode four, i.e., TtT PTCH in a dedicated TtT subframe.

#### 3.1 Mode One: TtT TTCH in MAC PDU

The TTCH LCID is defined in the MAC layer. The TTCH and all other logical channels are mapped to the DL-SCH or UL-SCH in one MAC PDU (**Fig. 2**).



▲ **Figure 2.** TtT Mode 1: TtT TTCH in MAC PDU.



## Terminal-to-Terminal Calling for GEO Broadband Mobile Satellite Communication

Qing Wang, Minjong Zhu, Jie Zhou, Zhen Gao, and Jinsheng Yang

In this mode, the physical layer is not modified. However, it is inefficient to multiplex logical channels because useless control information has to be processed in the satellite during TtT transmission.

### 3.2 Mode Two: TtT TCH in PDSCH

In TCH transmission, the MAC PDU only bears the TTCH. When the TCH is mapped to the PDSCH (Fig. 3), the TCH is identified along with other transmission channels by using the T-RNTI, which is similar to the PCH, or by using one bit in the PDCCH when the same RNTI is used with the PCH or DL-SCH. Mode two is highly efficient because only the TTCH needs to be processed. Also, a separate TCH enables greater flexibility to support network coding. However, search complexity is doubled when the T-RNTI is added, and the physical layer has to be modified.

### 3.3 Mode Three: TtT PTCH in Dedicated PRBs

The TCH is periodically mapped to the PTCH using dedicated PRBs, which are similar to PBCHs. With the PRCH, three PRBs are scheduled every 20 ms (Fig. 4). In this mode, one vertical protocol path is added without interfering with the original protocol. However, in this mode, resource efficiency is reduced for dedicated PRBs if no TtT services are required, and the physical layer also has to be modified.

### 3.4 Mode Four: TtT PTCH in Dedicated TtT Subframe

The TCH is periodically mapped to the PTCH using a dedicated subframe, which is similar to the PMCH. The TtT control channel (TCCH) and TTCH are mapped two-to-one to the TCH and is then mapped one-to-one to the PTCH. TtT data are

scheduled by higher level signaling. The PDCCH is only allocated uplink resources but not for PTCH transmission (Fig. 5).

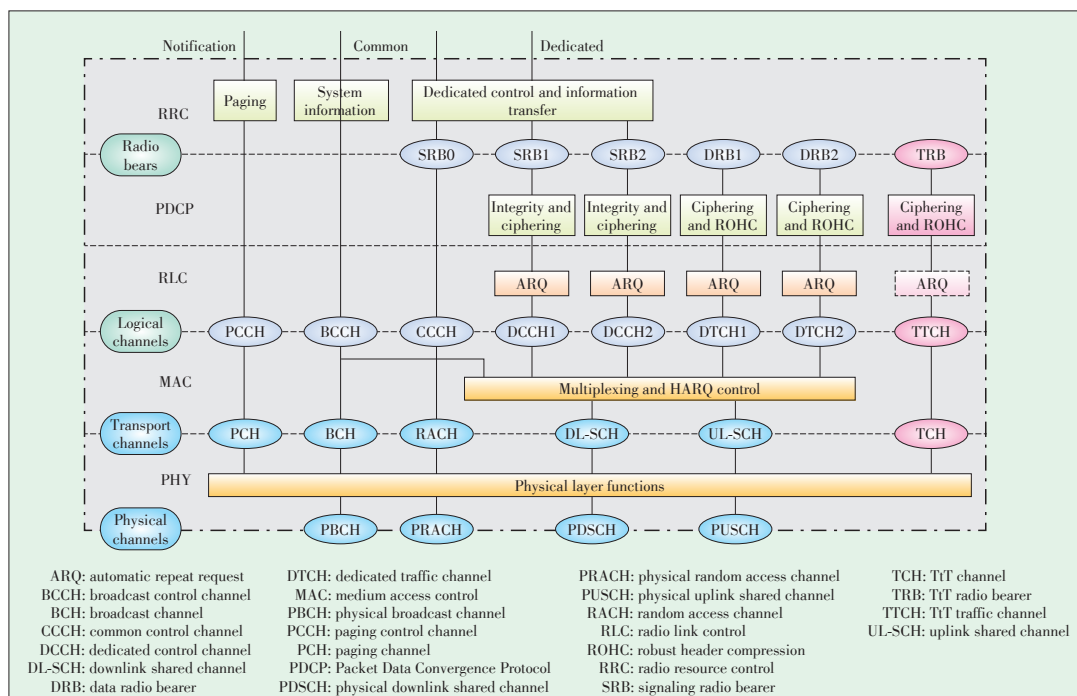
A UE that is measuring a neighboring cell does not need to know in advance the allocation of TtT and non-TtT subframes. The UE can take advantage of the fact that a different reference signal pattern and cyclic prefix are used in TtT subframes. An extended cyclic prefix (CP) is used, i.e., the prefix is approximately 17  $\mu$ s instead of approximately 5  $\mu$ s. In this mode, the reference symbols are spaced closer in the frequency domain than they are in non-MBSFN transmission. The separation is decreased to every other subcarrier rather than every sixth subcarrier.

In this mode, one vertical protocol path is added without affecting the original protocol. However, resource efficiency is lower for the dedicated subframe if there are not enough TtT users. In this case, the physical layer has to be modified.

## 4 Cooperation Between SAT-GW and Satellite

For TtT services with a semi-static packet rate, semi-persistent scheduling may be needed to reduce the control signaling overhead.

The SAT-GW is responsible for non-TtT service processing, legal interception, and semi-persistent configuration of TtT service. Semi-persistent scheduling involves allocating resources to both TtT and non-TtT services and leaving TtT PRBs in the DL-MAP blank. The satellite inserts TtT resource blocks into the DL-MAP for multiplexing with non-TtT services. TtT resource blocks are produced by an additional TtT processing module at the satellite.

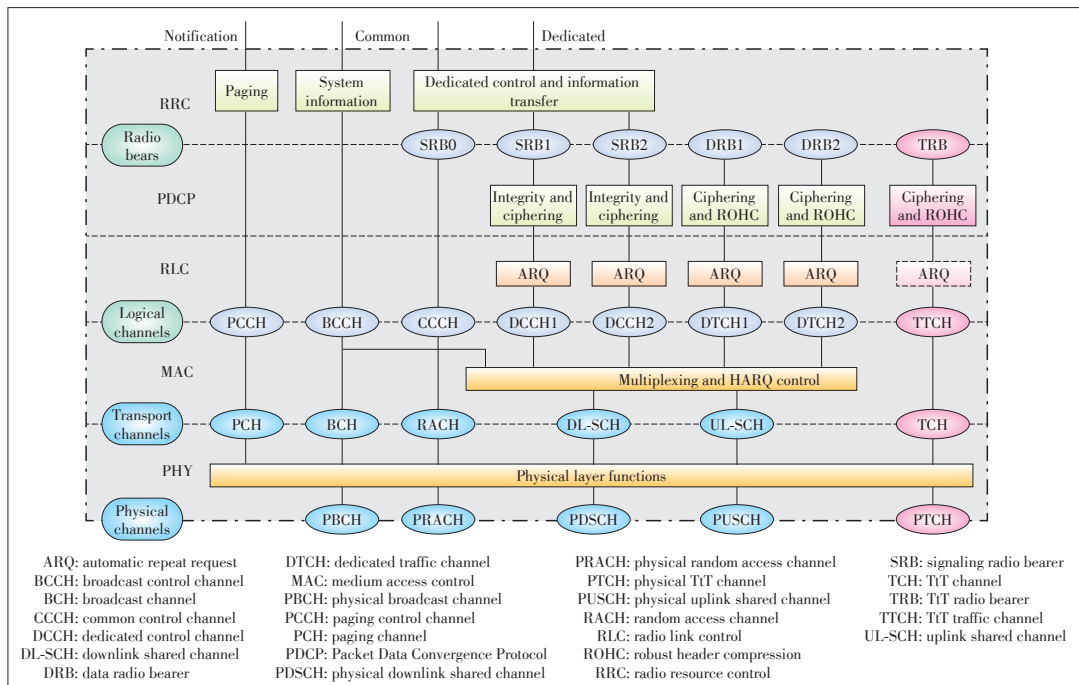


◀ Figure 3.  
Mode 2: TtT TCH in PDSCH.

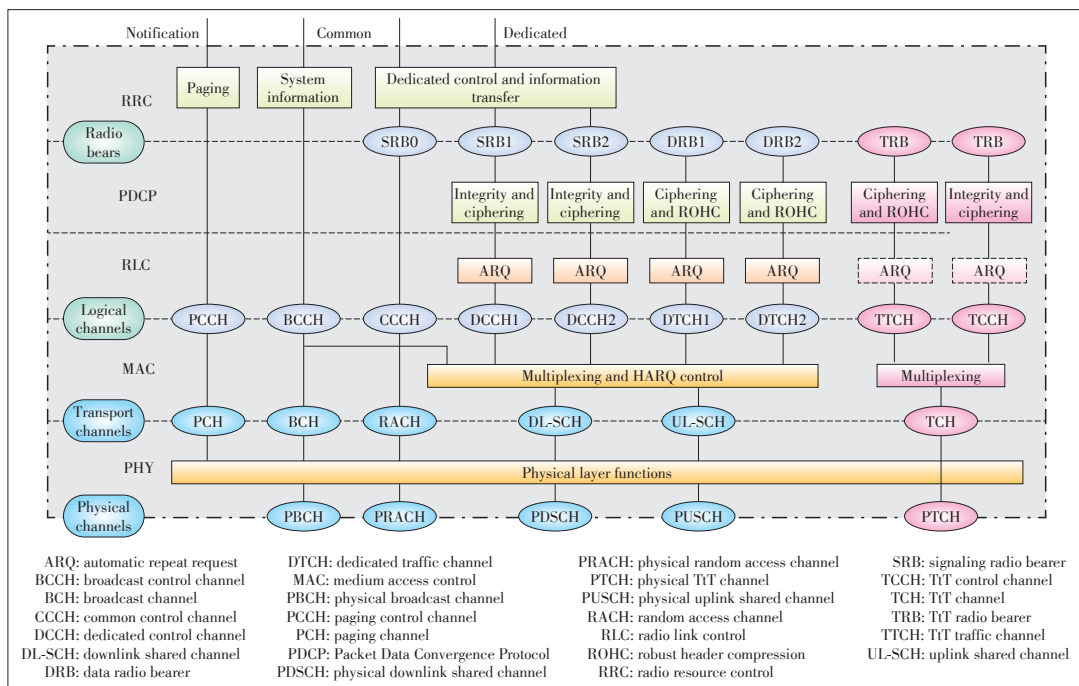


## Terminal-to-Terminal Calling for GEO Broadband Mobile Satellite Communication

Qing Wang, Minjiong Zhu, Jie Zhou, Zhen Gao, and Jinsheng Yang



◀ **Figure 4.**  
TtT Mode 3: TtT PTCH in  
dedicated PRBs.



◀ **Figure 5.**  
TtT Mode 4: TtT PTCH in  
dedicated TtT subframe.

The tasks performed between the SAT-GW and satellite are shown in **Fig. 6**.

## 5 TtT Call Processing

The signaling procedures for TtT call processing, which include random access, paging and handover, are completed in double-hop mode, as with LTE.

A TtT call can only be made in RRC-connected state and us-

ing TRB bearing (**Fig. 7**).

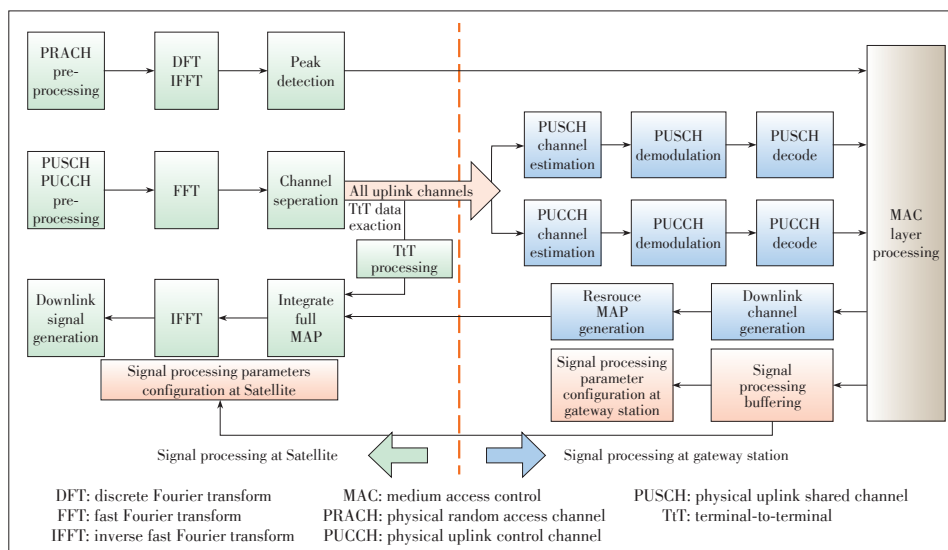
### 5.1 TtT Call Establishment

A TtT call is established in double-hop mode. The signaling process includes paging, random access, and establishment of an RRC connection and is coordinated with LTE.

After receiving the initial UE message, the Evolved Packet Core (EPC) recognizes that a TtT call is being established between two MESSs, i.e., TtT users. The EPC starts EPS bearing

## Terminal-to-Terminal Calling for GEO Broadband Mobile Satellite Communication

Qing Wang, Minjiong Zhu, Jie Zhou, Zhen Gao, and Jinsheng Yang



▲ Figure 6. Division of tasks between the SAT-GW and satellite.

and sends the initial context setup request to SAT-GW. This request includes the TtT setup. Security is established on the RRC connection, and the radio bearer, including TRB, is also established on the connection. A virtual circuit for the call is established between the TtT UEs, both of which are informed of the TtT states. A dedicated control channel (DCCH) between the SAT-GW and satellite is established. The SAT-GW configures the satellite parameters, which include downlink and uplink TtT resource allocation results and TtT mode, through the control channel. The SAT-GW also informs UEs of the downlink and uplink TtT resource allocation results. The SAT-GW generates the downlink MAP (DL-MAP) for non-TtT services and transmits it to the satellite through DCCH. TtT RBs are left blank in the DL-MAP.

In TtT mode one, the PRBs are semi-scheduled for DL-SCH with TTCH in PD-SCH. In TtT mode two, the PRBs are semi-scheduled for TCH in PDSCH. In TtT mode three, the PRBs for PTCH are periodically scheduled. And in TtT mode four, the subframes for PTCH are periodically scheduled.

After receiving the DL-MAP, the satellite sends a TtT transmission start signaling to both the UEs to indicate that call establishment is finished. At this time, the TtT call changes to signaling double-hop/voice single-hop mode.

### 5.2 TtT Voice Communication

In voice communication, TtT voice data is transmitted in single-hop mode.

#### 5.2.1 TtT UE Sending TtT Traffic

TtT uplink traffic sent by a TtT UE is carried by the TRB and mapped to the TTCH. In mode one, the TTCH is mapped to the UL-SCH, multiplexed with other logical channels, and transmitted via the PUSCH. In mode two, the TTCH is mapped to the TCH and transmitted in the PUSCH. In mode three, the

TTCH is mapped to the TCH and transmitted via the PTCH in dedicated PRBs. In mode four, the TTCH is mapped to the TCH and transmitted via the PTCH in dedicated subframes.

#### 5.2.2 TtT Processing at the Satellite

The satellite extracts the TtT user data from the uplink traffic and generates downlink TtT RBs in the TtT processing module. Fig. 8 shows the TtT processing module.

The satellite separates TtT data from received uplink traffic according to the parameters provided by the SAT-GW. The uplink resource allocation is used to:

- localize the UL-SCH transport block bearing the TTCH and separate it from the PUSCH, which includes other logical control channel information in TtT mode one
- localize the TCH transport block bearing the TTCH and separate it from the PUSCH, which only includes TTCH logical channel in TtT mode two
- localize the TCH transport block bearing the TTCH and separate it from the PTCH, which only includes the TTCH logical channel in TtT mode three
- localize the TCH transport block bearing the TTCH and separate it from the PTCH subframe, which only includes the TTCH logical channel in TtT mode four.

The satellite then finishes TtT transport block decoding, which involves channel estimation, equalization, IDFT, demodulation, descrambling, deinterleaving, deconcatenation, and channel decoding. Finally, the satellite recovers the bitstream of the UL-SCH or TCH transport block.

In TtT mode one, the recovered UL-SCH transport block bit stream includes other logical channel data. However, in TtT modes two to four, the recovered TCH transport block bit stream includes only TTCH logical channel data.

Next, the satellite encodes the TtT transport block again according to the downlink TtT resource allocation. This re-encoding requires rate-matching based on the number of REs in the allocated RB.

For VoIP services, 244 bits of user data are generated in 20 ms, and the whole packet is approximately 300 bits after padding the headers of layers two and three. When QPSK modulation is taken into account, a minimum of three PRBs are required when  $ITBS = 7$ ,  $NPRB = 3$ , and the transport block size is 328 bits [11, Sec. 7.1.7.2]. The number of usable REs in an allocated RB depends on whether one, two, or three OFDM symbols are used for the control signal. Thus, the number of REs in each RB is 126, 138 or 150. If there are three OFDM control symbols, the downlink channel coding rate is:

# Terminal-to-Terminal Calling for GEO Broadband Mobile Satellite Communication

Qing Wang, Minjiong Zhu, Jie Zhou, Zhen Gao, and Jinsheng Yang

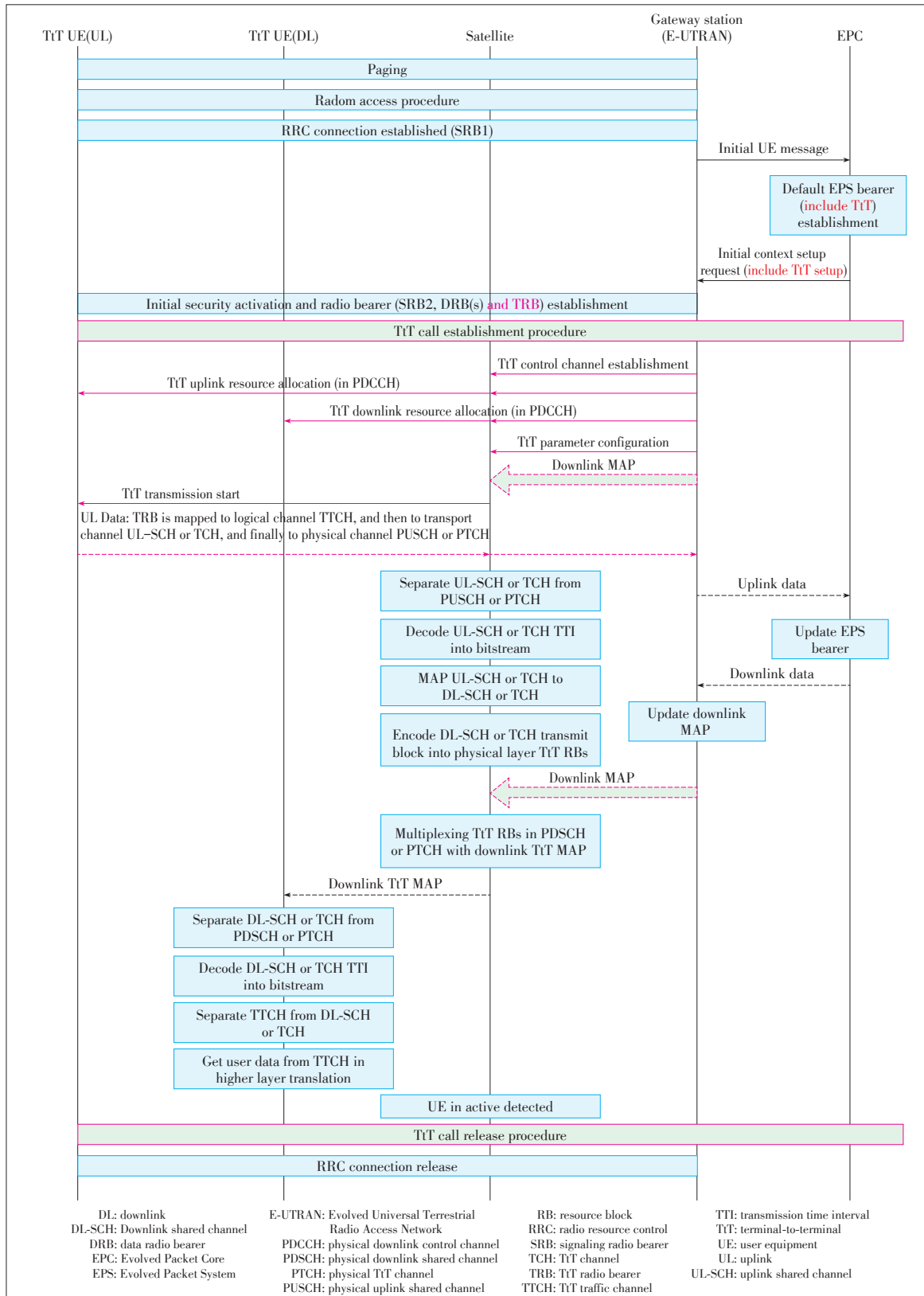


**Figure 7.** TtT calling process.

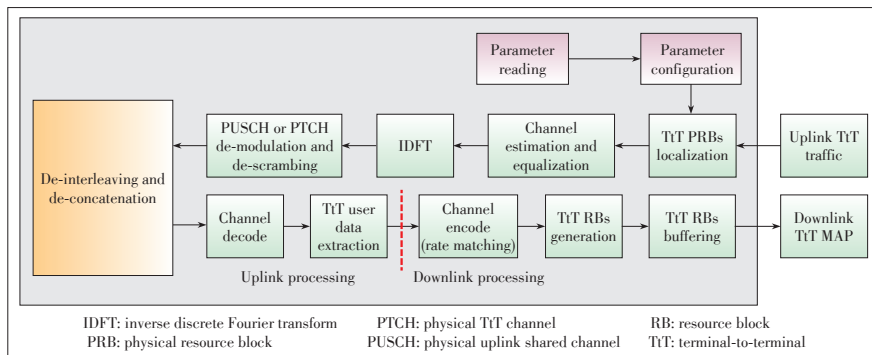
$$\frac{382 + 2(CRC)}{126 + 2(QPSK) \times 3} = 0.4656$$

(1)

After rate-matching and encoding, TtT RBs are generated. As the time is synchronized, the TtT RBs are buffered for the

## Terminal-to-Terminal Calling for GEO Broadband Mobile Satellite Communication

Qing Wang, Minjiong Zhu, Jie Zhou, Zhen Gao, and Jinsheng Yang



▲ Figure 8. TtT processing module.

downlink TtT MAP.

The TtT RBs are read by the buffer and mapped to the DL-SCH or TCH and are then combined with the DL-MAP (according to downlink TtT resource allocation) to generate the downlink TtT MAP. In this case, the TtT RBs are mapped to the DL-SCH in TtT mode one and to the TCH in the other three modes. The TtT RBs are scheduled in TtT modes one and two. PTCH PRBs and PTCH subframe are scheduled in TtT modes three and four, respectively.

### 5.2.3 TtT UE Receiving Downlink TtT MAP

In TtT modes one and two, TtT UE in the downlink decodes PDSCH and the corresponding DL-SCH according to CRC scrambling codes, such as SI-RNTI, P-RNTI, RA-RNTI, SPS-C-RNTI, C-RNTI, and T-RNTI. In order to recover the DL-SCH bitstream in TtT mode one, and to retrieve the TCH bitstream in TtT mode two, PDCCH uses the DCI information. This information is used to decide the size of the transport block and modulation order. Then, the PDCCH separates TTCH from the DL-SCH/TCH bitstream and recovers the user data in a higher layer.

In TtT modes three and four, the TtT PTCH RBs are extracted, and the bitstream of the TCH transport block, the TTCH, and the user data are recovered step by step.

### 5.2.4 TtT Call Release

The SAT-GW releases the TtT virtual circuit and RRC connection when the UE is inactive. Call release is signaled in double-hop mode, as in an LTE system.

## 6 Conclusion

In this paper, we have proposed a protocol architecture based on LTE/LTE-A for GEO mobile satellite TtT communication. We also designed a detailed call procedure. Four TtT modes for this architecture were then introduced and compared, and the scheme for cooperation between SAT-GW and the satellite was analyzed. Our next step is to come up with a more comprehensive design within this protocol architecture in the areas of frequency synchronization, time control, ciphering,

and interception schemes.

### References

- [1] F. Bastia, C. Bersani, E. A. Candreva, et al., "LTE adaptation for mobile broadband satellite networks," *EURASIP Journal on Wireless Communications and Networking*, pp. 1–13, 2009. doi:10.1155/2009/989062.
- [2] *Vision and Requirements for the Satellite Radio Interface (s) of IMT-Advanced*, ITU Std. Rep.ITU-R M.2176, 2010.
- [3] *BMSat Radio Interface Specifications; Introduction to the BMSat Family*, CCSA Std. BMSat-36.001.2, 2013.
- [4] *LTE; E-UTRA; Physical Channels and Modulation*, 3GPP Std. 3GPP TS36.211, 2013.
- [5] *LTE; E-UTRA; Multiplexing and Channel Coding*, 3GPP Std. 3GPP TS36.212, 2013.
- [6] *LTE; E-UTRA; Physical Layer Procedures*, 3GPP Std. 3GPP TS 36.213, 2013.
- [7] H. W. Kim, K. Kang, and B.-J. Ku, "Narrowband uplink transmission in LTE-based satellite radio interface," in *Fourth International Conference on Advances in Satellite and Space Communications*, Chamonix, France, 2012, pp. 104–107.
- [8] K. Ebina, N. Kataoka, M. Ueba, and H. Mizuno, "Investigation of single-hop connections between user terminals in geostationary mobile satellite communication systems," in *Global Telecommunications Conference*, 2001, vol. 4, pp. 2764–2768. doi: 10.1109/GLOCOM.2001.966277.
- [9] *GEO-Mobile Radio Interface Specifications; Part 3: Network Specifications; Sub-Part 18: Terminal-to-Terminal Call (TtT)*, ETSI Std. GMR-103.296 (ETSI TS 101 376-3-18), 2001.
- [10] S. Sesia, I. Toufik, and M. Baker, *LTE - The UMTS Long Term Evolution: From Theory to Practice*. Torquay, UK: Wiley, 2009.
- [11] *BMSat Radio Interface Specifications; Evolved Universal Satellite Radio Access (E-USRA) and Evolved Universal Satellite Radio Access Network (E-USRAN); Physical layer procedures (Release 1)*, CCSA Std. BMSat-36.213, 2013.

Manuscript received: 2014-11-21

## Biographies

**Qing Wang** (wqelaine@tju.edu.cn) received her BEng, MEng., and PhD degrees in electronic engineering from Tianjin University, China, in 2004, 2007, and 2010. Since 2010, she has worked in the School of Electronic and Information Engineering, Tianjin University, and is currently an associate professor there. From October 2007 to April 2009, she was a visiting scholar in the School of Electrical and Electronic Engineering, Nanyang Technological University, Singapore. Her research interests include wireless communication, passive radar, and radio propagation.

**Minjiong Zhu** (zhuminjiong@sina.cn) received his BS degree in electronic information engineering from Tianjin University, China, in 2014. He is currently pursuing the MS degree there. His research include software-defined networking and 5G mobile communication.

**Jie Zhou** (zhoujie\_tju@163.com) received her BS and MS degrees in communication engineering from Tianjin University, China, in 2011 and 2015. Her research interests include architecture design for wireless mobile communication, especially for satellite mobile communication systems, as well as physical-layer algorithms in wireless mobile communication.

**Zhen Gao** (zgao@tju.edu.cn) received his BS, MS and PhD degrees in electrical and information engineering from Tianjin University, China, in 2005, 2007 and 2011. From October 2008 to November 2010, he was a visiting scholar at Georgia Tech, USA, working on the design and implementation for OFDM-based cooperative communication. From July 2011 to November 2014, he was an assistant researcher with the Wireless and Mobile Communication Research Center, Tsinghua University, China. He has been an associate professor at Tianjin University since December 2014. His research interests include mobile satellite communication, fault-tolerant signal processing, and wireless communication systems.

**Jinsheng Yang** (jsyang@tju.edu.cn) is an associate professor in the School of Electronic Information Engineering, Tianjin University, China. His research interests include the channel characterizations and modeling for wireless communications and networking-based information solutions.

# Community Discovery with Location-Interaction Disparity in Mobile Social Networks

Danmeng Liu<sup>1</sup>, Wei Wei<sup>2</sup>, Guojie Song<sup>1</sup>, and Ping Lu<sup>2</sup>

(1. Peking University, Beijing 100871, China;

2. ZTE Corporation, Shenzhen 518057, China)



## Abstract

With the fast-growth of mobile social network, people's interactions are frequently marked with location information, such as longitude and latitude of visited base station. This boom of data has led to considerable interest in research fields such as user behavior mining, trajectory discovery and social demographics. However, there is little research on community discovery in mobile social networks, and this is the problem this work tackles with. In this work, we take advantage of one simple property that people in different locations often belong to different social circles in order to discover communities in these networks. Based on this property, which we referred to as Location-Interaction Disparity (LID), we proposed a state network and then define a quality function evaluating community detection results. We also propose a hybrid community-detection algorithm using LID for discovering location-based communities effectively and efficiently. Experiments on synthesis networks show that this algorithm can run effectively in time and discover communities with high precision. In real-world networks, the method reveals people's different social circles in different places with high efficiency.



## Keywords

mobile social network; community detection; LID

## 1 Introduction

Nowadays, mobile social network (MSN) services with location support have become a part of people's lives. This trend has produced a mass of location data that can be used to study human migration patterns and social structure.

Community detection is a field of social network research related to the social groups that people belong to. Communities are groups of people in a social network, and the amount of interaction within these groups is greater than that between different groups [1]. Group information is useful for further study on viral marketing [2], behavior modeling [3], and network visualization [4].

Introducing location information into community discovery opens up possibilities for practical application. Advertisers can use location information to push advertisements in specific places and target specific user groups. Friend recommendation for SNS sites can be more location specific when users use social networking applications on mobile devices. What's more, location information of users often contains time information, communities of one user formed in different places are actually communities formed in different time. Thus social relationship of users in different places can help social network miners understand users' activity patterns better.

Our fundamental task is to utilize both social relation data and location information to discover communities in MSN. Traditionally, community discovery works are on pure networks that do not take contents of networks into consideration [5], [6]. Recently, much research has been done on location-based social network mining, and the focus of these works is mainly revealing the relationship between human interactions and location. However, most of these works deal with local properties of a social actor, such as social connection strength [7] and user trajectories [8], and no research is being done on community discovery with location information. In reality, it is common for a person to behave quite differently in different locations. For example, a worker might contact colleagues when at work, talk with family when in a metro station heading home, and interact with close friends at home. Therefore it is natural for one actor in a location-marked social network to have multiple communities in different places. Taking advantage of these properties can be helpful for community discovery in MSN.

There can be several challenges in integrating location information into community discovery. First, the scale of the problem can be several times larger because users can be in multiple places with social connections in every place. Therefore efficient algorithms need to be designed to tackle large datasets. Second, traditional measures of user similarity for community discovery only comprise of social interactions, but no location information is included in the measurement. Finally, a new data model needs to be built for both location and social interaction information.

In this paper, we tackle the problem of finding communities in MSN by establishing a model that integrates location and social interaction features. We then design an efficient, high-precision algorithm for this model. First, we examine and confirm that it is common for users to have different communities when they are in different locations. We name this sort of disparity as Location-Interaction Disparity (LID). Then inspired by LID

This work is supported by the National High Technology Research and Development Program of China under Grant No. 2014AA015103, Beijing Natural Science Foundation under Grant No. 4152023, the National Natural Science Foundation of China under Grant No. 61473006, and the National Science and Technology Support Plan under Grant No. 2014BAG01B02.



## Community Discovery with Location-Interaction Disparity in Mobile Social Networks

Danmeng Liu, Wei Wei, Guojie Song, and Ping Lu

we propose a state network model for detecting community structure, where one state denotes one user in a specific location and links represent users interact in different locations. This model can easily describe the phenomenon of people in different locations belonging to different communities. After that, we define a quality function for state model based on modularity. Then we propose a community detection algorithm integrated with LID for effective and efficient community discovery. This algorithm has a conglomerating step and divisive step and is called a hybrid community detection algorithm. Experiments on synthesis data set verified the superiority of our proposed algorithm. We also conduct experiments on real-world data, which shows that users can be in different types of communities indicating different activities.

The primary contributions of this paper are as follows.

- 1) We propose a state network model for discovering communities in MSN with location interaction disparity.
- 2) We design a quality function based on modularity for state networks communities.
- 3) We propose an efficient algorithm to discover communities in MSN with state network model and quality function.
- 4) We present experiments on both synthesis and real-world data sets to show that our methods are effective and efficient.

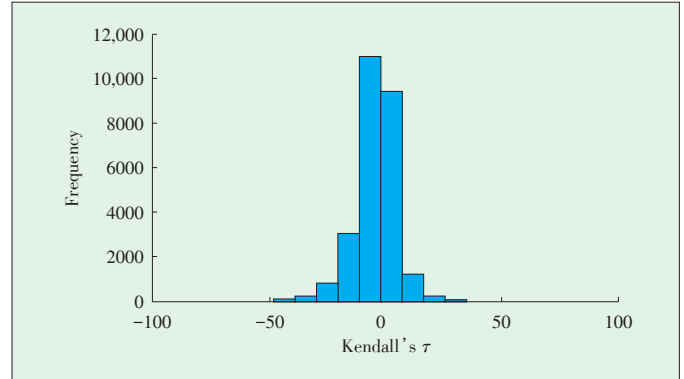
## 2 Model and Problem Definition

### 2.1 Location-Interaction Disparity

People tend to have different social relations in different places. For example, when people are at work, they tend to contact their colleagues, and when they are at home, they tend to contact their friends in private circles. This phenomenon, called LID, also happens on virtual spaces such as cyber-spaces where different websites tend to provide different services, thus leading to different types of social relations.

We investigate LID in a real-world MSN. This network is originally represented as a collection of  $(u_i, l_{i,t}, u_j, l_{j,t}, t)$ , where  $(u_i, l_{i,t})$  means that at time  $t$ , person  $u_i$  in location  $l_{i,t}$  calls person  $u_j$  in location  $l_{j,t}$ . The location of every user  $u_i$  is given by  $L_i = \{l_{i,t} | \exists (u_i, l_{i,t}, u_j, l_{j,t}, t) \in D\}$  where some communications are made in these locations. We generate a communication feature vector  $c_{i,l}$  for every  $l \in L_i$ , such that  $c_{i,l}(j) = |\{(u_i, l, u_j, l_{j,t}, t)\}|$ . These vectors actually record the communication frequency of user  $u_i$  to others in different places.

To simplify the investigation, we take users with marked home and work cells, or  $O$  cells and  $D$  cells, to show that LID exists widely in human communication networks. Both  $O$  and  $D$  cells are marked via the methods proposed in [9], and the differences between different locations are measured with Kendall's  $\tau$  [10] to avoid non-normality in degree distribution. For every  $u_i$ , we measure Kendall's  $\tau$  between  $c_{i,O_i}$  and  $c_{i,D_i}$  and plot  $9\tau n(n-1)/2(2n+5)$  (Fig. 1). We transform  $\tau$  in this way because the distribution of  $\tau$  is approximated with normal distribution  $N(0, 2(2n+5)/9n(n-1))$ .



▲ Figure 1. Kendall's  $\tau$  between  $c_{i,O_i}$  and  $c_{i,D_i}$  for every  $u_i$ .

bution  $N(0, 2(2n+5)/9n(n-1))$ .

In Fig. 1, most users have negative correlation between their  $O$  and  $D$  feature vectors. With a confidence level of 95%, we show that 65.2% of all the users show LID between home and work. This result shows that LID phenomenon is common in people's daily lives.

### 2.2 State Network

To effectively discover communities in MSNs with LID, we need to make sure that two locations for one person with significant LID are separated. Following this idea we introduce a state network model for discovering communities in MSN.

In our work, a state network has several sets of nodes and links between these nodes. The sets are called entities and the nodes are called states. In a real scenario, an entity represents a single person and a state represents a person location tuple  $(u, l)$ , when user  $u$  appears in  $l$ . There is an edge exists between two states  $(u_1, l_1)$  and  $(u_2, l_2)$  only if two entities  $u_1$  and  $u_2$  interact when they are in  $l_1$  and  $l_2$  respectively, or in real scenario, two people have contacted each other in two different locations. For example, if there are two users  $u_1$  and  $u_2$ , their home and work places are  $h_{u1}, w_{u1}$  and  $h_{u2}, w_{u2}$ , respectively. We call  $\langle u_1, h_{u1} \rangle$  and  $\langle u_1, w_{u1} \rangle$  two states for  $u_1$ . An edge between  $\langle u_1, h_{u1} \rangle$  and  $\langle u_2, h_{u2} \rangle$  means that  $u_1$  and  $u_2$  made phone calls when  $u_1$  is in  $h_{u1}$  and  $u_2$  is in  $h_{u2}$ . The weights of edges are the number of calls made between two linked states.

To give a formal definition, we define our network as an undirected graph  $G = \langle V, \Gamma, A \rangle$ , where  $V$  is the set of states and  $\Gamma$  is the set of entities which satisfies  $V = \bigcup_{\gamma_i \in \Gamma} \gamma_i$ ,  $\gamma_i \neq \emptyset$  and  $\gamma_i \cap \gamma_j = \emptyset$  for all  $1 \leq i < j \leq |\Gamma|$ .  $A \in R^{|\Gamma| \times |\Gamma|}$  is the adjacency matrix for the state network. We require that  $A_{ij} = 0$  if  $\exists \gamma_k$  so that  $v_i, v_j \in \gamma_k$ , because there should be no links within a single entity. For convenience, we define  $s_i$  as the entity index of  $v_i$ , i.e.  $s_i = j$  only if  $v_i \in \gamma_j$ .

Fig. 2 shows the configuration of a state network. In this network, there are four entities,  $\gamma_1$  to  $\gamma_4$ , marked as ovals in the bottom and for every entity, there are several states, marked as circles. The dotted lines in Fig. 2 show the belonging relationship between states and entities.

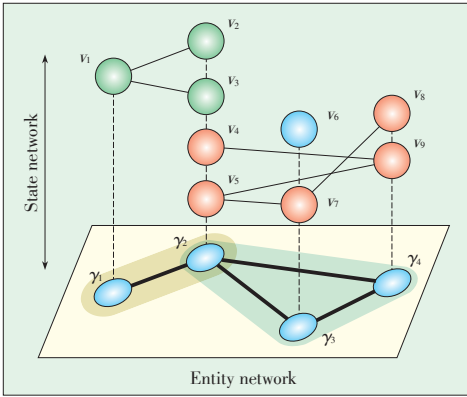


Figure 2. State network and its corresponding entity network.

With the definition of state network we can give the definition of communities. In our network, communities are defined as unoverlapped sets of states. In Fig. 2, there are two state communities, one marked with light gray and another is marked with dark gray. States belonging to  $\gamma_2$  are divided into two different communities. This overlap is due to the disparity of interaction of  $\gamma_2$  between  $v_2, v_3$  and  $v_4, v_5$ . States in  $\gamma_2$  with LID are explicitly separated in this model.

However, when two states in one entity do not show significant LID, these two states should not be separated into two communities, which do not show explicitly in our model.

### 2.3 Modularity for State Network

Now that we have our state network, we need to define a quality function for community division. We use Newman's modularity to evaluate the quality of community detection in our state network. In [11], Newman's modularity calculates the difference between the real adjacency matrix and a null model, and the null model is a randomized graph where nodes are reconnected with a property proportional to their degrees and thus community structure is removed. The expression of Newman's modularity is shown below.

$$Q = \frac{1}{2m} \sum_{i,j} \left( A_{ij} - \frac{k_i k_j}{2m} \right) \quad (1)$$

The definition of state network we defined above is actually a multipartite network with no edges between states within the same entity. Given this property, we modify the definition of null model to make sure that no links exist between nodes within the same state. Note that term  $k_i k_j / 4m^2$  in Newman's modularity in (1) show that in the original null model, the probability that two nodes connect together is proportional to the number of stubs (i.e., half-edges) they own respectively. In our modification of modularity, we use this idea to define modularity on state networks. Given that number of pairs of stubs is:

$$\hat{M} = 4m^2 - \sum_{\gamma_i \in \Gamma} \left( \sum_{v_j \in \gamma_i} k_j \right)^2 + \sum_{v_i \in \gamma_i} k_i^2 \quad (2)$$

and for every pair of nodes  $v_i$  and  $v_j$ , the number of stubs each node own are  $k_i$  and  $k_j$ , we can have our modularity for state net-

works defined as:

$$\hat{Q} = \sum_{i,j} \left( \frac{A_{ij}}{2m} - \frac{k_i k_j}{\hat{M}} \right) (1 - \delta_{s_i, s_j}) \delta_{c_i, c_j} \quad (3)$$

The multiplier  $1 - \delta_{s_i, s_j}$  means that, for states within one entity, the probability that two states links is equal to 0.

With the definition of modularity, we can discover communities within our state network by maximizing  $Q_b$ . In addition, we can also discuss the problem in Section 2.2. Given that directly bridging LID and modularity is not easy, we turn to solve an alternative problem, which is given as Theorem 1.

**Theorem 1.** Merging states  $i$  and  $j$  in a state network with  $\delta_{s_i, s_j} \delta_{c_i, c_j} = 1$  does not affect  $Q_b$ , which means that optimal community division is stable against merge and separation of states.

The proof of this theorem can be simply done by calculating the new modularity value after merging  $i$  and  $j$ . This theorem guarantees that separating and merging states in one entity within the same community does not change the value of modularity. That is, multiple states for one entity in the same group do not affect community discovery.

The last step is to show that the problem of maximizing  $\hat{Q}$  is NP-hard. For a random graph, we assume that every node is a single state entity. In this case,  $M_c = 4m^2$  and  $\hat{Q} = Q + \sum_i k_i^2 / \hat{M}$ . As stated by Brandes *et al.* [12], modularity maximization on undirected network is NP-hard, hence maximizing our modified modularity is also NP-hard, as  $\sum_i k_i^2 / \hat{M}$  is a constant for a fixed graph.

### 2.4 Problem Definition

We give a formal definition of the problem we need to solve. Suppose that we have a database D with records in vectors like  $\langle u_i, l_{i,t}, u_j, l_{j,t}, t \rangle$ , where  $\langle u_i, l_{i,t} \rangle$  denotes person  $u_i$  in location  $l_{i,t}$  while person  $u_j$  in location  $l_{j,t}$  at specific time  $t$  and they communicated. This kind of records appear in a wide scope, from mobile phone calls to check-in data from location-based social network services. Thus we define a state network as  $G = \langle V, \Gamma, A \rangle$ , where  $V = \{ \langle u_i, l_j \rangle \}$ ,  $\gamma_i = \{ \langle u_i, l_j \rangle \}$  and  $A_{pq} = |\{ t | \exists \langle u_i, l_{i,t}, u_j, l_{j,t}, t \rangle \text{ s.t. } \langle u_i, l_{i,t} \rangle = v_p \text{ and } \langle u_j, l_{j,t} \rangle = v_q \}|$ . We need to discover a community division  $C$  that maximizes  $Q_b$  as is defined in (3). As is stated in Section 2.3, maximizing  $Q_b$  is an NP-hard problem.

## 3 Algorithm

We first discuss the spectral algorithm for state networks, SASN, then the greedy algorithm for state networks, GASN. We combine these two methods together with integrated LID information to create a hybrid community detection algorithm (HCD).

### 3.1 Spectral Algorithm for State Networks

SASN is based on Newman's work [13], which is a popular

## Community Discovery with Location-Interaction Disparity in Mobile Social Networks

Danmeng Liu, Wei Wei, Guojie Song, and Ping Lu

approach to calculating optimal community discovery results. In that work, the basic steps of the algorithm is to perform binary divisions, while each division step is done by calculating  $S$  that maximizes  $\Delta Q = \text{Tr}(S^T B^{(C)} S)$  and divide given signs of  $S$ , where  $B^{(C)}$  is the generalized modularity matrix defined as

$$B_{ij}^{(C)} = B_{ij} - \delta_{ij} \sum_{l \in C} B_{il}, i, j \in C \quad (4)$$

The method is a spectral method because  $S$  is computed via eigen decomposition of  $B_{ij}^{(C)}$ .

For SASN, we need to calculate  $B_{ij}^{(C)}$  for MSN and then follow the framework of the original iterative division framework. Given that existing implementations of the spectral approach, such as the igraph package [14], use Lanczos algorithm to solve eigenvectors of modularity matrices, and in Lanczos algorithm, all we need to compute eigenvectors of a matrix  $M$  is to define a function multiplying  $M$  with a random vector  $S$  [15], we provide the result of multiplication for  $B_b^{(C)} S$  instead of  $B_b^{(C)}$  for SASN as follows:

$$\hat{B}^{(C)} S = BS - \text{diag}\{B1_n\}S \quad (5)$$

$$BS = \left( \frac{A}{2m} - \frac{kk^T}{2m} \right) S + \frac{1}{\hat{M}} \sum_{p=1}^{|\Gamma|} k^{(i)} k^{(i)T} S^{(i)} - \frac{1}{\hat{M}} \text{diag}\{k_i^2\} \quad (6)$$

As there is no overlap between states, the complexity to compute  $\hat{BS}$  is  $O(n)$ . Hence, the total time complexity is  $O(kn)$ , where  $k$  is the number of iterations.

### 3.2. Greedy Algorithm for State Networks

Given that in SASN, iteration number of  $k$  can be quite large, we need to find a faster algorithm. Therefore we propose an algorithm base on FastGreedy algorithm proposed by Newman and Girvan [13], which is often used as a fast approach towards large-scale networks. This algorithm initializes every single node as a community and then iteratively merge connected community pairs with maximal value of  $\Delta Q_{C_u, C_v} = 1/2m(e_{uv} - a_u a_v / 2m)$ . This value computes the gain when communities  $C_u$  and  $C_v$  are merged. In our work, as we use MSN instead of original modularity,  $\Delta Q_{C_u, C_v}$  can be computed as (7).

$$\Delta Q_{C_u, C_v} = \frac{e_{uv}}{2m} - \frac{a_u a_v}{\hat{M}} + D_{C_u, C_v} \quad (7)$$

$$D_{C_u, C_v} = \frac{1}{\hat{M}} \sum_{p=1}^{|\Gamma|} a_u^{(p)} a_v^{(p)} \quad (8)$$

where  $e_{uv} = \sum_{i \in C_u, j \in C_v} A_{ij}$ ,  $a_u = \sum_{i \in C_u} k_i$  and  $a_u^{(p)} = \sum_{i \in C_u} k_i^{(p)}$ .

The time cost of computing  $\Delta Q_{C_u, C_v}$  mainly falls on computing  $D_{C_u, C_v}$ . A naive idea for computing  $D_{C_u, C_v}$  is to calculate summation of  $a_u^{(p)} a_v^{(p)}$  directly. In this way, time complexity for calcu-

lating  $D_{C_u, C_v}$  is therefore  $O(|\Gamma|)$ . When  $|\Gamma|$  is comparable to  $n$ , which is often the case, this complexity can deteriorate to  $O(n)$ . Thus, the overall computational complexity for the algorithm is  $O(n|E|d \log n)$  assuming that  $d$  is the depth of iteration, which is intolerable for very large  $n$ .

We improve the performance of this algorithm and derive GASN by exploiting the properties of item  $D_{C_u, C_v}$ . We notice that  $a_u^{(p)} a_v^{(p)} \neq 0$  if and only if  $\gamma_p \cap C_u \neq \emptyset$  and  $\gamma_p \cap C_v \neq \emptyset$ . We say that in this case, entity  $p$  is shared by  $C_u$  and  $C_v$ . This property shows that an entity is affected if and only if it is shared by different communities, which give us a way to optimize the naive algorithm.

We generate an entity clique graph (ECG) to help us computing  $D_{C_u, C_v}$  efficiently. An ECG is a multigraph where every node denotes a community and every edge means that there is one entity shared by two communities. Given this definition, there can be multiple edges between two nodes denoting multiple entities shared by two communities, each representing one entity. We denote these edges as  $(u, v, p)$ , meaning that entity  $p$  is now shared by  $C_u$  and  $C_v$ . What's more, nodes in ECG form a clique when they shared states from one entity. If  $a_u^{(p)} a_v^{(p)} \neq 0$  and only if there is an edge  $(u, v, p)$  exists for entity  $\gamma_p$  connecting nodes representing  $C_u$  and  $C_v$ .

In many implementations of FastGreedy algorithms, such as Newman and Girvan's original work [13], Wakita [6] and Schuetz's optimized version [16], there are two fundamental steps: the update step and the merge step. In the update step,  $\Delta Q_{C_u, C_v}$  is updated for every community pair affected by the merge. That is, if one community in a community pair is merged by a community outside the current pair, its  $\Delta Q$  should be updated for further merges. In our algorithm, an extra item,  $D_{C_u, C_v}$  is calculated and added to the original  $\Delta Q$ . The update step is shown in detail in **Algorithm 1**.

#### Algorithm 1. Update Step in GASN

```

1: function UPDATE PAIR( $v_i, v_j$ )
2:   for all  $w$  s.t.  $(v_i, w) \in E \wedge (v_j, w) \in E$  do
3:      $\Delta Q_{v_i, w} \leftarrow \Delta Q_{v_i, w} + \Delta Q_{v_j, w}$ 
4:   end for
5:   for all  $w$  s.t.  $(v_i, w) \in E \wedge \neg(v_j, w) \in E$  do
6:      $D_{v_j, w} \leftarrow \sum_{(v_j, w, p) \in ECG} a_{v_j}^{(p)} a_w^{(p)}$ 
7:      $\Delta Q_{v_j, w} \leftarrow \Delta Q_{v_j, w} - (a_{v_j} a_w + D_{v_j, w}) / \hat{M}$ 
8:   end for
9:   for all  $w$  s.t.  $\neg(v_i, w) \in E \wedge (v_j, w) \in E$  do
10:     $D_{v_i, w} \leftarrow \sum_{(v_i, w, p) \in ECG} a_{v_i}^{(p)} a_w^{(p)}$ 
11:     $\Delta Q_{v_i, w} \leftarrow \Delta Q_{v_i, w} - (a_{v_i} a_w + D_{v_i, w}) / \hat{M}$ 
12:   end for
13: end function

```

In the merge step, two selected communities are merged into

one community. In this step,  $a_i$  and  $a_i^{(p)}$  are updated given the merge from  $C_f$  to  $C_i$ . The merge step for GASN is shown in **Algorithm 2**.

---

**Algorithm 2.** MERGE\_PAIR( $v_f, v_i$ )
 

---

```

1:  $a_i \leftarrow a_i + a_f$ 
2: for all  $(v_i, v_f, p) \in ECG$  do
3:    $a_i^{(p)} \leftarrow a_i^{(p)} + a_f^{(p)}$ 
5: end for
6: Merge community  $t$  into  $f$  by changing the index.
7: end function

```

---

We analyze the efficiency of the algorithm within Newman and Girvan's original FastGreedy framework (NGFG) because existing derivative works only have difference in time costs in constant multipliers, and it is easy to replace update and merge steps in these algorithms with GASN. In NGFG, only one community pair with maximum  $\Delta Q_{C_u, C_v}$  is selected and merged, while all  $\Delta Q_{C_u, C_w}$  and  $\Delta Q_{C_v, C_w}$  values are updated to reflect the merge. The merge continues until  $Q$  stops to increase, or there is only one community left. The election of maximum  $\Delta Q$  takes  $O(n \log n)$  if a max-heap is used.

Then we analyze the complexity of update and merge steps, which is based on the dendrogram of merges. The merge depth is defined as the maximal depth of two nodes involved in the merge. It is easy to see that communities never overlap in merges with same depth, which provide us convenience for the analysis of the update step. For update steps in merges with same depth, number of edges updated can be at most  $2|E|$ , as one edge in state network can be updated at most twice. It is the same for ECG. Therefore the time complexity for update steps in merges with the same depth is  $O(|E| \log |E|) + O(|E_{ECG}| \log |E_{ECG}| \log n)$  if efficient lookup data structures are employed. Therefore the total time cost for the update step is  $O(|E| d \log^2 n)$  for the whole algorithm, where  $d$  is the depth of dendrogram. For the merge step, the most time-consuming step is to calculate  $a_i^{(p)}$ , and this can take  $O(|E_{ECG}| \log |E_{ECG}|)$  for the whole algorithm. Summing all these up we get the whole computation complexity as  $O(|E| d \log^2 n)$ . Given that in a real scenario,  $|\gamma_i|$  can be relatively small,  $|E_{ECG}| \leq \sum_{1 \leq p \leq |\Gamma|} |\gamma_p|^2 \leq O(n)$ . Hence the expression of complexity can be further simplified to  $O(|E| d \log^2 n)$ , which is significantly less than the naive approach.

### 3.3 Hybrid Community Detection

SASN runs quite slowly because there can be a large number of iterations before it converges. On the other hand, GASN can be quite biased as it might generate many communities

with only one or two members, even if heuristics efforts such as that introduced by Schuetz *et al.* [16] to balance the merge are taken. We get an applicable method for large networks with high quality. It is common for people to behave differently in different places, which naturally led to different communities. This LID feature can be made use of in our algorithm.

To take advantage of the LID feature, we combine SASN and GASN to create a hybrid community detection algorithm with two stages for the proposed state network. The first stage is called the conglomerating stage, where GASN is used to conglomerate all the states into communities. In this stage, LID information is used to stop two communities from merging if these two communities both have states from one entity and show significant disparity in interaction. This guarantees that at the end of the execution of GASN, the network is divided into several small fragments, not merely one large network. The second stage is called the divisive stage, where SASN is executed on every divided fragment of the network to get refined results. Given that each fragment is significantly smaller than the original network, SASN can run much faster than running on the original data set. The algorithm framework is shown in **Algorithm 3**.

---

**Algorithm 3.** Hybrid Community Detection
 

---

```

1: Initialize every state node as one-node communities.
2: Calculate  $\Delta Q_u$  for every edge  $(u, v)$  and push into a heap  $H$ .
3: while  $H \neq \emptyset$  do. //The conglomerating stage
4: Pop  $(t, f)$  with maximal  $\Delta Q_u$ .
5:   if  $(t, f)$  is inhibited by known LID info then
6:      $H \leftarrow H - \{(t, f)\}$ 
7:   continue
8:   end if
9:   if  $\Delta Q_u < 0$  then break
10:  Update Pair( $v_f, v_i$ )
11:  Merge Pair( $v_f, v_i$ )
12: end while
13: repeat // The divisive stage
14: Get the largest fragment as  $C$ 
15:  $(\lambda, V) = \text{Eigen}(B_b^{(C)})$ 
16: if  $\lambda_1 < 0$  then break
17: Divide  $C$  given positiveness of  $V_1$ 
18: until enough number of communities generated

```

---

## 4 Experiments

In this section, we evaluate the efficiency and correction of SASN, GASN, and HCD. Typically, it is not possible for a real-world network to provide data on community membership; thus, we first conduct experiment on the synthesis network to evaluate the correctness of these algorithms. Then we turn to real-world data to evaluate the efficiency of these algorithms as



## Community Discovery with Location-Interaction Disparity in Mobile Social Networks

Danmeng Liu, Wei Wei, Guojie Song, and Ping Lu

well as the features extracted by these algorithms.

### 4.1 Experiments on Synthesis Data

We build stochastic networks for the experiment. These networks all have 2000 state nodes. These nodes are divided into 10 communities and every community has 200 states. We create links within these communities with probability  $p_i = 30\%$  and links between different communities with varying  $p_o$ , which will be shown later. Furthermore, we put all these state nodes into 1400 entities. 700 entities have only one state, 400 entities have two, while the rest have three. The reason for the entity sizes is that in real-world networks, more users tend to have a few locations of interest, while some users can have many such locations. The state-entity relationship is generated randomly. Finally, we pick state nodes within one entity but assigned to different communities and randomly select 50% of them to form an LID pair set. Normalized mutual information (NMI) [17] is used to measure the clustering performance of algorithms. The value of NMI ranges between 0 and 1, and a larger NMI indicates a better clustering result. When  $NMI = 1$ , two communities are exactly the same.

We vary  $p_o$  from 0.0025 to 0.025 with a 0.0025 step to create networks with different density of edges outside the communities. For every algorithm and every  $p_o$  setting, we generate and execute our algorithm 50 times to get an average performance. When  $p_o = 0.0025$ , the community structure is quite explicit. However, when  $p_o = 0.025$ , for communities with 200 nodes, number of expected edges from the same community is close to the number of expected edges from the whole network. Thus the community structure is not so explicit.

**Fig. 3a** shows the clustering performance in terms of NMI. Three lines from top to bottom show the performance for HCD, GASN and SASN, respectively. HCD performs the best, and SASN performs the worst. This can be explained by the power of LID. For GASN the performance is good for small  $p_o$ . However, the result deteriorates to the level of SASN when more noise is added to the network. We investigate the result of communities generated by GASN and discover that when the network densifies, FastGreedy became so biased that small com-

munities with only one or two members were generated, which hamper the performance. We also mark variance for every data point. HCD is the most stable method of all three algorithms when the network is sparse, which is guaranteed by its divisive step.

**Fig. 3b** shows the running time for these three algorithms. HCD runs slower than GASN, as it needs more computation on division step. But HCD still outperforms SASN in sparse networks, as the fragment to be divided by spectral method is smaller than the original SASN. When the network becomes denser, time cost of HCD grows because more  $\Delta Q$  on edges need to be updated, and the size of fragments of the network generated by the conglomerate step grow. This leads to slower convergence of divisive step. These results show that HCD outperforms other algorithms referred to in our experiment especially in sparse networks. As real-world networks are mostly sparse, HCD is more competitive than other methods.

### 4.2 Experiments on Real-World Data

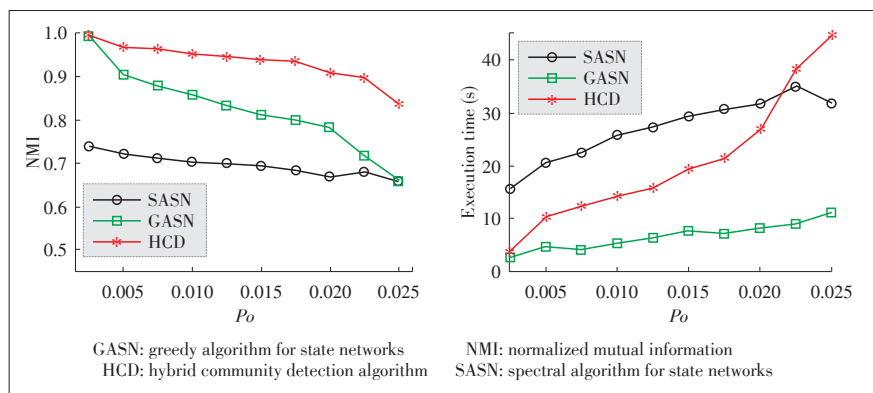
After evaluating our algorithms on synthesis network, we evaluate our algorithm on real-world data sets. Our data are collected from cellphone call records in a medium city in China with a population of about 400,000 in 14 days. Different from data used in other researches, phone records in our phone call record contain cell information for both the calling and called people. We also obtained information on virtual phone networks (VPN) users join. These VPNs are user groups established by companies for their employees to enjoy free calls within the company, which provide us another source of validation of user belongings.

We first extract telephone calls from the largest four VPNs to conduct our experiments. We define every user as an entity and every user-location pair as a state node if the user has made more than five calls in this location. Given that there can be a number of disconnected components in the extracted graph, we take the largest connected component for the subsequent analysis. This component has 5927 state nodes, 3364 entities and 8571 edges. **Fig. 4a** shows that degree distribution of this component observes power law. Therefore this component

is a typical complex network. **Fig. 4b** shows the number of states owned by entities. Most of the people only make phone call frequently in one single place while some people make phone calls in different places.

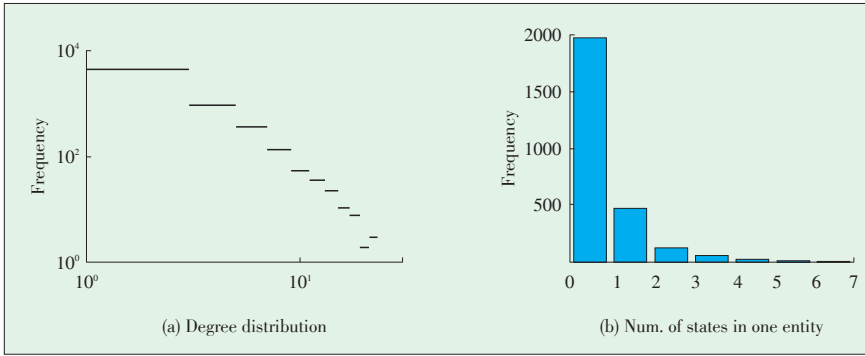
We also evaluate the number of links between different VPNs and the result is shown in **Table 1**. We can see that the number of links inside a VPN is larger than the number of links outside a VPN. This means that VPN data in our dataset have some properties as communities, which can be taken advantage of to evaluate our algorithm.

First, we borrow the conception of NMI.



▲ Figure 3. Performance of three algorithms on synthesis data.





▲ Figure 4. Features of real-world data set.

▼ Table 1. Links between VPNs

	$N_1$	$N_2$	$N_3$	$N_4$
$N_1$	41,921	7948	1338	2690
$N_2$	7948	47,204	2148	2208
$N_3$	1338	2148	4258	533
$N_4$	2690	2208	533	11,962

Given that traditional definition of NMI by Strehl *et al.* [17] only takes unoverlapped communities into account, we instead propose an extended version of NMI that takes overlaps in our model into account. Given one divisions of state network  $X = \{C_1^X, C_2^X, \dots, C_\gamma^X\}$  and another division of entity network  $Y = \{C_1^Y, C_2^Y, \dots, C_\delta^Y\}$ , our extended version of NMI can be calculated as follows:

$$mNMI(X, Y) = I(X, Y) / H(X)H(Y) \quad (9)$$

$$I(X, Y) = \sum_{u,v} B_{XY}(u, v) \log \frac{n B_{XY}(u, v)}{O_X(u) |C_v^Y|} \quad (10)$$

$$H(X) = \sum_u O_X(u) \log \frac{O_X(u)}{n} \quad (11)$$

where

$$B_{xy}(u, v) = \sum_{p \in C_u^X \cap C_v^Y} \frac{1}{|\gamma_{s_p}|} \quad (12)$$

$$O_X(u) = \sum_{p \in C_u^X} \frac{1}{|\gamma_{s_p}|} \quad (13)$$

In this definition, when an entity is completely in one community, it will be accounted as 1 in the calculation. Otherwise it will only be accounted as  $|C_u^X \cap \gamma_{s_p}| / |\gamma_{s_p}|$  for community  $u$ . Therefore for multiple communities sharing one entity, every community only own part of the entity, which is proportional to the number of states it owns.  $mNMI$  is equivalent to the original version when every entity only owns one state node.

We conduct experiment on this of network by using HCD al-

gorithm as we have proved that HCD outperforms other algorithms on synthesis data, and LID set generated from user's calling behavior in different locations and selected with Kendall's  $\tau$  with 95% confidence. First, we show the correctness of communities generated with HCD on state networks. We vary the number of communities to be generated and run traditional spectral algorithm on entity network and HCD on state networks because there is no inhibition information available in entity network. Extended NMI is computed for community number from 50 to 200 between discovered communities and VPN data, and the result is shown in Fig. 5a. Communities generated from state network have slightly higher NMI than entity network. Thus HCD on state network is slightly better than original approaches.

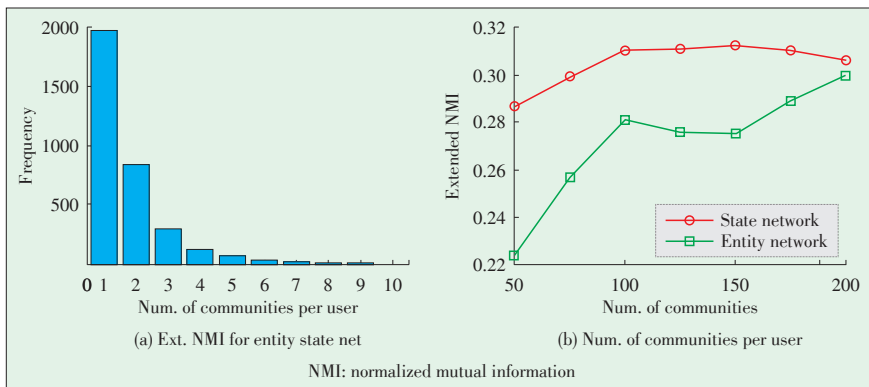
Then we investigate the communities owned by users. As is shown in Fig. 5b, many users only belong to one single community, and the rest belong to multiple communities. This result shows that many users belong to different communities in different locations. To illustrate this more explicitly, we investigate these communities by case study.

We extract phone call records within every community and calculate histograms of these calls for every community and then put these histograms into clusters by cosine distances. From these clusters, we observed two different types of communities: daytime, where phone calls are mostly made during the day, and nighttime, where calls are made at night. These two types of communities reveal different activity patterns of people. Given that in our work, one person can belong to multiple communities, it is natural that they might belong to daytime communities and night communities simultaneously. There are 157 people who belong to both daytime clusters and night clusters. Fig. 6 shows two communities of one single user. The histogram on the left is a typical daytime community, while the one on the right is a night community showing that one user have different social circle in different time.

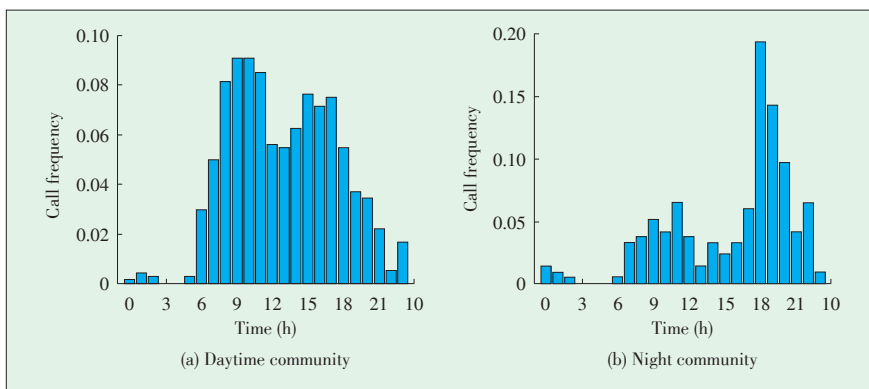
As we generate states by locations, we also analyze the locations of these nodes. We have already noted that users have different contact behavior in different places; thus, people should have different communities in these places. In our result, we see 75.6% O-D pairs are separated in different communities in the result of HCD. Fig. 7 shows the locations of one single user appeared in a map. According to the method proposed by Huang *et al.* [9], to mark O and D of users, two locations in the bottom-right corner was recognized as O and D of one user. However, in the result generated by HCD, we can see two communities:  $C_{147}$  in the top-left corner of the map and  $C_{169}$  in the bottom-right corner. Two locations in  $C_{169}$  recognized as different locations are actually in one community in our result. Looking up information on the map, we discover that the bottom-right corner is a residential area, and the top-left corner has a

## Community Discovery with Location-Interaction Disparity in Mobile Social Networks

Danmeng Liu, Wei Wei, Guojie Song, and Ping Lu



▲ Figure 5. Communities in real-world networks.



▲ Figure 6. Call pattern of two communities of one user.



◀ Figure 7. Location properties.

power plant. Phone call record also reveal that time of calls the user made in the bottom - right corner varies through all the day, and the time of calls made in the top-left corner are all in working hours. This show that locations on the top-left corner are more likely to be work locations, while the bottom-right to be home locations. This show that community discovery in MSN can discover communities with location properties.

Finally we investigate the scalability of our algorithms. We merge nodes from the largest VPN to the smallest and form 10 networks sizing from 5881 to 88427 and run SASN, GASN and HCD on these networks. In Fig. 8, SASN run fastest, while HCD run slower, as it need to split large communities in the divisive stage. SASN run slowest, and its time cost become intolerable as the number of states grow larger than  $5 \times 10^4$ . The re-

sult shows that HCD can run efficiently with higher accuracy and acceptable time cost comparing to GASN.

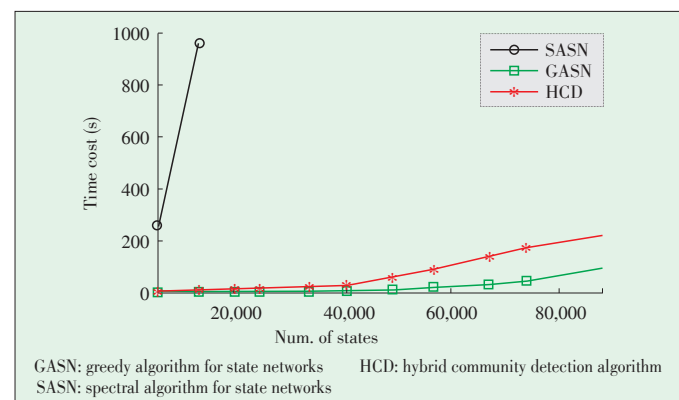
## 5 Related Works

There have been many existing works studying the relationship between social links and locations of social actors. Eagle *et al.* [18] and Li *et al.* [7] measure user similarities given locations or trajectories of users. The Method proposed by these authors can achieve satisfactory results on link prediction. Cho *et al.* [8] study the differences between trajectories caused by activity patterns of users and trajectories caused by movements of users, and then create a model of user mobility given link information. However, most of these works are only concerned with local information, i.e., trajectories and friends of one single user.

Another related field is the modification of modularity to find communities. There have been many attempts to extend modularity in (1) for specific types of graphs. Barber *et al.* [19] extend modularity from normal graphs to bipartite graphs by restricting links between nodes with different colors in the null model.

Mucha *et al.* [20] make a further step by creating a model for multi - slice networks. The author model temporal changes in networks by dividing the network into different slices and calculate modularity for two types of links, i.e., links between slices and links within every slice. However, for networks combined with location information, the method to divide nodes into slices is to be studied.

Some researchers pay attention to the combination of link and content to discover communities. Gomez *et al.* [21] add negative links into network and modify modularity by replacing the target function with a linear combination of positive



▲ Figure 8. Scalability of algorithms.

modularity and negative modularity. Yang *et al.* [22] integrate content model into link analysis, which can be another method for integrating location information.

For community detection algorithms, Lancichinetti *et al.* [23] give a comprehensive comparison of existing community discovery algorithms. Many existing community discovery algorithms have computational complexity greater than  $O(n^2)$ , which mean that these algorithms are not applicable for large scale networks. Therefore we select spectral approach and FastGreedy for our work.

## 6 Conclusion

MSN data are now growing fast, revealing people's interactions in different locations. In this work, we propose an approach to detecting communities in this type of network. We observe location interaction disparity and define a state model in which states represent user-location tuples and entities represent users. This model leverages location interaction disparity. We extend traditional definition of modularity to our model and formally describe community detection problem for location-based social network. Then we modify existing spectral approach and FastGreedy algorithm to create SASN and GASN with efficiency optimization. Given the time cost and precision of these two algorithms we propose HCD for higher precision and lower time cost. LID can be easily integrated into this algorithm as heuristics.

Experiments on synthesis data show that HCD outperforms SASN and GASN in precision. For the aspect of time cost, HCD runs slower than GASN since it uses GASN as the first step, but significantly faster than SASN when the network is sparse. This property holds both on synthesis data and real-world data. We show in real world data that many users belong to different communities in different places. In a case study we find that users can be in different types of communities, indicating different activities for users in different locations.

## References

- [1] M. Girvan and M. E. J. Newman, "Community structure in social and biological networks," *Proceedings of the National Academy of Science*, vol. 99, pp. 7821–7826, Jun. 2002.
- [2] M. Richardson and P. Domingos, "Mining knowledge-sharing sites for viral marketing," in *8th ACM SIGKDD International Conference on Knowledge Discovery and Data Mining*, Edmonton, Canada, Jul. 2002, pp. 61–70.
- [3] L. Tang, X. Wang, and H. Liu, "Uncovering groups via heterogeneous interaction analysis," in *9th IEEE International Conference on Data Mining*, Miami, USA, Dec. 2009, pp. 503–512.
- [4] H. Kang, L. Getoor, and L. Singh, "Visual analysis of dynamic group membership in temporal social networks," *Sigkdd Explorations*, vol. 9, no. 2, pp. 13–21, Dec. 2007. doi: 10.1145/1345448.1345452.
- [5] M. E. J. Newman and M. Girvan, "Finding and evaluating community structure in networks," *Physical Review E*, vol. 69, 026113, 2004. doi: 10.1103/PhysRevE.69.026113.
- [6] K. Wakita and T. Tsurumi, "Finding community structure in mega-scale social networks," in *16th International Conference on World Wide Web*, Banff, Canada, 2007, pp. 1275–1276. doi: 10.1145/1242572.1242805.
- [7] Q. Li, Y. Zheng, X. Xie, *et al.*, "Mining user similarity based on location history," in *16th ACM SIGSPATIAL International Conference on Advances in Geo-*

*graphic Information Systems*, Irvine, USA, Nov. 2008, no. 34. doi: 10.1145/1463434.1463477.

- [8] E. Cho, S. A. Myers, and J. Leskovec, "Friendship and mobility: user movement in mobile social network," in *17th ACM SIGKDD International Conference on Knowledge Discovery and Data Mining*, San Diego, USA, Aug. 2011, pp. 1082–1090.
- [9] W. Huang, Z. Dong, N. Zhao, *et al.*, "Anchor points seeking of large urban crowd based on the mobile billing data," in *6th International Conference on Advanced Data Mining and Applications*, Chongqing, China, Nov. 2010, pp. 346–357.
- [10] M. G. Kendall, "A new measure of rank correlation," *Biometrika*, vol. 30, no. 1/2, pp. 81–93, 1938.
- [11] M. E. J. Newman, "Detecting community structure in networks," *The European Physical Journal B Condensed Matter*, vol. 38, no. 2, pp. 321–330, Mar. 2004.
- [12] U. Brandes, D. Delling, M. Gaertler, *et al.*, "On modularity clustering," *IEEE Transactions on Knowledge and Data Engineering*, vol. 20, no. 2, pp. 172–188, Feb. 2008.
- [13] M. E. J. Newman, "Finding community structure in networks using the eigenvectors of matrices," *Physical Review E*, vol. 74, 036104, Sep. 2006. doi: 10.1103/PhysRevE.74.036104.
- [14] G. Csardi and T. Nepusz, "The igraph software package for complex network research," *InterJournal Complex Systems*, no. 1695, 2006.
- [15] G. H. Golub and C. F. Van Loan, *Matrix Computations*, 3rd ed. Baltimore, USA: Johns Hopkins University Press, 1996.
- [16] P. Schuetz and A. Caflisch, "Efficient modularity optimization by multistep greedy algorithm and vertex mover refinement," *Physical Review E*, vol. 77, 046112, 2008. doi: 10.1103/PhysRevE.77.046112.
- [17] A. Strehl and J. Ghosh, "Cluster ensembles — a knowledge reuse framework for combining multiple partitions," *The Journal of Machine Learning Research*, vol. 3, pp. 583–617, Mar. 2003. doi: 10.1162/153244303321897735.
- [18] N. Eagle and A. Pentland, "Eigenbehaviors: identifying structure in routine," *Behavioral Ecology and Sociobiology*, vol. 63, pp. 1057–1066, 2009.
- [19] M. J. Barber, "Modularity and community detection in bipartite networks," *Physical Review E*, vol. 76, 066102, 2007. doi: 10.1103/PhysRevE.76.066102.
- [20] P. J. Mucha, T. Richardson, K. Macon, *et al.*, "Community structure in time-dependent, multiscale, and multiplex networks," *Science*, vol. 328, no. 5980, pp. 876–878, May 2010. doi: 10.1126/science.1184819.
- [21] S. Gomez, P. Jensen, and A. Arenas, "Analysis of community structure in networks of correlated data," *Physical Review E*, vol. 80, 016114, 2009. doi: 10.1103/PhysRevE.80.016114.
- [22] T. Yang, R. Jin, Y. Chi, and S. Zhu, "Combining link and content for community detection: a discriminative approach," in *15th ACM SIGKDD International Conference on Knowledge Discovery and Data Mining*, Paris, France, 2009, pp. 927–936. doi: 10.1145/1557019.1557120.
- [23] A. Lancichinetti and S. Fortunato, "Community detection algorithms: a comparative analysis," *Physical Review E*, vol. 80, 056117, 2009. doi: 10.1103/PhysRevE.80.056117.

Manuscript received: 2015-04-21

## Biographies

**Danmeng Liu** (liudanmeng@pku.edu.cn) received his Bachelor degree from Wuhan University. He is a Master candidate at school of School of Electronic Engineering and Computing Science, Peking University. His research interests include data mining and social network analysis.

**Wei Wei** (wei.wei118.zte.com.cn) received her MS degree in communication and information engineering from Chongqing University of Posts and Telecommunications. Her research interests include location technology and business intelligence.

**Guojie Song** (gjsong@pku.edu.cn) is an associate professor of the School of Electronic Engineering and Computing Science, and vice director of Research Center of Intelligent Information Processing, at Peking University. He received the PhD degree from Department of Computer Science, Peking University in 2004. He is currently interested in various techniques of data mining, machine learning, as well as their applications in intelligent traffic system, and social networks etc.

**Ping Lu** (lu.ping@zte.com.cn) received his ME degree in automatic control theory and applications from South East University. He is the chief executive of the Service Institute of ZTE Corporation. His research interests include augmented reality and multimedia services technologies.

## New Members of ZTE Communications Editorial Board



**Fa-Long Luo**, PhD, is the chief scientist of two leading international companies dealing with software-defined radio and wireless multimedia with headquarters in Silicon Valley, USA. He was the Founding Editor-in-Chief of *International Journal of Digital Multimedia Broadcasting* from 2007 to 2011. Fa-Long Luo was the chairman of IEEE Industry DSP Standing Committee and Technical Directional Board Member of IEEE Signal Processing Society from 2011 to 2012. He is now an associate editor of *IEEE Access* and *IEEE Internet of Things Journal* as well as an editorial board member of *St. Petersburg State Polytechnical University Journal*. He has 31 years of research and industrial experience in multimedia, communication and broadcasting with real-time implementation, applications and standardizations with receiving worldwide attention and recognition. He has authored/edited 4 books, more than 100 technical papers and 18 patents in these and closely related fields. His fifth book *Signal Processing for 5G: Algorithms and Implementations* will be published by Wiley and appear in November of 2015. He was elected Fellow of IET/IEE and awarded Fellowship by the Alexander von Humboldt Foundation, Germany.



**Guifang Li** received the PhD degree from The University of Wisconsin at Madison and is a professor of Optics, Electrical & Computer Engineering and Physics at University of Central Florida (UCF), USA. His research interests include optical communication and networking, RF photonics and all-optical signal processing. He has collaborated widely with academic institutions and industry. He was the director of the NSF IGERT program in Optical Communications and Networking at UCF. He received the Research Incentive Award in 2007 and was a founder of Optium, UCF's first venture-back startup. He also received the Teaching Incentive Award in 2004 and 2015. He is the recipient of the NSF CAREER award and the Office of Naval Research Young Investigator award. He was an IEEE EDS Distinguished Lecturer in 2004–2005 and an IEEE IPS Distinguished Lecturer in 2014–2015. Dr. Li is a fellow of IEEE, the Optical Society of America, and SPIE. He currently serves as a deputy editor for *Optics Express*, and associate editors for *Chinese Optics Letters* and for *Photonics Technology Letters*.



**Shuguang Cui** received the PhD degree in Electrical Engineering from Stanford University, USA, in 2005. He has been working as a professor in Electrical and Computer Engineering at the Texas A&M University, College Station, USA. His current research interests focus on data oriented large-scale information analysis and system design, including large-scale distributed estimation and detection, information theoretical approaches for large data set analysis, complex cyber-physical system design, and cognitive network optimization. He was selected as the Thomson Reuters Highly Cited Researcher and listed in the Worlds' Most Influential Scientific Minds by ScienceWatch in 2014. He was the recipient of the IEEE Signal Processing Society 2012 Best Paper Award. He has served as the TPC co-chairs for many IEEE conferences. He has also been serving as the area editor for *IEEE Signal Processing Magazine*, and associate editors for *IEEE Transactions on Big Data*, *IEEE Transactions on Signal Processing*, *IEEE JSAC Series on Green Communications and Networking*, and *IEEE Transactions on Wireless Communications*. He was the elected member for IEEE Signal Processing Society SPCOM Technical Committee (2009–2014) and the elected Vice Chair for IEEE ComSoc Wireless Technical Committee (2015–2016). He is a member of the Steering Committee for *IEEE Transactions on Big Data* and a member of the IEEE ComSoc Emerging Technology Committee. He was elected as an IEEE Fellow in 2013 (within 8 years after PhD, one of the quickest in IEEE history) and an IEEE ComSoc Distinguished Lecturer in 2014.



**Wanlei Zhou** received the PhD degree from The Australian National University, Australia, in 1991, in Computer Science and Engineering. He also received a DSc degree from Deakin University, Australia in 2002. He is currently the Alfred Deakin Professor and Chair of Information Technology, School of Information Technology, Deakin University. Dr. Zhou was the head of School of Information Technology twice (Jan. 2002–Apr. 2006 and Jan. 2009–Jan. 2015) and the associate dean of Faculty of Science and Technology in Deakin University (May 2006–Dec. 2008). Before joining Deakin University, Dr. Zhou served as a lecturer in University of Electronic Science and Technology of China, a system programmer in HP at Massachusetts (USA), a lecturer in Monash University (Australia), and a lecturer in National University of Singapore. His research interests include distributed systems, network security, bioinformatics, and e-learning. Dr. Zhou has published more than 300 papers in refereed international journals and refereed international conferences proceedings. He has also chaired many international conferences and has been invited to deliver keynote speeches in many international conferences. He is a senior member of the IEEE.



**Weihua Zhuang** received the PhD degree from the University of New Brunswick, Canada, in electrical engineering. In October 1993, she joined the Department of Electrical and Computer Engineering, University of Waterloo, Canada, as an assistant professor. She was promoted to the rank of associate professor with tenure in July 1997, and then to full professor in July 2002. Since May 2010, she has been a Tier I Canada Research Chair in wireless communication networks. Her current research focuses on resource allocation and QoS provisioning in wireless networks, and on smart grid. Dr. Zhuang is a co-recipient of several Best Paper Awards from the IEEE International Conferences. She received the Outstanding Performance Award 4 times since 2005 from the University of Waterloo, and the Premier's Research Excellence Award in 2001 from the Ontario Government.

Dr. Zhuang is a fellow of IEEE, a fellow of the Canadian Academy of Engineering (CAE), a fellow of the Engineering Institute of Canada (EIC), the VP Mobile Radio, and an elected member of the Board of Governors (BoG) of the IEEE Vehicular Technology Society. She was the Editor-in-Chief of *IEEE Transactions on Vehicular Technology* (2007–2013), an editor of *IEEE Transactions on Wireless Communications* (2005–2009), the Technical Program Committee (TPC) Symposia Chair of the IEEE Globecom 2011, the TPC Co-Chair for Wireless Networks Symposium of the IEEE Globecom 2008, and an IEEE Communications Society Distinguished Lecturer (2008–2011).



**Yi Pan** is a Distinguished University Professor of the Department of Computer Science and an Interim Associate Dean at Georgia State University, USA. He received the M.Eng. degrees in computer engineering from Tsinghua University, China, in 1984, and the PhD degree in computer science from the University of Pittsburgh, USA, in 1991. His profile has been featured as a distinguished alumnus in both Tsinghua Alumni Newsletter and University of Pittsburgh CS Alumni Newsletter. Dr. Pan's research interests include parallel and cloud computing, wireless networks, and bioinformatics. Dr. Pan has published more than 150 journal papers with over 50 papers published in various IEEE journals. In addition, he has published over 150 papers in refereed conferences. He has also co-authored/co-edited 37 books. His work has been cited more than 4000 times. Dr. Pan has served as an editor-in-chief or editorial board member for 15 journals including 7 IEEE Transactions. He is the recipient of many awards including IEEE Transactions Best Paper Award, IBM Faculty Award, JSPS Senior Invitation Fellowship, IEEE BIBE Outstanding Achievement Award, NSF Research Opportunity Award, and AFOSR Summer Faculty Research Fellowship. He has organized many international conferences and delivered over 40 keynote speeches at various international conferences around the world.



**Yueping Zhang** received the PhD degree from the Chinese University of Hong Kong, in 1995. He worked at the University of Liverpool, UK, from 1990 to 1992, and City University of Hong Kong from 1996 to 1997. From 1997 to 1998, he taught at the University of Hong Kong. He is now a professor of Electronic Engineering at Nanyang Technological University, Singapore. He has researched extensively in the field of radio science and technology. He has published numerous papers and taken various US patents. Dr. Zhang serves as an editor of *ETRI Journal* and an associate editor of the *IEEE Transactions on Antenna and Propagation*. He also serves on the Editorial Boards of a large number of Journals including the *IEEE Transactions on Microwave Theory and Techniques* and *ZTE Communications*.

He was the recipient of the Sino-British Technical Collaboration Award (1990) for his contribution to the advancement of subsurface radio science and technology, the Best Paper Award of the 2nd IEEE/IET International Symposium on Communication Systems, Networks and Digital Signal Processing, and the Best Paper Prize of the 3rd IEEE International Workshop on Antenna Technology. He was also the recipient of a William Mong Visiting Fellowship of the University of Hong Kong (2005) and the S. A. Schelkunoff Transactions Prize Paper Award of the IEEE Antennas and Propagation Society (2012).



# ***ZTE Communications Guidelines for Authors***

## **• Remit of Journal**

*ZTE Communications* publishes original theoretical papers, research findings, and surveys on a broad range of communications topics, including communications and information system design, optical fiber and electro-optical engineering, microwave technology, radio wave propagation, antenna engineering, electromagnetics, signal and image processing, and power engineering. The journal is designed to be an integrated forum for university academics and industry researchers from around the world.

## **• Manuscript Preparation**

Manuscripts must be typed in English and submitted electronically in MS Word (or compatible) format. The word length is approximately 4000 to 7000, and no more than 6 figures or tables should be included. Authors are requested to submit mathematical material and graphics in an editable format.

## **• Abstract and Keywords**

Each manuscript must include an abstract of approximately 150 words written as a single paragraph. The abstract should not include mathematics or references and should not be repeated verbatim in the introduction. The abstract should be a self-contained overview of the aims, methods, experimental results, and significance of research outlined in the paper. Five carefully chosen keywords must be provided with the abstract.

## **• References**

Manuscripts must be referenced at a level that conforms to international academic standards. All references must be numbered sequentially in-text and listed in corresponding order at the end of the paper. References that are not cited in-text should not be included in the reference list. References must be complete and formatted according to *ZTE Communications* Editorial Style. A minimum of 10 references should be provided. Footnotes should be avoided or kept to a minimum.

## **• Copyright and Declaration**

Authors are responsible for obtaining permission to reproduce any material for which they do not hold copyright. Permission to reproduce any part of this publication for commercial use must be obtained in advance from the editorial office of *ZTE Communications*. Authors agree that a) the manuscript is a product of research conducted by themselves and the stated co-authors, b) the manuscript has not been published elsewhere in its submitted form, c) the manuscript is not currently being considered for publication elsewhere. If the paper is an adaptation of a speech or presentation, acknowledgement of this is required within the paper. The number of co-authors should not exceed five.

## **• Content and Structure**

*ZTE Communications* seeks to publish original content that may build on existing literature in any field of communications. Authors should not dedicate a disproportionate amount of a paper to fundamental background, historical overviews, or chronologies that may be sufficiently dealt with by references. Authors are also requested to avoid the overuse of bullet points when structuring papers. The conclusion should include a commentary on the significance/future implications of the research as well as an overview of the material presented.

## **• Peer Review and Editing**

All manuscripts will be subject to a two-stage anonymous peer review as well as copyediting, and formatting. Authors may be asked to revise parts of a manuscript prior to publication.

## **• Biographical Information**

All authors are requested to provide a brief biography (approx. 150 words) that includes email address, educational background, career experience, research interests, awards, and publications.

## **• Acknowledgements and Funding**

A manuscript based on funded research must clearly state the program name, funding body, and grant number. Individuals who contributed to the manuscript should be acknowledged in a brief statement.

## **• Address for Submission**

magazine@zte.com.cn

12F Kaixuan Building, 329 Jinzhai Rd, Hefei 230061, P. R. China



# ZTE COMMUNICATIONS



► *ZTE Communications has been indexed in the following databases:*

- Cambridge Scientific Abstracts (CSA)
- China Science and Technology Journal Database
- Chinese Journal Fulltext Databases
- Inspec
- Norwegian Social Science Data Services (NSD)
- Ulrich's Periodicals Directory
- Wanfang Data—Digital Periodicals